THE MECHANICAL FACTORS WHICH INFLUENCE THE SEMI-RANDOM BEHAVIOR OF GREAT EARTHQUAKES

A Thesis Submitted
to the Temple University Graduate Board

---

in Partial Fullfiment
of the Requirement for the Degree

MASTER OF ARTS

---

by

Alex Ko-Chien Tung

1981

DEPARTMENT COPY

THE MECHANICAL FACTORS WHICH INFLUENCE THE SEMI-RANDOM BEHAVIOR OF GREAT EARTHQUAKES

ALEX KO-CHIEN TUNG

A THESIS SUBMITTED IN PARTIAL FULFILLMENT
OF THE REQUIREMENTS FOR
THE MASTER OF ARTS DEGREE IN GEOLOGY,
COLLEGE OF LIBERAL ARTS,

TEMPLE UNIVERSITY
PHILADELPHIA, PENNSYLVANIA
1981

APPROVED BY _____

THESIS ADVISOR

ABSTRACT

The apparent randomness in patterns of earthquake activity are modeled using a quasi-static, truss-fault block analogy of earthquake occurrence. The earthquake belt is modeled utilizing a series of fault blocks which are initially subject to a set of randomly generated stresses. The model indicates that fault blocks along a seismic belt can experience either enhanced or suppressed seismic activity immediately after and during the years that follow a modeled earthquake. However, the regions that adjoin the block which has experienced a modeled earthquake, are primarily affected by the enhancing or the suppressive effects of a modeled earthquake.

Seismic gaps are attributed to the complex interaction between fault blocks and the manner in which modeled earthquakes redistribute forces to an elastic truss, which represents the oceanic lithosphere. Due to the enhancing and suppressive seismic effects, seismic gaps within the model are filled by earthquakes that occur in a different order from one modeled earthquake cycle to another. Thus the truss-fault block model produces a semi-random pattern of earthquake occurrence, although there are similarities between modeled earthquake cycles. Model behavior is not unlike the space-time distribution patterns observed in nature.

Owing to the semi-random character of the model, the recurrence interval within each fault block is different and the recurrence interval changes from cycle to cycle. Also the recurrence interval increases if a fault block is interrupted by the suppressive effects of earthquakes in adjacent areas.

ACKNOWLEDGEMENTS

I wish to acknowledge with gratitude the aid and guidance given by my thesis committees, Dr. Gene C. Ulmer and Dr. David E. Grandstaff. I also wish to thank Dr. Robert Stone in the College of Engineering Technology for his instruction of structural analysis. I would particularly like to thank my thesis advisor, Dr. Richard E. Bischke, for his suggestions and critical comments during the course of study. I also appreciate Temple University for its financial support and computer facilities over the past two and a half years.

In addition, I am grateful to Mrs. Mildred Shapiro, Mrs. Randy Blau, and Terry O'Reilly for their help and kindness.

DEDICATION

I would like to dedicate this work to my parents and my wife, who gave their special care and encouragement during the years of my graduate study.

TABLE OF CONTENTS

INTRODUCTION

It has long been recognized that great earthquakes occur along several active seismic belts, the most obvious earthquake zone being the Ring of Fire. One of the most noticeable characteristics of great earthquakes is that they recur in the same areas within time intervals of several tens to hundreds of years (Sykes, 1971; Kelleher et al., 1973). This interesting feature has been employed by a number of investigators as a primary constraint when modeling great earthquakes (Savage and Prescott, 1978; Turcotte et al., 1979; Ito, 1980; Shimazaki and Nakata, 1980). By utilizing earthquake models investigators try to understand the mechanisms of great earthquakes and to account for earthquake periodicity and regularity. Knopoff (1971), however, has criticized this approach, and he believes that earthquakes are statistically random events. Although this is true for earthquakes of small to large magnitude, most seismologists point to the existence of regularities in the return pattern of great and very large earthquakes (Sykes, 1971, 1972; Kelleher, 1973; Ito, 1980).

Based on Burridge and Knopoff's (1967) simple dynamic model of coupled mass or fault blocks, Cohen (1977, 1979) generated a complex and apparently random sequence of modeled earthquakes. For example, a random space-time earthquake sequence can be produced by randomly distributing a friction parameter applied to each fault block. Cohen concluded that

the periodic reoccurrence of similar type events is observed in cases where the parameters of the fault and the fault blocks are nearly homogeneous from location to location within an earthquake model. Seismic gaps are more likely to occur where there are large variations in the elastic or frictional parameters of a modeled fault zone. Ito (1980), however, has proposed an electric analogue model of coupled fault blocks that reproduces nonperiodic behavior of seismic events without introducing a heterogeneous friction parameter into the model. He emphasized that interaction between seismic events may play an important role in causing the apparent random behavior of earthquake occurrence. He also showed that interaction between fault blocks may contribute to the partial release of seismic energy particularly in blocks adjacent to a block which has experienced a modeled earthquake. This suggests a suppressive effect of earthquake occurrences in adjacent blocks, an effect which should suppress seismic migration (Mogi, 1968a). Although the mathematics and the logic of Ito's electric analogue model is rather complex, it suggests an alternative mechanism of generating seismic randomness without resorting to an inhomogeneous fault friction parameter.

In this thesis I present a quasi-static, truss-fault block earthquake model to study the apparent random behavior of earthquake occurrence. Expanding on Ito's work, I will show that a semi-random earthquake sequence can be generated

by a simple deterministic model, without making any use of variable mechanical factors such as time-dependent fault friction. This study will concentrate on modeling the great earthquakes which occur along subduction zones, as these earthquakes have been shown not to be completely random but exhibit at least some spatial and temporal regularities (Sykes, 1971, 1972). In addition, great thrust fault earthquakes tend to occur within certain restricted zones and can, therefore, be modeled in two dimensions, utilizing a truss-fault block analogue. Although highly idealized models may not yield adequate representations of naturally occurring events, more realistic models tend to be so complex in detail as to obscure the physical significance of the model. Thus, the model employed in this study may not be the best of all possible earthquake models. It does, however, model fault block interactions, it employs a relatively simple mathematical development, and it permits an analysis of the complex coupling between adjoining fault blocks allowing a determination of the mechanisms which cause strain accumulation within each model element. Perhaps the most interesting feature of the model is that it generates a semi-random space-time distribution pattern of great earthquakes from a physically homogeneous yet deterministic fault model.

SEISMIC GAP THEORY

Fedotov (1965) was the first seismologist to envision the concept of a seismic gap. From a plot of the focal zones of great shallow earthquakes located along the Japan-Kurile-Kamchatka arc, Fedotov noticed that there were several gaps in the seismic activity. These gaps had not ruptured for many years and thus were the most probable sites for future large earthquakes. Since the time of Fedotov's initial study in 1965, great earthquakes occurred within the seismic gaps on May 16, 1968 (M_w=8.2), on August 11, 1969 (M_w=8.2) (Kanamori, 1977), and on December 15, 1971 (M=7.8) (Kelleher et al., 1973) (Fig. 1).

Furthermore, Mogi (1968b) realized that the aftershock zones of great earthquakes filled the circum-Pacific seismic belt without significant overlap. In addition, Mogi found that great earthquakes migrated along and successively filled the seismic belt, and that the seismic gaps were filled by great earthquakes without appreciable overlap (Mogi, 1969). Utilizing seismic gap theory, Mogi (1969) studied the focal regions of large earthquakes along the coastal areas of south-eastern Japan and correctly predicted the location of a great earthquake on August 11, 1969 (M_w=8.2). Additional work has been conducted by Kelleher et al. (1973). They examined the most active portions of the plate margins and found that these regions were filled by the rupture zones of large shallow

earthquakes. They also successfully predicted the site for an earthquake which occurred in the Yakataga gap, a part of the Alaska-Aleutian seismic zone.

By examining the space-time diagram shown in Figure 2, Kelleher et al. (1973) realized that tectonic strain had been accumulating in the gap since the last great earthquake occurred in the Yakataga region in 1899. On February 28, 1979, the eastern part of the gap experienced the M_S=7.7 Saint Elias earthquake (Fig. 3). Only a small part of the gap has been filled, and thus their results strongly suggest the possibility of another great shock filling the remaining area of the gap within the very near future. Although the seismic gap theory can not predict the exact time of future large or great earthquakes, the theory delineates the future sites of earthquakes, and enhances our understanding of the mechanisms involved in earthquake recurrence and seismic migration.

FAULT BLOCKS

In Fedotov's early work (1965), he noticed that the focal areas of great earthquakes were spatially bounded and emphasized the sharp lateral termination of each focal zone. Utilizing seismic gap theory and analyzing the patterns of seismic migration, a number of other seismologists concluded that the seismic belts seem to be composed of a series of fault segments which terminate laterally (Fig. 4) (Mogi, 1968a, 1968b; Sykes, 1971; Kelleher et al., 1973; Anderson, 1975; McCann et al., 1980; Sykes et al., 1980; Davies et al., 1981). For example, to explain the very sharp limits of observed aftershock activity following the 1965 Rat Island earthquake (M_w=8.2) in the Aleutian Islands, Jordan et al. (1965) proposed that the earthquake zone was segmented into a series of block-like regions. They were also able to correlate the boundaires of aftershock activity to transverse geological structures. Mogi (1968a, 1968b) was the first to recognize that many focal zones terminated along transverse features and Kelleher et al. (1973) have come to the similar conclusions.

By utilizing evidences from both seismology and volcanology, Carr et al. (1973, 1974) and Carr and Stoiber (1977) presented a segmented structural model to explain changes in seismic and volcanic activity along the central American convergent plate margin. They summarized that this continental margin is broken by transverse structures and that each

structural segment (i.e. fault block) is a few hundred kilometers long (Fig. 5).

TRUSS-FAULT BLOCK ANALOGY

In this study, a convergent plate margin is divided into three regions; an oceanic lithospheric region which loads the plate margin, a zone of stress drop that characterizes the regions of large and great earthquakes, and a relatively stable region, the continental lithospheric plate (Fig. 6,7). According to this interpretation the seismic zone experiences relatively large strain variations, whereas the surrounding lithospheric plates are subject to relatively small internal deformations during the years separate large or great earthquakes.

Due to the strong geologic, seismologic, and volcanologic evidence suggesting that earthquake zones are partitioned into block-like regions, a modeled seismic belt will be studied using a truss-fault block analogy (Fig. 6). In the truss-fault block analogue of earthquake occurrence the seismic zone is segmented into a series of externally connected blocks that are independently linked to an elastic truss (Fig. 7). Thus each block supports a different level of stress and strain which varies from block to block. Each individual fault block (Fig. 8) can be subject to an imposed stress drop in the form of a modeled earthquake, and the fault block deforms viscoelastically during the period of time which divides modeled earthquakes.

The oceanic lithosphere is modeled using an elastic

truss which is uniformly loaded by constant forces (F_T) applied to the left edge of the truss (Fig. 7,8). In nature the oceanic lithosphere should be subject to elastic deformations which warp the regions where the oceanic plate loads the plate margin. This warping of the oceanic plate is caused by the release and the recovery of stress within the seismic zone. Therefore, an elastic truss should model the type of deformation that is to be expected in nature.

The seismic zone is composed of individual fault block elements (Fig. 7) that experience large deformations between earthquakes. This zone is divided into two sections, an upper elastic zone which is subject to stress drops and a lower viscoelastic zone which is continuously creeping (Kasahara, 1975; Thatcher, 1975a, 1975b; Scholz and Kato, 1978). Thus, the total deformation to be experienced by the fault blocks is both elastic and viscous (i.e. viscoelastic). If the upper portion of the fault block behaves according to Hooke's Law and the lower portion of the block in both an elastic and Newtonian viscous manner, then the total deformation in the seismic zone behaves as a standard linear solid (Ramsay, 1967; Flügge, 1975; Findley et al., 1976; Bischke, 1981). The standard linear solid element which describes that type of deformation considered here, is composed of an upper elastic spring in parallel with a lower elastic spring and viscous

dashpot in series (Fig. 9). In this study the continental lithosphere is taken to be perfectly rigid body experiencing no internal deformations, i.e. the deformations at the plate margin occur entirely within viscoelastic blocks and the elastic truss.

As the elastic truss represents the converging oceanic lithospheric plate (Fig. 7), the level of strain within each fault block is not totally independent of the amount of strain in the adjoining fault blocks. Thus, the manner in which each fault block deforms depends primarily upon the amount of strain within several adjoining fault blocks. Each fault block is complexly linked to its neighbouring blocks through the elastic truss, and thus the fault blocks mutually interact depending upon the level of strain within each block. For example, if a modeled earthquake occurs in one fault block, a stress drop will be generated within the block due to the release of elastic strain energy. A portion of the strain energy lost by the block experiencing a modeled earthquake is transferred to the elastic truss, causing the truss to deform (i.e. warp) along its length and the adjoining blocks to support more of the externally applied load. The deformation in the truss due to the earthquake will be larger in those blocks adjacent to the block which has experienced the modeled earthquake, and the deformation will diminish along the entire length of the truss.

In some models of earthquake occurrence, the effects of an earthquake are primarily local (Anderson, 1975; Savage and Prescott, 1975; Shimazaki and Nakata, 1980). In Ito's (1980) electric analogue model and the truss-fault block analogue model, the effects of a modeled local earthquake are distributed along the entire length of the modeled earthquake belt, although the adjoining fault block elements are more affected. Even though each fault block is laterally discontinuous relative to adjoining fault blocks, the manner in which the forces are transferred between the truss and each fault block element must be somewhat analogous to what exists in nature. A precise description of how this loading force redistribution is accomplished is discussed in Appendix A.

MODEL FORMULATION AND PROCEDURES

In order to model the repetitive patterns of stress release and accumulation inherent in the earthquake cycle, it is necessary to discuss the mechanisms responsible for plate motion, particularly the origin of the driving force or forces. According to plate tectonic theory, the outermost portions of the earth are composed of lithospheric plates which exhibit elastic behavior. At depth, high temperatures cause the rock to behave in a viscoelastic fashion, and thus the plates move over a viscous like asthenosphere (Savage and Burford, 1970; Turcotte and Spence, 1974). It has been shown that the largest forces acting upon the plates originate at the trenches (Forsyth and Uyeda, 1975; Cappel and Tullis, 1977). This slab-pull force, as defined by Forsyth and Uyeda (1975), can be resolved into a horizontal force which loads the oceanic lithosphere in a direction that is perpendicular to the plate boundaries. In Figure 7 the force F_T acting on the truss is the horizontal resolution of the slab-pull force or any other force which loads the lithosphere. As shown in Figures 8 and 9 the force F_n, which results from the force F_T, acts along the right hand side of the truss. Force F_n is then resolved into forces F_G and F_μ which act within each fault block. Force F_G loads the upper locked section and force F_μ loads the lower creeping section of each fault block (Fig. 9). Thus the truss which models the elastic oceanic lithosphere loads

each fault block along the entire length of the fault zone.

The length of each truss element is arbitrarily assigned value of 300 Km as shown in Figure 7. Therefore, the rupture length for an earthquake is 300 Km and the short term elastic thickness of lithosphere is about 100 Km (Fig. 7). In the model (Fig. 8) the total force (F_T) is constant and is uniformly applied to each truss joint along the oceanic side of the modeled lithosphere. The force F_n applied to each fault block is resolved according to procedures described in Appendix A. As each fault block behaves in a viscoelastic manner (Fig. 9), the time-dependent behavior of the model is determined by the methods outlined in Appendix B.

Once the truss is subject to the loading force F_T and random initial stresses are applied to each fault block using a random number generator (Fig. 10), the stress and strain start to accumulate until the failure stress level is reached. It is assumed that the failure level within each block is uniform and that failure occurs at 1000 bars. Even with this assumption the cyclic pattern of modeled earthquakes will be semi-random. When the accumulated stress exceeds the failure level, the block is subject to an imposed stress drop, here taken to be approximately 30 bars, and a modeled earthquake is triggered. By solving equation (A12) of Appendix A the redistributed forces (F_n) which load the fault blocks along

the length of truss are determined, and the suppressive or enhancing effect of redistributed forces (F_n) is applied to every fault block. In the model those fault blocks which adjoin the fault block which experienced the imposed stress drops are primarily affected by the force redistribution. After a modeled earthquake, the stress and the strain in each fault block accumulate until the stress reaches 1000 bars, and the next earthquake is triggered.

Although a truss may not be the best possible analogue of the oceanic lithosphere, it does model the elastic character inherent in the oceanic lithosphere. Most of all, it offers a media in which to transfer forces from block to block and simulates the effects that an earthquake should have upon the oceanic lithosphere. In order to simulate the natural situation, each fault block is initially subject to randomly generated stresses (or stiffnesses) (Fig. 10). This procedure generates a random distribution of earthquake occurrence along the modeled seismic belt, which is similar to the patterns observed in nature. The parameters used in the model are listed in Table 1.

FORCE REDISTRIBUTION SURROUNDING A MODELED EARTHQUAKE

Initially the earthquake model is subject to randomly generated forces (F_n) which act along the right hand edge of the truss. This procedure subjects the fault blocks to a randomly distributed set of displacements or stresses that range in value from 952.5 bars in block 24 to 981.5 bars in block 46 (Fig. 10). After the fault blocks are loaded by the random stresses, the stress within each block accumulates incrementally according to equation (B6) of Appendix B. When the accumulating stress within a block exceeds the failure threshold, here assumed to be 1000 bars, the block is subject to an approximate 30 $\pm$ 1.0 bar stress drop. The failure stress and the stress drop within each block are assumed to be uniform throughout the model.

When a modeled earthquake occurs, the adjacent blocks are primarily affected, and the resulting force disturbance dies out along the entire length of the truss. The resultant force redistribution is computed by equation (A12) of Appendix A.

The following discussion describes how this force redistribution occurs. Figure (11) shows that the stress in block 26 has reached 1000 bars and, therefore, a modeled earthquake is triggered in this element (Fig. 12). After imposing a 30.2 bar stress drop in block 26, Figure (13) gives the results of the force redistribution at the end of the

modeled event. Figure (13) summarizes the effects of a modeled earthquake in block 26 upon the other fault blocks, and illustrates the overall net effect of the force redistribution. The effect of an earthquake in block 26 is to increase the stress in blocks 24, 25, 27, 28, 0.068 bar, 3.00 bar, 3.03 bar, and 0.072 bar, respectively. The force redistribution diminishes very quickly away from the failed block, increasing the stress in the four elements that adjoin block 26 and reducing the stress in the remaining or more distant elements (Fig. 13).

Ito's (1980) electric analogue model produced very similar results. Ito's states that the short-term effect of a modeled earthquake is to increase the energy in those elements adjacent to the element which experienced the modeled earthquake, while the energy in distant element decreases. Thus a modeled earthquake has the immediate effect of enhancing earthquake activity in adjacent blocks while suppressing earthquake activity along the remaining portions of the modeled seismic belt. This effect may cause the immediate triggering of large or great earthquakes along the earth's seismic belts.

EARTHQUAKE TRIGGERING AND MODEL

After a modeled earthquake, the force redistribution (Fig. 13) has the effect of increasing stress levels in neighbouring blocks, enhancing their seismic activity, while decreasing the stress levels in the remaining blocks, thus suppressing seismic activity along the remaining portions of the modeled seismic belt. Evidently the blocks surrounding the site of a modeled earthquake have a greater potential of experiencing a modeled earthquake, particularly if the stress in the adjoining blocks is very near the failure stress.

The following discussion details how a modeled earthquake either enhances or suppresses modeled seismic activity. In Figure 14 a modeled earthquake occurs in block 27. Notice that the stress level in blocks 8, 11, 18, and 28 are very close to the threshold stress of 1000 bars. Since block 28 is adjacent to the failed block 27, and is within the region affected by the enhancing effect, a modeled earthquake is immediately induced in block 28 (Fig. 15), even though the stress levels in blocks 8, 11, and 18 are higher than the level in block 28 (Fig. 14). On the other hand, the stress level in block 18 is suppressed by 0.0003 bar (compare Figs. 14 and 15). As blocks 8 and 11 are too far away from block 27, the stress changes are minor.

If, after a modeled earthquake, the stress levels in

those blocks influenced by the enhancing effect are not high enough to immediately exceed the failure level, then a suppressive effect influences earthquake activity in the zones which experienced the enhancing effect, i.e. in the years following a modeled earthquake, there is a small stress drop within the blocks where were enhanced by the earthquake. For example, the earthquake that occurred in block 26 (Fig. 11) did not raise the stress level in the adjacent blocks to the failure stress (1000 bars) (Fig. 12). However in the two year time interval following the modeled earthquake in block 26, the stress level in blocks 25 and 27 are suppressed by 5.42 and 5.49 bars, respectively (compare Figs. 12 and 16). The suppressive effect in blocks 25 and 27 in the two years following a modeled earthquake is illustrated in Figure 17. This result is consistant with Ito's (1980) long-term effect, i.e. the long-term interaction between fault segments is to suppress the next main event in adjacent blocks.

Therefore, in the years immediately following a modeled earthquake the regions experiencing the enhancing effect will experience suppressed seismic activity, provided that the enhancing effect does not immediately (or very shortly) trigger a modeled earthquake. Furthermore, those regions at a distance from the failed region which are slightly suppressed by the modeled earthquake will be slightly

enhanced during the years which followed a modeled earthquake.

Apparently the regions adjacent to an area which experiences an earthquake will have a higher probability of experiencing an earthquake very shortly, but only if the elements are very near the failure stress. The complicated interaction of fault blocks discussed above may very possibly produce the random seismic activity inherent in the circum-Pacific seismic belt.

SEISMIC GAP MODEL

According to seismic gap theory (Mogi, 1968b), great earthquakes tend to fill in seismic belts without significant overlap. This means that during one earthquake cycle most of the fault segments along the seismic belt should fail at least once, and that the remaining unfailed segments are categorized as seismic gaps. Figure 18a diagrams the failed and unfailed fault blocks near the end of the initial random stress distribution pattern. There are eight unfailed blocks or seismic gaps; blocks 12, 17, 19, 24, 25, 31, 35, and 43; each gap represents a potential site for a future earthquake.

In subsequent years these gaps are filled in, one by one in the following order, blocks 25 & 43, 24, 17 & 35, 19, 31, and 12, respectively (Fig. 18b-g). Figure 19 illustrates the stress distribution pattern very near the beginning of the first modeled earthquake cycle. Near the end of the first modeled earthquake cycle, seismic gaps exist in blocks 12, 17, 24, 31, 35, 38, 40, and 43 (Fig. 20a), and these gaps fill up in a different order from that of the initial pattern. Now the order of modeled earthquakes filling the gaps at the end of the first cycle is 24, 38, 40, 35 & 43, 31, 17, and 12 (Fig. 20b-h). Figure 21 is near the beginning of the second cycle. During the second cycle the earthquake return order is 25, 38, 31 & 40, 35 & 43, 17, and 12, and the order of the third cycle is 25 & 31 & 38, 35 & 40 & 43, 17, and 12.

Figures 22 and 23 show the space-time distribution patterns near the beginnings of the third and fourth cycles.

By comparing Figure 18a and 20a, blocks 4, 14, 15, 19, 22, 27, 28, and 39 are enhanced (accelerated), and blocks 11, 13, 17, 30, 32, 34, 35, 36, 42, 43, and 44 are suppressed (deaccelerated). The tendancy of blocks to be accelerated or deaccelerated results from the complex interaction between the truss and fault blocks via the force redistribution function (equation (A12), Appendix A),i.e. the random initial stress (or stiffness) distribution within each fault block causes some fault blocks to be enhanced and other to be suppressed by the model.

Cohen (1977, 1979) has attributed seismic gaps to large variations in the elastic or frictional parameters of a modeled fault zone. However, in the truss-fault block analogy model, seismic gaps are attributed to the complex interaction between fault blocks and the manner in which modeled earthquakes redistribute forces to the elastic truss. The manner in which this stress redistribution occurs depends upon the interactive effect of the elastic stiffness of each fault (foundation) block. In general, stiffer or unfailed fault blocks support more strain energy (or stress) relative to the less stiff or failed blocks, whereas the failed fault blocks support less strain energy and transfer this strain energy to neighboring unfailed blocks.

SEMI-RANDOMNESS IN THE PATTERN OF EARTHQUAKE OCCURRENCE

The truss-fault block model is initially subject to a set of randomly generated stresses and Figure 10 shows the initially random stress distribution pattern. According to equation (B6) of Appendix B, the stress within each block accumulates incrementally. After all of the fault blocks have experienced a modeled earthquake, the next complete earthquake cycle begins (Fig. 19, 21, 22, 23), and the stress distribution patterns are similar to the initial pattern shown in Figure 10. However, due to the enhancing and suppressive effects discussed in the previous sections, the stress distribution patterns are not identical.

If subsequent stress distribution patterns are totally unrelated to the previous pattern, then there will not be any regularities between the first and the second complete earthquake cycles. On the other hand, if the second pattern is exactly identical to the initial pattern, then predicting the future sites of great earthquakes would be trivial exercise. However, both of the cases hypothesized above are contradictory to what is observed in nature. The truss-fault block model of earthquake occurrence lies somewhere between these two extremes, and generates a semi-random space-time earthquake distribution pattern. Figure 24 and 25 represent two earthquake space-time distribution patterns using two different sets of randomly distributed initial stresses. The figures

illustrate two space-time diagrams for the first four modeled earthquake cycles. The sequence of earthquake patterns is similar from cycle to cycle, although the amount of stress within each fault block may change, i.e. the amount of stress either being higher than or lower than the amount of stress in previous or subsequent earthquake cycles.

However, there exists regularities in the semi-random patterns of earthquake occurrence (Fig. 24, 25), which are very similar to the space-time distribution patterns observed in nature. Although the truss-fault block model is very idealized, the model simulates the natural patterns of earthquake occurrence.

RECURRENCE INTERVAL OF THE TRUSS-FAULT BLOCK ANALOGY

The recurrence interval of modeled earthquake is controlled by several factors such as the amount of stress drop and the effective viscosity of the creeping portion of the fault zone. However, in this study the amount of stress drop is held approximately constant and thus the effective viscosity primarily controls recurrence times, as it controls the rate of stress transfer from the lower creeping section to the upper locked section of the modeled fault blocks. Equation (B6) of Appendix B demonstrates that the larger the effective viscosity, the smaller the displacement rate, the lower the rate of stress transfer from the lower creeping section to the upper locked section, and thus the longer the recurrence interval; i.e. the recurrence interval is proportional to the effective viscosity.

Given the conditions listed in Table 1, the recurrence interval for the first modeled earthquake cycle (Fig. 24) ranges from 96 years in block 19 to 130 years in blocks 12, 38, and 44. For the second, third, and fourth cycles, the recurrence interval varies from 76 years in blocks 19 and 24 to 130 years in blocks 20, 32, and 34, from 84 years in block 8 to 140 years in block 26, and from 80 years in block 19 to 148 year in block 20, respectively (Fig. 24). This range of values for the recurrence interval is similar to recurrence intervals for the Nankaido area of Shikoku, Japan (Imamura,

1928), and suggests that, to the first approximation, model parameters were properly chosen.

Table 2 gives the recurrence interval in each block during the different earthquake cycles. The average recurrence interval of the first, second, third, and fourth cycles are 121 years, 116 years, 122 years, and 121 years, respectively. Obviously, during the same cycle, the recurrence interval varies from block to block, and the recurrence interval also varies within the same block from cycle to cycle (Table 2). These differences in the recurrence intervals result from the enhancing and suppressive effects of modeled earthquake activity, as was described previously.

THE VARIATIONS OF STRESS AND STRAIN OF THE TRUSS-FAULT BLOCK ANALOGY

According to equation (B6) of Appendix B, the stress and the strain accumulate incrementally. Initially the model was run at ten year time interval until the first earthquake was generated. After the first earthquake was generated, the time interval is reduced to two years so that a more detailed earthquake-time sequence was produced by the model.

Figure 26 and 27 show the incrementally increasing amounts of stress and strain in block 18. Notice that there are four complete cycles of modeled earthquake occurrence. For block 18, the first, second, third, and fourth cycles have a recurrence interval of 128 years, 122 years, 134 years, and 122 years, respectively (Fig. 26 and 27; Table 2). Except the first cycle, the stress and strain diagrams are interrupted once or, sometimes, twice by the suppressive effect of an earthquake in the adjoining blocks. This suppressive effect causes a small stress drop in block 18, and extends the recurrence interval between modeled earthquakes.

Even though block 18 is accelerated relative to the other blocks, the suppressive effects of the adjoining earthquakes delays the fourth model earthquake in block 18. Notice that the rate of strain accumulation is very small and uniform (approximately 2.22×10^{-14} per second) (Fig. 27). Therefore, the strain accumulation is nearly constant except where the

curve is broken by adjacent earthquakes.

Figure 28 is a summation of the total number of earthquakes generated by the model. Model results demonstrate that the initial stress pattern, and the first, second, and third complete earthquakes cycles end at 176 years, 306 years, 432 years, and 560 years, respectively (Fig. 19, 21, 22, 23, 24). However, on Figure 28, there is no obvious distinction between the different earthquake cycles. Thus, the accumulative earthquake curve (Fig. 28) is approximately a straight line, and the number of great earthquakes generated each year is roughly constant. However, the curve does not repeat the same pattern from cycle to cycle, indicating that the model generates a semi-random earthquake-time sequence.

CONCLUSION

It has been shown that a simple truss-fault block model can produce semi-random patterns of earthquake occurrence without resorting to a variable fault friction parameter (Cohen, 1977, 1979). Thus, the truss-fault block model suggests an alternative procedure for studying the apparent randomness inherent in the earthquake cycle. Model results seem fundamental to the understanding of earthquake mechanisms.

It is the contension of this study that following a very large or great earthquake, a force redistribution function primarily affects the regions adjoining the source areas of an earthquake, enhancing seismic activity in these regions. Therefore, the regions adjacent to an earthquake have higher probability of shortly experiencing another earthquake, provided that these regions are close to the failure stress.

Due to the complex interaction of fault blocks along a seismic belt, seismic gaps exist at the end of each complete earthquake cycle (e.g. Fig. 18a, 20a), and these gaps are filled by earthquakes that need not repeat the same pattern from cycle to cycle (e.g. Fig. 18b-g, 20b-h). It seems reasonable to believe that seismic zones are influenced by the mechanical effects which are incorporated within truss-fault block earthquake model. This earthquake model assumes that there is a force transfer between fault blocks caused by

the effects of an earthquake and a complex interaction between the seismic zone of fault blocks and the oceanic lithosphere. Thus, individual fault blocks and the entire seismic belt may be enhanced and suppressed by the effects of earthquakes, some regions being accelerated relative to adjoining regions, others being deaccelerated. This causes the recurrence interval to vary from region to region, and from one earthquake cycle to another cycle within a particular fault block.

Analysis of Figure 24 demonstrates that several fault blocks tend to be triggered as a pair. This results in a larger earthquake affecting a larger area. Examples of earthquake pairs occur in blocks 8 & 9 & 10, 14 & 15, 21 & 22, 27 & 28, and 32 & 34 (Fig. 24). Figure 24 also shows several cases of earthquake propagation sequences similar to the earthquake propagation patterns along the Chilean coast (Kelleher et al., 1973) and along the Aleutian arcs (Sykes et al., 1980) (Fig. 4). A number of blocks (38, 40, 43) are triggered consecutively in time, at 156 years, 160 years, and 164 years, then at 286 years, 288 years, and 292 years, and then at 410 years, 414 years, and 416 years, respectively. Blocks 41, 37, and 34 & 32 repeat this pattern at 114 years, 116 years, and 118 years, then at 242 years, 244 years, and 246 years, then at 368 years, 370 years, and 372 years, then at 498 years, 500 years, and 502 years, and then

at 626 years, 628 years, and 630 years, respectively. Regardless of the enhancing and suppressive effects, some modeled earthquakes tend to propagate along the modeled earthquake belts, an effect which is consistant with the seismic migration observed in nature (Mogi, 1968a).

The prediction of great earthquakes is a complicated subject, and although the truss-fault block model has the potential of predicting great earthquakes, further studies and possible refinements of the model are required. In particular, the stiffness of the truss is not precisely known. As the stiffness of the truss influences the manner in which the truss deforms, and as the truss is meant to model the oceanic lithosphere, the truss-fault block model may not properly reproduce the force redistribution function in an adequate manner.

The model does, however, predict that fault blocks which have not experienced a model earthquake for many years, have, in general, a greater potential to fail than fault blocks that have recently experienced a model earthquake. Thus, the model supports seismic gap theory. If the amount of stress and stiffness within each fault block were known, then the truss-fault block model may adequately describe future earthquake activity.

On the basis of physical arguments (Ito, 1980; and this study), it is very likely that fault blocks may experience

enhancing or suppressive seismic effects, making the model prediction of great earthquake a very difficult task to say the least. It appears likely that natural seismic belts contain fault blocks that accelerate ahead of other blocks, while some blocks lag their neighbors. Thus, this purely mechanical factor should be taken into consideration when modeling great earthquakes.

APPENDIX A--STATICALLY INDETERMINATE PLANE TRUSS

A truss is composed of consecutive triangles containing j pinned joints and m members. If the external reactions and internal forces are determined by a unique set of equilibrium equations (i.e. the rules of statics), then the truss is statically determinate. If, however, the truss has a greater number of external reactions and/or internal forces than the number of independent equilibrium equations, then the truss is statically indeterminate (Den Hartog, 1949; Parcel & Moorman, 1955; Laursen, 1969). The forces which act on the joints are 1) the internal member forces, 2) the external loading forces, and 3) the external reactions. For each joint in a plane truss there are two equations, $\Sigma F_X=0$, and $\Sigma F_Y=0$. Thus, for the entire truss we can write 2j equilibrium equations. The unknown forces to be determined are the member forces and components of the reaction forces. Therefore, we can make the following general statements concerning the relations between j, the number of joints; and m, the number of members; and r, the number of reaction components.

If (1) $2j < m + r$, then the number of unknowns exceeds the equilibrium equations, and the structure is statically indeterminate.

If (2) $2j = m + r$, then the number of unknowns can be obtained from the 2j equilibrium equations, and the structure is statically determinate.

If (3) $2j > m + r$, then there are an insufficient number of constraints, and the structure is unstable.

The truss employed in the truss-fault block analogy for great earthquakes is statically indeterminate, or condition (1) above. In other words, due to an insufficient number of equilibrium equations, the unknowns in the earthquake model can not be uniquely determined by the equilibrium equations available. However, by utilizing virtual work method of structural analysis and the concept of redundant forces, the problem can be solved according to the procedures described below.

In Figure 29a, $j=13$, $m=23$, and $r=8$, and according to condition (1) (i.e. $2j < m + r$), the truss is statically indeterminate, i.e. there are not enough equilibrium equations to determine the unknown member forces and reaction components. By subtracting $2j$ from $m + r$, we find that five more equations are required to solve the problem. The problem can be solved in the following manner. First, we remove the roller supports from joints 3, 5, 7, 9, and 11, and treat the reactions at these points as redundant forces. After removing the supports, the truss (Fig. 29b) becomes statically determinate and its internal member forces and external reactions can represented by $2j$ equilibrium equations (i.e. condition (2) above). By utilizing the method of joints (Brown, 1967; Laursen, 1969), all the member forces, S', can be determined in terms of the

externally applied loads.

Next, a unit load, D_3, is applied at joint 3 to determine the magnitude of the member forces (u^3's) which result from the applied unit load, D_3 (Fig. 29C). In turn, unit loads D_5, D_7, D_9, and D_{11} are applied at joints 5, 7, 9, and 11 respectively (Fig. 29d, 29e, 29f, 29g). These unit loads determine the member forces, u^5's, u^7's, u^9's, and u^{11}'s, in terms of unit loads D_5, D_7, D_9, and D_{11}, respectively.

Lastly, the deflection at each joint can be determined by the virtual work method (Parcel & Moorman, 1955; Laursen, 1969). The deflection at joint 3 (Δ_3) due to the externally applied loading forces (ΣF_T) is

$$\Delta_3 = \frac{L}{AE} \left(\sum_{i=1}^{m} S_i u_i^3\right)/1, \qquad \text{(A1)}$$

where

Δ_3 = the deflection at joint 3 due to the external loading forces,

L = the length of each truss member,

A = the cross-sectional area of each truss member,

E = the modulus of elasticity of the truss,

S_i = the force in the i^{th} member due to the external loads,

u_i^3 = the force in the i^{th} member due to unit load, D_3, applied at joint 3.

i = member number designation,

m = the total number of members,

1 = the unit load applied at joint 3.

The deflection at joint 3 (Δ_3') due to all unit loads applied at 3, 5, 7, 9, and 11 is

$$\Delta_3' = (\frac{L}{AE}(R_3 \sum_{i=1}^{m}(u_i^3 u_i^3) + R_5 \sum_{i=1}^{m}(u_i^3 u_i^5) + R_7 \sum_{i=1}^{m}(u_i^3 u_i^7) + R_9 \sum_{i=1}^{m}(u_i^3 u_i^9) + R_{11} \sum_{i=1}^{m}(u_i^3 u_i^{11}))/1 \qquad (A2)$$

where

Δ_3' = the deflection at joint 3 due to unit loads D_3, D_5, D_7, D_9, and D_{11},

R_3, R_5, R_7, R_9, R_{11} = the redundant forces at joints 3, 5, 7, 9, and 11, respectively, and

1 = the unit load applied at joint 3.

Since joint 3 does not displace in the vertical direction (Fig. 29a), the deflection, Δ_3, at joint 3 due to external loading forces must equal the deflection, Δ_3', resulting from the unit loads. Thus,

$$\Delta_3 = \Delta_3', \qquad (A3)$$

and from equation (A1) and (A2), we obtain

$$\frac{L}{AE}\left(\sum_{i=1}^{m} S_i u_i^3\right) = \frac{L}{AE}\left(R_3 \sum_{i=1}^{m} (u_i^3 u_i^3) + R_5 \sum_{i=1}^{m} (u_i^3 u_i^5)\right.$$

$$+ R_7 \sum_{i=1}^{m} (u_i^3 u_i^7) + R_9 \sum_{i=1}^{m} (u_i^3 u_i^9)$$

$$\left. + R_{11} \sum_{i=1}^{m} (u_i^3 u_i^{11})\right). \qquad \text{(A4)}$$

Rewriting equation (A4) in terms of a truss stiffness coefficient, K^T, and simplifying the summation symbols, we have

$$\frac{\Sigma S u^3}{K^T} = R_3\left(\frac{\Sigma u^3 u^3}{K^T}\right) + R_5\left(\frac{\Sigma u^3 u^7}{K^T}\right) + R_7\left(\frac{\Sigma u^3 u^7}{K^T}\right)$$

$$+ R_9\left(\frac{\Sigma u^3 u^9}{K^T}\right) + R_{11}\left(\frac{\Sigma u^3 u^{11}}{K^T}\right), \qquad \text{(A5)}$$

where

$K^T = AE/L$, the stiffness coefficient,

$$\Sigma = \sum_{i=1}^{m}$$

Utilizing the same method of analysis as above, we can write four similar equations for supports: 5, 7, 9, and 11. The resulting five equations can be written in matrix form as follows:

$$\begin{bmatrix} \frac{\Sigma u^3 u^3}{K^T} & \frac{\Sigma u^3 u^5}{K^T} & \frac{\Sigma u^3 u^7}{K^T} & \frac{\Sigma u^3 u^9}{K^T} & \frac{\Sigma u^3 u^{11}}{K^T} \\ \frac{\Sigma u^5 u^3}{K^T} & \frac{\Sigma u^5 u^5}{K^T} & \frac{\Sigma u^5 u^7}{K^T} & \frac{\Sigma u^5 u^9}{K^T} & \frac{\Sigma u^5 u^{11}}{K^T} \\ \frac{\Sigma u^7 u^3}{K^T} & \frac{\Sigma u^7 u^5}{K^T} & \frac{\Sigma u^7 u^7}{K^T} & \frac{\Sigma u^7 u^9}{K^T} & \frac{\Sigma u^7 u^{11}}{K^T} \\ \frac{\Sigma u^9 u^3}{K^T} & \frac{\Sigma u^9 u^5}{K^T} & \frac{\Sigma u^9 u^7}{K^T} & \frac{\Sigma u^9 u^9}{K^T} & \frac{\Sigma u^9 u^{11}}{K^T} \\ \frac{\Sigma u^{11} u^3}{K^T} & \frac{\Sigma u^{11} u^5}{K^T} & \frac{\Sigma u^{11} u^7}{K^T} & \frac{\Sigma u^{11} u^9}{K^T} & \frac{\Sigma u^{11} u^{11}}{K^T} \end{bmatrix} X \begin{bmatrix} R_3 \\ R_5 \\ R_7 \\ R_9 \\ R_{11} \end{bmatrix} = \begin{bmatrix} \frac{\Sigma S u^3}{K^T} \\ \frac{\Sigma S u^5}{K^T} \\ \frac{\Sigma S u^7}{K^T} \\ \frac{\Sigma S u^9}{K^T} \\ \frac{\Sigma S u^{11}}{K^T} \end{bmatrix} \quad (A6)$$

The equations are now in the standard matrix form, AX=B. If we invert symmetric matrix A (A^{-1})the unknown column matrix X can be determined,

$$X = (A^{-1})B, \quad (A7)$$

and the redundant forces R_3, R_5, R_7, R_9, and R_{11} can be computed.

Thus the above technique can be used to solve the problem of a statically indeterminate truss, utilizing the concept of externally applied redundant forces. However, in the truss-fault block analogy of earthquake occurrence, the supports are replaced by foundation (i.e. fault) blocks (Fig. 30a). Each foundation block is a three-dimensional body that deforms as a standard linear solid element (Fig. 30b). Equation (A3) is no longer adequate to solve the indeterminate problem since

all of the supports are now represented by visco-elastic foundations which deform in the vertical direction. The net displacement at each joint is now dependent upon the foundation stiffness coefficient, K^F.

$$\Delta_n - \Delta_n' = \delta_n,$$

where

Δ_n = the maximum deflection of the supported joint along the bottom chords of the truss,

Δ_n' = the elastic deformation of the foundation block,

δ_n = the net displacement of each foundation block,

n = the number of the supported joints along the bottom chords of the truss which equals the number of foundation blocks.

The net displacement at each joint is actually the displacement within each foundation block. Therefore, the net elastic (i.e. time-dependent) deformation of the support can be defined by the following linear relationship (see Appendix C)

$$\delta_n = \frac{-R_n}{K_n^F}, \qquad \text{(A9)}$$

where

R_n = the redundant force at joint n, and $-R_n$ is the force stored within foundation block n,

K_n^F = the linear time-dependent stiffness coefficient of the foundation block n.

By using the correspondance principle, viscoelastic deformations are incorporated into this analysis following procedures described in Appendix B.

Substituting equation (A9) into (A8) and writing in matrix form, yields

$$\begin{bmatrix} \frac{\Sigma u^3 u^3}{K^T} & \frac{\Sigma u^3 u^5}{K^T} & \frac{\Sigma u^3 u^7}{K^T} & \frac{\Sigma u^3 u^9}{K^T} & \frac{\Sigma u^3 u^{11}}{K^T} \\ \frac{\Sigma u^5 u^3}{K^T} & \frac{\Sigma u^5 u^5}{K^T} & \frac{\Sigma u^5 u^7}{K^T} & \frac{\Sigma u^5 u^9}{K^T} & \frac{\Sigma u^5 u^{11}}{K^T} \\ \frac{\Sigma u^7 u^3}{K^T} & \frac{\Sigma u^7 u^5}{K^T} & \frac{\Sigma u^7 u^7}{K^T} & \frac{\Sigma u^7 u^9}{K^T} & \frac{\Sigma u^7 u^{11}}{K^T} \\ \frac{\Sigma u^9 u^3}{K^T} & \frac{\Sigma u^9 u^5}{K^T} & \frac{\Sigma u^9 u^7}{K^T} & \frac{\Sigma u^9 u^9}{K^T} & \frac{\Sigma u^9 u^{11}}{K^T} \\ \frac{\Sigma u^{11} u^3}{K^T} & \frac{\Sigma u^{11} u^5}{K^T} & \frac{\Sigma u^{11} u^7}{K^T} & \frac{\Sigma u^{11} u^9}{K^T} & \frac{\Sigma u^{11} u^{11}}{K^T} \end{bmatrix} \times \begin{bmatrix} R_3 \\ R_5 \\ R_7 \\ R_9 \\ R_{11} \end{bmatrix} = \begin{bmatrix} \frac{\Sigma Su^3}{K^T} - \frac{R_3}{K_3^F} \\ \frac{\Sigma Su^5}{K^T} - \frac{R_5}{K_5^F} \\ \frac{\Sigma Su^7}{K^T} - \frac{R_7}{K_7^F} \\ \frac{\Sigma Su^9}{K^T} - \frac{R_9}{K_9^F} \\ \frac{\Sigma Su^{11}}{K^T} \frac{R_{11}}{K_{11}^F} \end{bmatrix} \quad \text{(A10)}$$

and rearranging equation (A10), we have

$$\begin{bmatrix} (\frac{\Sigma u^3 u^3}{K^T} + \frac{1}{K_3^F}) & \frac{\Sigma u^3 u^5}{K^T} & \frac{\Sigma u^3 u^7}{K^T} & \frac{\Sigma u^3 u^9}{K^T} & \frac{\Sigma u^3 u^{11}}{K^T} \\ \frac{\Sigma u^5 u^3}{K^T} & (\frac{\Sigma u^5 u^5}{K^T} + \frac{1}{K_5^F}) & \frac{\Sigma u^5 u^7}{K^T} & \frac{\Sigma u^5 u^9}{K^T} & \frac{\Sigma u^5 u^{11}}{K^T} \\ \frac{\Sigma u^7 u^3}{K^T} & \frac{\Sigma u^7 u^5}{K^T} & (\frac{\Sigma u^7 u^7}{K^T} + \frac{1}{K_7^F}) & \frac{\Sigma u^7 u^9}{K^T} & \frac{\Sigma u^7 u^{11}}{K^T} \\ \frac{\Sigma u^9 u^3}{K^T} & \frac{\Sigma u^9 u^5}{K^T} & \frac{\Sigma u^9 u^7}{K^T} & (\frac{\Sigma u^9 u^9}{K^T} + \frac{1}{K_9^F}) & \frac{\Sigma u^9 u^{11}}{K^T} \\ \frac{\Sigma u^{11} u^3}{K^T} & \frac{\Sigma u^{11} u^5}{K^T} & \frac{\Sigma u^{11} u^7}{K^T} & \frac{\Sigma u^{11} u^9}{K^T} & (\frac{\Sigma u^{11} u^{11}}{K^T} + \frac{1}{K_{11}^F}) \end{bmatrix} \times \begin{bmatrix} R_3 \\ R_5 \\ R_7 \\ R_9 \\ R_{11} \end{bmatrix} = \begin{bmatrix} \frac{\Sigma Su^3}{K^T} \\ \frac{\Sigma Su^5}{K^T} \\ \frac{\Sigma Su^7}{K^T} \\ \frac{\Sigma Su^9}{K^T} \\ \frac{\Sigma Su^{11}}{K^T} \end{bmatrix} \quad \text{(A11)}$$

The redundant forces R_3, R_5, R_7, R_9, and R_{11} can now be determined from equation (A11).

The problem of a statically indeterminate plane truss can be solved for any number of supports. Equation (A11) can be generalized for n foundation blocks as follows.

$$\begin{bmatrix} \left(\frac{\Sigma u^3 u^3}{K^T} + \frac{1}{K_3^F}\right) & \frac{\Sigma u^3 u^5}{K^T} & \cdots & \frac{\Sigma u^3 u^{n-1}}{K^T} & \frac{\Sigma u^3 u^n}{K^T} \\ \frac{\Sigma u^5 u^3}{K^T} & \left(\frac{\Sigma u^5 u^5}{K^T} + \frac{1}{K_5^F}\right) & \cdots & & \frac{\Sigma u^5 u^n}{K^T} \\ \cdots & \cdots & \cdots & \cdots & \cdots \\ \cdots & \cdots & \cdots & \cdots & \cdots \\ \frac{\Sigma u^n u^3}{K^T} & \cdots & \cdots & \left(\frac{\Sigma u^n u^n}{K^T} + \frac{1}{K_n^F}\right) & \end{bmatrix} \times \begin{bmatrix} R_1 \\ R_2 \\ \cdot \\ \cdot \\ \cdot \\ \cdot \\ R_n \end{bmatrix} = \begin{bmatrix} \frac{\Sigma S u^3}{K^T} \\ \frac{\Sigma S u^5}{K^T} \\ \cdot \\ \cdot \\ \cdot \\ \cdot \\ \frac{\Sigma S u^{11}}{K^T} \end{bmatrix} \quad \text{(A12)}$$

The model used to study earthquake occurrence contains 51 foundation blocks (n=49). Due to the size of the matrix (49 x 49), matrix inversion is accomplished on the Temple University CDC CYBER 174 computer using the GELS subroutine of matrix inversion which is available in the Temple University Program Library.

APPENDIX B--TIME-DEPENDENT BEHAVIOR OF TRUSS-FAULT BLOCK ANALOGY

Mogi (1968a) has noticed that the aftershock areas of great earthquakes cover the circum-Pacific seismic belt without significant overlap. This strongly suggests that the seismic belt is segmented into a series of independently acting fault segments (Davies et al., 1981), i.e. "fault blocks." Therefore, the fault zone of the modeled seismic belt is partitioned into a series of fault blocks (Fig. 6), each block being a potential site for a large earthquake. The lateral edge of each fault block is taken to represent the marginal region between the aftershock zones of great earthquake (Mogi, 1968b), i.e. a structural discontinuity separates each adjoining fault block.

In this study the fault blocks are linked to an elastic truss (Fig. 7), and each fault block is modeled as a standard linear solid element sandwiched between the elastic truss and a rigid foundation (Fig. 8). In Figure 7 the total force (ΣF_T) acting on the truss which represents the oceanic lithosphere, is apportioned to each fault block depending upon the properties of each block (i.e. the stiffness of each block). The sum of the apportioned forces (F_n) that are applied to each fault block must be equal to the sum of the loading forces (F_T) (Fig. 7, 8). Therefore, the force balance equation for the truss-fault block analogue model is

$$\Sigma F_T = \Sigma F_n, \tag{B1}$$

where

F_T = the loading force applied along the left hand edge of the truss,

F_n = the nodal force applied to each block along the right hand edge of the truss. From now on F_n will be written simply F, i.e. $F_n = F$.

Since each fault block is composed of an upper elastic section and a lower creeping or viscous section, the force balance equation for each fault block is

$$F = F_G + F_\mu \ , \qquad \text{(B2)}$$

where

$F = F_n$, the nodal force,

F_G= the force acting upon the upper locked section of the fault block, and

F_μ= the force acting upon the lower creeping section of the fault block.

This means that the truss nodal force (F) is apportioned between the locked and the creeping sections of each fault block.

The differential equation governing the behavior of each fault block (or its analogue, a standard linear solid) is

$$F = (\mu A_u + \mu G_2 A_G / G_1)\dot{\gamma} + G_2 A_G \gamma, \qquad \text{(B3)}$$

(For derivation see procedures outlined in Ramsay, 1967 and Bischke, 1981)

where

μ = the effective viscosity in the lower creeping section of the fault block,

G_1, G_2 = the shear modulus in the (G_1) and creeping (G_2) sections of the fault block, $G_1=G_2=G^s$,

A_μ = the area of the creeping section of the fault block,

A_G = the area of the locked section of the fault block,

γ = the strain within the fault block.

(See Figures 8 and 9)

The solution to equation (B3) has been derived by Bischke (1981), and is

$$\gamma_t = (F_t/A_G G^s)(1 - \exp(-t/R)) + \gamma_0 \exp(-t/R), \qquad \text{(B4)}$$

where

F_t = the time-dependent nodal force,

γ_t = the time-dependent strain,

$$R = (\mu/G^s)(A_\mu/A_G + 1) \qquad \text{(B5)}$$

= the retardation time of the fault block,

γ_0 = the initial strain in the fault block at t=0, and

t = the time designition.

Thus in equation (B4), the total strain (γ_t) and the nodal force (F_t) are functions of time (t). In this study, modeled earthquakes are generated by imposing an initial strain to the modeled fault block. As the initial strain or the force drop varies according to time in each fault block, this problem has

to be solved incrementally on the computer. For small time intervals (Δt), equation (B4) is rewritten as

$$\gamma_{t+\Delta t} = (F_t/A_G G^S)(1 - \exp(-\Delta t/R)) + \gamma_t \exp(-\Delta t/R), \quad \text{(B6)}$$

where

$\gamma_{t+\Delta t}$ = total shear strain at the end of each time increment, provided that F_t and γ_t are constant throughout the time interval (Δt) and change abruptly at the end of the time interval (Zienkiewicz, 1968).

Rewriting equation (B6) in terms of displacement, X, and stiffness, K^F, we have

$$X_{t+\Delta t} = (F_t/K^F)(1 - \exp(-\Delta t/R)) + X_t \exp(-\Delta t/R), \quad \text{(B7)}$$

or

$$\begin{matrix}\text{Final} \\ \text{Displacement}\end{matrix} = \begin{matrix}\text{Incremental} \\ \text{Displacement}\end{matrix} + \begin{matrix}\text{Initial} \\ \text{Displacement},\end{matrix} \quad \text{(B8)}$$

where

$K^F = A_G G^S/L$, the foundation stiffness of the fault block,

G^S = the shear modulus of the fault block, and

L = the length of the fault block (Fig. 7),

with the understanding that F_t is constant during the time interval and changes abruptly at the end of each time interval (Zienkiewicz, 1968). In equation (B7) the first, second, and third terms represent the final displacement, the incremental displacement, and the initial displacement within each fault block, respectively. Thus the incremental displacement is

equal to the final displacement minus the initial displacement, i.e.

$$(F_t/K^F)(1-\text{expt}(-\Delta t/R)) = X_{t+\Delta t} - X_t\exp(-\Delta t/R), \quad \text{(B9)}$$

or

$$(F_t/K^F)(1-\exp(-\Delta t/R)) = \Delta X_v, \quad \text{(B10)}$$

where

ΔX_v = the incremental displacement which represents a change in displacements.

Multiplying equation (B7) by the stiffness, K^F, yields

$$KX_{t+\Delta t} = F_t(1-\exp(-\Delta t/R)) + KX_t\exp(-\Delta t/R). \quad \text{(B11)}$$

As stiffness times displacement is the total nodal force, equation (B11) can be written in terms of forces, or

$$F_{t+\Delta t} = \Delta F_t + F_t, \quad \text{(B12)}$$

or

$$\begin{matrix}\text{Total}\\ \text{Force}\end{matrix} = \begin{matrix}\text{Incremental}\\ \text{Force}\end{matrix} + \begin{matrix}\text{Initial}\\ \text{Force}\end{matrix}, \quad \text{(B13)}$$

where

$$F_{t+\Delta t} = KX_{t+\Delta t}, \quad \text{(B14)}$$

= the total nodal force acting upon the fault block,

$$\Delta F_t = F_t(1 - \exp(-\Delta t/R)), \quad \text{(B15)}$$

= the force change within each fault block after a time interval, Δt,

$$F_t = KX_t \exp(-\Delta t/R), \tag{B16}$$

= the initial force acting upon the fault block.

Equations (B8) and (B13) indicate the incremental character of the truss-fault block analogy for great earthquakes, and owing to this property, the analysis is most readily solved on the computer.

For an elastic block subject to an initial displacement or an incremental displacement (Padlop et al., 1968), we obtain

$$F_t = K_e(\Delta X_e), \tag{B17}$$

where

K_e = the time-independent stiffness of the elastic block,

ΔX_e = an initial or incremental displacement within the elastic block.

By rearranging equation (B7), we derive

$$F_t=(K^F/(1-\exp(-\Delta t/R))(X_{t+\Delta t} - X_t(\exp(-\Delta t/R)), \tag{B18}$$

or

$$F_t = (K^F/(1-\exp(-\Delta t/R))(\Delta X_v) \tag{B19}$$

where

$$\Delta X_v = X_{t+\Delta t} - X_t \exp(-\Delta t/R), \tag{B20}$$

= the incremental displacement change within the viscoelastic block over a given time interval (see equation (B10)).

In order to model viscoelastic behavior within each fault block, the correspondence principle (Biot, 1965), is employed to study the time-dependent deformations in the modeled fault zone. This principle of continuum mechanics states that the behavior of any linear viscoelastic substance is governed by equations which may be derived from the theory of elasticity. Once the elastic equations are derived, viscoelastic behavior is introduced into the elastic equations by simply substituting the proper viscoelastic operator for the elastic coefficients (Biot, 1965).

The viscoelastic operator which defines the time-dependent deformation of each fault block can be obtained by comparing equation (B17), which represents the time-independent (incremental) elastic equation, to equation (B19), which represents the time-dependent (incremental) viscoelastic equation, since $\Delta X_v = \Delta X_e$ for any given time, and as the correspondence principle requires that the elastic coefficient be replaced by the viscoelastic operator, therefore, we have

$$B = K^F/(1-\exp(-\Delta t/R)) = K_e \qquad \text{(B21)}$$

where

B = the time-dependent viscoelastic operator.

Thus, we can introduce viscoelastic behavior into elastic equation (B17) by simply replacing K_e by the corresponding viscoelastic operator, B. Therefore,

$$F_t = B(\Delta X_e) \tag{B22}$$

or

$$F_t = (K^F/(1-\exp(-\Delta t/R))(\Delta X_e). \tag{B23}$$

Thus, equation (B23) introduces viscoelastic displacements into the foundation blocks that support the truss.

But $\Delta X_e = \Delta X_v = X_{t+\Delta t} - X_t \exp(-\Delta t/R)$, so equation (B23) becomes

$$F_t = (K^F/(1-\exp(-\Delta t/R))(X_{t+\Delta t} - X_t \exp(-\Delta t/R)). \tag{B24}$$

Rewriting equation (B24) in terms of strain, we have

$$\gamma_{t+\Delta t} = (F_t/A_G G^S)(1-\exp(-\Delta t/R)) + \gamma_t \exp(-\Delta t/R). \tag{B25}$$

Obviously equation (B25) is identical to equation (B6) and thus both equations are able to describe the viscoelastic behavior of each fault block. According to equation (B21), the viscoelastic operator, B, is solved incrementally, which is consistant with the incremental approach developed above.

At the end of each time interval, the time-dependent viscoelastic operator is recalculated using equation (B21). Thus, it is the time-dependent property of the viscoelastic

operator which produces time-dependent foundation stiffness changes and the time-dependent deformations in the model. After the time-dependent stiffness, $\mathbb{K}^F$, is determined for each fault block using equation (B21) the loading force acting upon the fault blocks is recalculated using equation (A12) of Appendix A. This permits a determination of the shear strain (see equation (B6)) within each block for the next time interval.

In above calculations, $\gamma_{t+\Delta t}$ and $F_{t+\Delta t}$ are derived for each time increment. By substituting the total strain ($\gamma_{t+\Delta t}$) and the total loading force ($F_{t+\Delta t}$) for the last time increment into equation (B6), the total strain ($\gamma_{t+\Delta t}$) for the next time increment is determined.

Figure 31 is a flow chart illustrating the steps taken to determine how the total strain ($\gamma_{t+\Delta t}$) is solved incrementally on the computer.

APPENDIX C -- HOOKE'S LAW

Consider a spring attached to a wall (Fig.32a). Let the origin, X=0, coincide with the endpoint of the spring in its unstretch state. If we stretch the spring so that its endpoint moves to a position X (Fig. 32b), the spring will exert an opposing force to its displacement X.

$$F = -KX, \qquad (C1)$$

where

F = the internal force exerted by and stored within the spring. This internal force is always directed toward the origin of the spring (Fig. 32b, 32c).

K = the spring stiffness coefficient.

Equation (C1) is known as Hooke's Law (Halliday, 1970). The direction of the stored force is always opposite to that of the displacement. When the spring is stretched, X>0, and the internal force is negative; when the spring is compressed, X<0, and the internal force is positive.

To stretch a spring we must exert a force F' equal to and opposite in direction to the force F exerted by the spring.

$$F = -F', \qquad (C2)$$

where

F' = the applied external force.

The force determined by subroutine GELS is the applied

external force F'. The force stored in the spring is the internal force F exerted by the standard linear solid upon the truss structure (Fig. 32c). Force F opposes force F', therefore, in equation (A9) and (A10) of Appendix A, $-R_n/K_n^F$ is substituted in the right hand side of the equation to provide consistant deformation.

BIBLIOGRAPHY

Anderson, D.L., Accelerated plate tectinics, Science, 187, 1077-1079, 1975.

Biot, M.A., Mechanics of incremental deformation, John Wiley & Sons, Inc., New York, 359, 1965.

Bischke, R.E., A model of convergent plate margins based on the recent tectonics of Shikokou, Japan, J. Geophys. Res., 79, 4845-4857, 1974.

Bischke, R.E., Secular horizontal displacements: a method for predicting great earthquakes and for assessing earthquake risk, J. Geophys. Res., 81, 2511-2516, 1976.

Bischke, R.E., A simple viscoelastic model of inter-plate and intra-plate earthquakes, in review, 1981.

Brown, E.H., Structural analysis, John Wiley & Sons, Inc., New York, 14-18, 1967.

Burridge, R. and L. Knopoff, Model and theoretical seismicity, Bull. Seismol. Soc. Amer., 57, 341-371, 1967

Capple, W.M. and T.E. Tullis, Evaluation of the forces that drive the plates, J. Geophy. Res., 82, 1967-1984, 1977.

Carr, M.J., R.E. Stoiber, and C.L. Drake, Discontinuities in the deep seismic zones under the Japenese arcs, Geol. Soc. Amer. Bull., 84, 2917-2930, 1973.

Carr, M.J., R.E. Stoiber, and C.L. Drake, The segmented nature of some continental margins, Geology of continental margin, edited by C.A. Burk and C.L. Drake, Springer-

Verlag, Hamsurg, 1974.

Carr, M.J. and R.E. Stoiber, Geologic setting of some destructive earthquakes in central America, Geol. Soc. Amer. Bull., 88, 151-156, 1977.

Cohen, S.C., Computer simulation of earthquakes, J. Geophys. Res., 82, 3781-3796, 1977.

Cohen, S.C., Numerical and laboratory simulation of fault motion and earthquake occurrence, Rev. Geophys. Space Phys., 17, 61-72, 1979.

Davies, J., L. Sykes, L. House, and K. Jacob, Shumagin Seismic Gap, Alaska Peninsula: history of great tectonic setting, and evidence for high seismic potential, J. Geophys. Res., 86, 1981.

Den Hartog, J.P., Strength of materials, Dover Publications, Inc., New York, 11, 1949.

Fedotov, S.A., Regularities of the distribution of strong earthquakes of Kamchatka, the Kurile Islands, and northeastern Japan, Tr. Inst. Fis. Zemli. Akad. Nauk SSSR, 36, 66-93, 1965.

Findley, W.N., J.S. Lai, and K. Onaran, Creep and relaxation of non-linear viscoelastic materials, North-Holland Publishing Co., Chapter 5, 1976.

Flügge, W., Viscoelasticity, 2nd ed. Springer-Verlag, New York, 17-20, 47-48, 1975.

Forsyth, D., and S. Uyeda, On the relative importance of the driving forces of plate motion, Geophys. J.R. Astr. Soc., 43, 163-200, 1975.

Gennaro, J.J., Computer methods in solid mechanics, The Macmillan Co., New York, 1975.

Holliday, D. and R. Resnick, Fundamentals of Physics, John Wiley and Sons, Inc., New York, 99-101, 1973.

Imamura, A. On the seismic activity of Central Japan, Jap. Jour. Astro. and Geophys., 6, 119-137, 1928.

Ito, K., Periodicity and chaos in great earthquake occurrence, J. Geophys. Res., 85, 1399-1408, 1980.

Jordan, J.N., J.F. Lauder, and R.A. Black, Aftershocks of the 4 February 1965 Rat Island earthquake, Science, 148, 1323-1325, 1965.

Kanamori, H., The energy release in great earthquakes, J. Geophys. Res., 82, 2981-2987, 1977.

Kasahara, K., Aseismic faulting following the 1973 Nemuro-Oki earthquake, Hokkaido, Japan (a possibility). Pure Appl. Geophys., 113, 127-139, 1975.

Kelleher, J., L. Sykes, J. Oliver, Possible criteria for predicting earthquake locations and their application to major plate boundaries of the Pacific and the Caribbean, J. Geophys. Res., 78, 2547-2585, 1973.

Knopoff, L., A stochastic model for the occurrence of main sequence earthquakes, Rev. Geophys. Space Phys., 9, 175-188, 1971.

Laursen, H., Structural analysis, McGraw-Hill Book Co., New York, 51, 59, and 187, 1969.

McCann, W.R., O.J. Perez, and L.R. Sykes, Yakataga gap, Alaska: seismic History and earthquake potential, Science, 207, 1309-1314, 1980.

Mogi, K., Migration of seismic activity, Bull. Earthq. Res. Inst., 46, 53-74, 1968a.

Mogi, K., Sequential occurrences of recent great earthquakes, J. Phys. Earth, 16, 30-36, 1968b.

Mogi, K., Some features of recent seismic activity in and near Japan, 2, activity before and after great earthquakes, Bull. Earthq. Res. Inst. Tokyo Univ., 47,395-417, 1969.

Padlop, J., R.D. Huff,and G.F. Holloway, The unelastic behavior of structure subjected to cyclic thermal and mechanical stressing conditions, Wright Air Development Div., TR60-271, 1968.

Parcel, J.I. and R.B.B. Moorman, Analysis of statically indeterminate structures, John Wiley & Sons, Inc., New York, 1, and 17, 1955.

Ramsay, J.G., Folding and fracturing of rock, McGraw-Hill, New York, 277-279, 1967.

Savage, J.C. and R.O. Burford, Accumulation of tectonic strain in California, Bull. Seismol. Soc. Amer., 60, 1877-1896, 1970.

Savage, J.C. and W.H. Prescott, Asthenosphere readjustment and the earthquake cycle, J. Geophys. Res., 83, 3369-3376, 1978.

Scholz, C.H. and T. Kato, The behavior of a convergent plate boundary crustal deformation in the south Kanto District, Japan, J. Geophys. Res., 83, 783-797, 1978.

Shimazaki, K. and T. Nakata, Time-predictable recurrence model for large earthquakes, Geophys. Res. Lett., 7, 279-282, 1980.

Sykes, L.R., Aftershock zones of great earthquakes, seismicity gap, and earthquake prediction for Alaska and the Aleutions, J. Geophys. Res., 76, 8021-8041, 1971.

Sykes, L.R., Seismicity as a guide to global tectonics and earthquake prediction, Tectonophysics, 13, 393-414, 1972.

Sykes, L.R., J.B. Kisslinger, L. House, J.N. Davies, and K.H. Jocob, Rupture zones of great earthquakes in the Alaska-Aleutian Arc, 1784 to 1980, Science, 210, 1343-1345, 1980.

Thatcher, W., Strain accumulation and release mechanism of the 1906 San Francisco Earthquake, J. Geophys. Res., 80, 4862-4872, 1975a.

Thatcher, W., Strain accumulation on the northern San Andreas fault zone since 1906, J. Geophys. Res., 80,4873-4880, 1975b.

Turcotte, D.L. and D.A. Spence, An analysis of strain accumulation on a strike slip fault, J. Geophys. Res., 79, 4407-4412, 1974.

Turcotte, D.L., R.T. Clancy, D.A. Spence, and F.H. Kulhawy, Mechanisms for the accumulation and release of stress on the San Andreas fault, J. Geophys. Res., 84, 2273-2282, 1979.

Zienkiewicz, O.C., M. Watson, and I.P. King, A numerical method of viscoelastic stress analysis, Int. J. Mech. Sci., 10, 807-827, 1968.

Table 1. Parameters used in the truss-fault block analogue model.

	Layer thickness (Km)	Shear modulus (Bars)	Effective viscosity, μ
Oceanic Lithosphere	100.0	4.0×10^5	-
Locked section	50.0	4.0×10^5	-
Creeping section	50.0	4.0×10^5	2.0×10^{22}

	Length (Km)	Width (Km)	Depth (Km)	Stiffness* (Dyne/cm)
Truss member	300.0	-	100.0	5.0×10^{18}
Fault block	300.0	100.0	100.0	

Loading stress (F_T) = 950.0 Bars

Failure stress = 1000.0 Bars

Stress drop = 30.0 $\pm$ 1.0 Bars

* Truss stiffness is defined as $K^T = AG/L$.

TABLE 2. RECURRENCE INTERVAL OF EACH FAULT BLOCK IN DIFFERENT MODELED EARTHQUAKE CYCLES.

BLOCK NUMBER	4	5	6	7	8	9	10	11	12	13	14	15
FIRST CYCLE	112	126	128	126	104	104	104	128	130	128	112	112
SECOND CYCLE	88	124	124	122	82	82	124	126	126	120	106	106
THIRD CYCLE	94	128	128	126	84	110	128	132	128	128	110	110
FOURTH CYCLE	90	132	128	132	86	104	120	128	108	126	112	112

BLOCK NUMBER	16	17	18	19	20	21	22	23	24	25	26	27
FIRST CYCLE	126	120	128	96	124	102	102	122	116	116	128	108
SECOND CYCLE	124	124	122	76	130	122	100	120	76	126	124	118
THIRD CYCLE	128	130	134	100	100	130	110	126	98	132	140	96
FOURTH CYCLE	126	128	122	80	148	110	116	132	102	124	134	120

BLOCK NUMBER	28	29	30	31	32	33	34	35	36	37	38	39
FIRST CYCLE	108	124	128	126	124	128	124	126	128	128	130	128
SECOND CYCLE	88	88	116	120	130	124	130	124	126	126	124	126
THIRD CYCLE	126	96	126	124	130	130	130	126	132	130	128	130
FOURTH CYCLE	94	124	124	124	128	128	128	126	128	128	128	128

BLOCK NUMBER	40	41	42	43	44	45	46
FIRST CYCLE	128	128	128	128	130	128	110
SECOND CYCLE	126	126	126	124	126	122	118
THIRD CYCLE	128	130	132	126	132	126	116
FOURTH CYCLE	128	128	130	126	128	126	110

THE AVERAGE RECURRENCE INTERVAL OF THE FIRST CYCLE IS 121 YEARS.

THE AVERAGE RECURRENCE INTERVAL OF THE SECOND CYCLE IS 116 YEARS.

THE AVERAGE RECURRENCE INTERVAL OF THE THIRD CYCLE IS 122 YEARS.

THE AVERAGE RECURRENCE INTERVAL OF THE FOURTH CYCLE IS 121 YEARS.

FIGURE CAPTIONS

Figure 1. Aftershock areas of great earthquakes along the Japan-Kurile-Kamchatka arc. The 1968 (M_W=8.2) earthquake near south-eastern Hokkaido, the 1969 (M_W=8.2) earthquake near Kurile Islands, and the 1971 (M=7.8) earthquake near northern Kamchatka are included in this figure. After Kelleher et al. (1973).

Figure 2. Large and great earthquakes in the Aleutians and the northeast Pacific. Yakataga gap is located in the area near 59°N and 142°S. The last earthquake that occurred in this area was in 1899. Various symbols denote individual aftershock sequences as follows. Corss, 1925, 1949, 1957, and 1964; squares, 1938, 1958, and 1965; open triangles, 1946, 1960, 1964, and 1970; solid triangles, 1940, 1948, and 1957; solid circles, others. Largest symbols denote most precise locations. Depth contours in fathoms. In space-time diagram below, lengths of aftershock zones, magnitudes of main shocks, and locations of main shocks are indicated. Aftershock locations for 1970 Queen Charlotte Islands (QCI) sequence are those of U.S. Coast and Geodetic Survey. FZ indicates latitudes of three fracture zones that offset magnetic anomaly pattern south of Aleutian trench. Taken from Sykes (1971).

Figure 3. The Yakataga Seismic gap. The eastern part of Yakataga seismic gap was filled in by the M_S=7.7 Saint Elias earthquake of 1979. The remaining portions of the gap have the potential of experiencing a large or great earthquake in the very near future. After Sykes et al. (1980).

Figure 4. Fault blocks in the Aleution arc. The seismic belt along the Aleutian trench is composed of a series of fault blocks which are separated by transverse structures. The space-time diagram below shows the length of each fault segment. For symbols refer to Figure 2. After Sykes et al. (1980).

Figure 5. Fault blocks in the Central American arc. Stippled bars indicate transverse structureal features; solid triangles are historically active volcanoes. After Carr and Stoiber (1977).

Figure 6. Convergent plate margin. The seismic zone is modeled as a series of fault blocks sandwiched between the elastic oceanic lithosphere (on the right), and the continental lithosphere (on the left). A fault block is composed of an upper locked (elastic) section and a lower creeping (viscous) section, denoted by A_G and A_μ respectively.

Figure 7. Truss-fault block analogue. The oceanic lithosphere is modeled utilizing a truss which is subject to elastic deformations, the seismic zone is modeled by a series of fault blocks which behave in both an elastic and viscous manner, and the rigid foundation represents the undeformed continental lithosphere. The modeled trench occurs at the contact between oceanic lithosphere and seismic zone. The geometry of the fault block is 300 Km long, 100 Km wide, and 100 Km deep. The loading forces (F_T) are applied to the left edge of the truss and distribute to each fault block as nodal force F_n.

Figure 8. The truss-fault block and the standard linear solid elements. Each fault block is modeled utilizing a standard linear solid rheology, i.e. each element behaves viscoelastically. The nodal force (F_n) acts upon each element.

Figure 9. Standard linear solid element. A standard linear solid element is composed of an upper locked section which is subject to stress drop (i.e. earthquakes), and a lower viscous section which continuously creeps.

Figure 10. The distribution pattern of randomly generated stresses in year 0.0. The first column represents the

number of each fault block, and the second column is the value of the stress in each block. The X-direction gives the level of the stress in each block, and the Y-direction gives the number (location) of the corresponding block. The first three and the last three blocks are omitted as they were subject to end effects.

Figure 11. Stress distribution pattern in year 78. The stress level in block 26 has reached the failure stress (1000 bars). The number on the plot is the number of modeled earthquakes within each block, e.g. block 26 just experienced its first earthquake, while block 30 (*) has not yet experienced any modeled earthquakes.

Figure 12. Stress distribution pattern in year 78 following a modeled earthquake. An earthquake occurred in block 26 after imposing a 30.2 bar stress drop in element 26.

Figure 13. The net effect of the stress redistribution after modeled earthquake in fault block 26. Notice that adjoining blocks 24, 25, 27, and 28 are primarily affected.

Figure 14. Stress distribution pattern in year 128. A modeled earthquake occurred in block 27. Notice that

the stress levels in blocks 8, 11, 18 and 28 are very close to failure stress (1000 bars).

Figure 15. Stress distribution pattern in year 128 following a modeled earthquake. A modeled earthquake is immediately induced by the earthquake in block 28, whereas block 18 is suppressed.

Figure 16. Stress distribution pattern in year 80. During the two years following an earthquake in block 26 (see Fig. 12), a suppressive effect occurs in blocks 25 and 27.

Figure 17. The net effect of stress redistribution in the two years following a modeled earthquake in block 26. Blocks 25 and 27 are now suppressed, although they were enhanced immediately following an earthquake (see Fig. 13).

Figure 18a-18g. Stress distribution patterns in years 162, 164, 164, 166, 166, 168, and 176, respectively.

a. Eight seismic gaps exist in blocks 12, 17, 19, 24, 25, 31, 35, and 43.
b. Blocks 25 and 43 are filled.
c. Block 24 is filled.
d. Blocks 17 and 35 are filled.

e. Block 19 is filled.

f. Block 31 is filled.

g. Block 12 is filled.

Figure 19. Stress distribution patterns in year 176. This diagram is at the end of the first complete earthquake cycle (i.e. all of the fault blocks have experienced at least one earthquake in this cycle).

Figure 20a-20h. Stress distribution patterns in years 280, 280, 286, 288, 292, 294, 296 and 306, respectively.

a. Eight seismic gaps exist in blocks 12, 17, 24, 31, 35, 38, 40, and 43.

b. Block 24 is filled.

c. Block 38 is filled.

d. Block 40 is filled.

e. Blocks 35 and 43 are filled.

f. Block 31 is filled.

g. Block 17 is filled.

h. Block 12 is filled.

Figure 21. Stress distribution pattern in year 306. This figure shows the stresses at the end of the second complete earthquake cycle. Notice that two blocks (blocks 22 and 46) have accelerated ahead of the others, and had experienced their third earthquakes.

Figure 22. Stress distribution pattern in year 432. Diagram shows the end of the third complete earthquake cycle. Notice that eight blocks (blocks 4, 8, 9, 14, 15, 22, 29, and 46) have had their fourth earthquakes.

Figure 23. Stress distribution pattern in year 560. It shows the end of the fourth complete earthquake cycle. Twelve blocks (4, 8, 9, 14, 15, 19, 21, 22, 24, 28, 29, and 46) have experienced their fifth earthquakes.

Figure 24. The space-time diagram of earthquake occurrence. The X-direction is the number of elements (fault block numbers), and the Y-direction is the time in years. The time increment is 2 years. This diagram contains four complete earthquake cycles.

Figure 25. The space-time diagram of earthquake occurrence. This diagram is generated by a different set of random stresses.

Figure 26. The variations of stress in block 18. X-direction is the amount of stress. Y-direction is the time. The actual amount of stress is given in the last column (under stress). This diagram has four complete earthquake cycles.

Figure 27. The variations of strain of block 18. The actual amount of strain is given in the last row (under strain). This diagram contains four complete earthquake cycles.

Figure 28. The cumulative curve of the total number of earthquakes in the model.

Figure 29. Simple truss model with 13 joints (j), 23 members (m), and 6 external loading forces (F_T) applied to the top of the truss. The number in the circle is the joint number. The number along the bar is the truss member number, which is arranged in accordance with the computer program.

a. This truss is fully supported by 1 pinned support and 6 roller supports. A pinned support supplies horizontal and vertical constraints to fix its position, while a roller support provides only vertical constraint and allows freedom of movement in the lateral direction. Therefore, for a pinned support, r=2, and for a roller support, r=1 (Brown, 1967). Thus, according to condition (1), $2j<m + r$, and the example truss is statically indeterminate.

b. A truss supported by a pinned support at joint 1 and a roller support at joint 13 (see Fig. 1a). The

total number of reaction components becomes three. According to condition (2), $2j = m + r$, the truss is statically determinate and, therefore, all member forces, S', can be determined in terms of the external loading forces (F_T).

c. A unit load D_3 is applied at joint 3 (see Fig. 1b). All of the member forces (u^3's) can be determined in terms of the unit load, D_3, applied at joint 3.

d. A unit load D_5 is applied at joint 5 (see Fig. 1b). All member forces (u^5's) can be determined in terms of the unit load, D_5, applied at joint 5.

e. A unit load D_7 is applied at joint 7 (see Fig. 1b). All member forces (u^7's) can be determined in terms of the unit load, D_7, applied at joint 7.

f. A unit laod D_9 is applied at joint 9 (see Fig. 1b). All member forces (u^9's) can be determined in terms of the unit load, D_9, applied at joint 9.

g. A unit laod D_{11} is applied at joint 11 (see Fig 1b). All member forces (u^{11}'s) can be determined in terms of the unit load, D_{11}, applied at joint 11.

Figure 30. The truss applied to the truss-fault block analogue.

a. A truss supported by foundation (i.e. fault) blocks. Each block has a stiffness coefficient, K^F, and is a rectangular solid box.

b. A truss supported by a viscoelastic foundation. Each foundation block behaves as a standard linear solid (see Fig. 9), when subject to time-dependent deformation.

Figure 31. The flow chart demonstrating the steps taken to determine how the total strain ($r_{t+\Delta t}$) is solved incrementally on the computer. At the end of each time interval the current solution is employed as an initial condition for the next incremental deformation.

Figure 32. The compression force is considered to be negative, whereas the extensional force is considered to be positive. F is the internal force stored within the spring. F' is the external force applied to the spring.

a. Unstretch state. X=0, F=0, F'=0.

b. Extensional state. X>0, F<0, F'>0.

c. Compressional state. X<0, F>0, F'<0. In the truss-fault block model the fault blocks are loaded and compressed by the external forces, i.e. the forces due to the moving plates (Fig. 6), therefore, Figure 32c illustrates what is happening in the model.

Figure 1

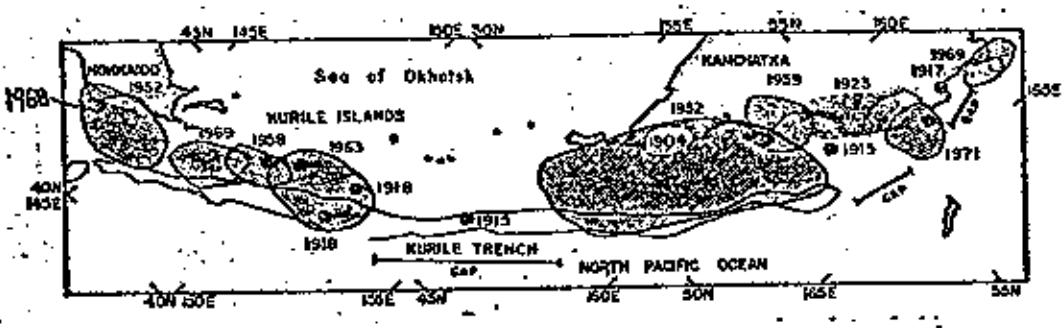
45N 145E
150E 50N
155E
55N
160E
HOKKAIDO
1952
Sea of Okhotsk
KAMCHATKA
1959
1923
1969
1917
1952
1904
1915
1971
1969
1958
1963
1918
1915
1918
KURILE TRENCH
GAP
NORTH PACIFIC OCEAN
40N 145E
40N 150E
150E 45N
45N 160E
50N
165E
55N

Figure 2

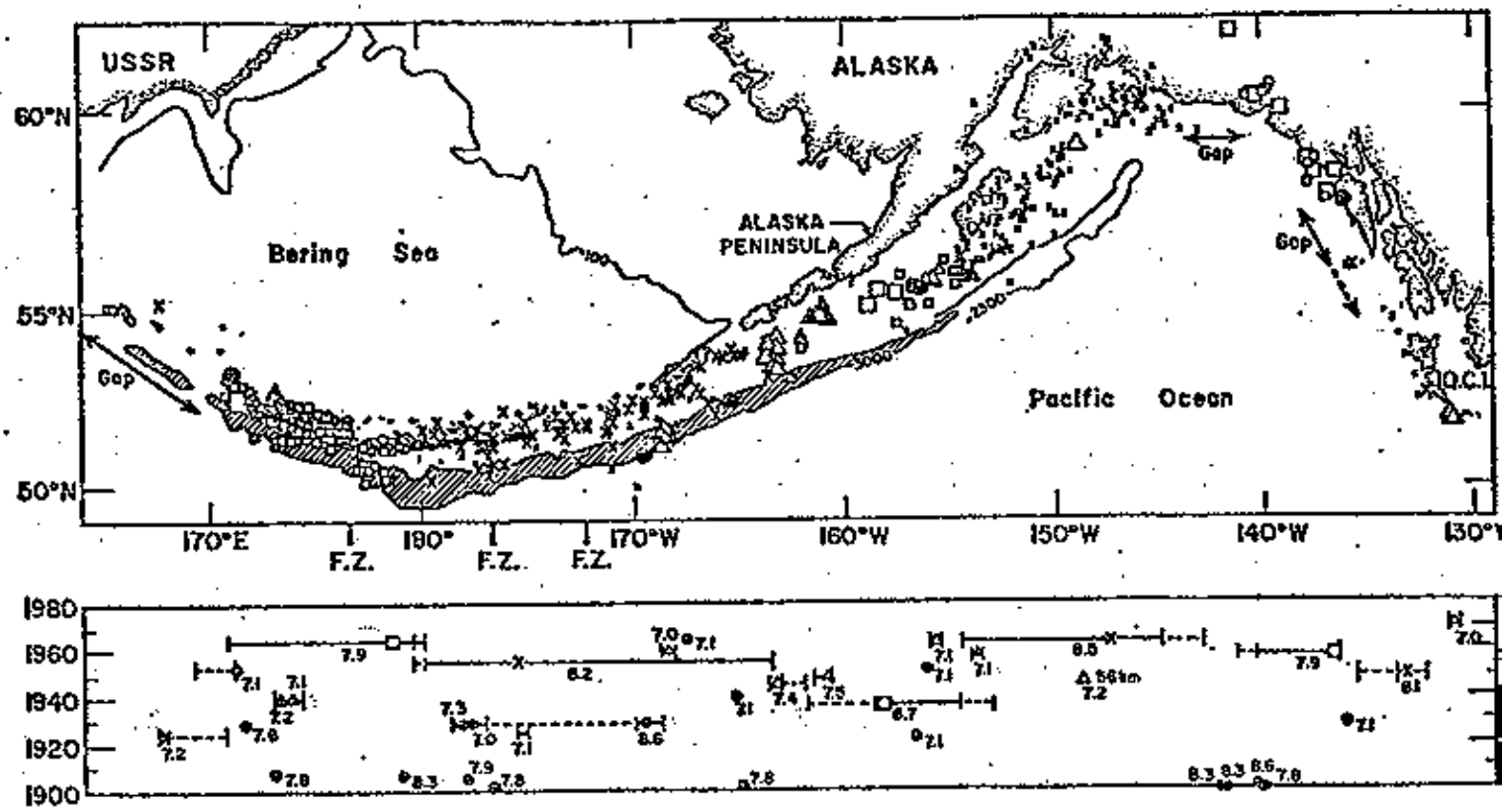
USSR
ALASKA
60°N
55°N
50°N
Bering Sea
ALASKA PENINSULA
Gap
Gap
Gap
Pacific Ocean
170°E
180°
170°W
160°W
150°W
140°W
F.Z.
F.Z.
F.Z.
1980
1960
1940
1920
1900

Figure 3

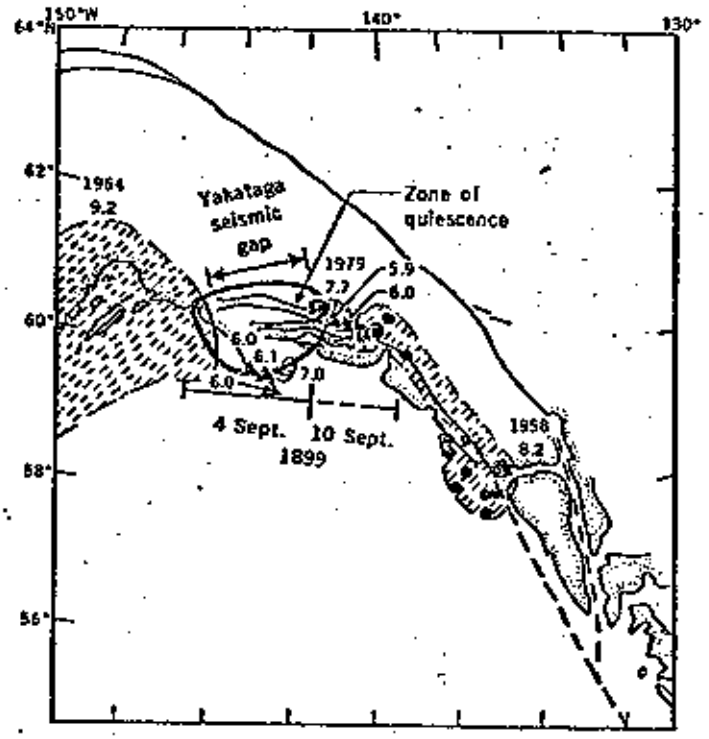
150°W
140°
130°
64°N
62°
60°
58°
56°
1964
9.2
Yakataga
seismic
gap
Zone of
quiescence
1979
7.2
5.9
6.0
6.0
6.1
7.0
6.0
4 Sept.
10 Sept.
1899
1958
8.2

Figure 4

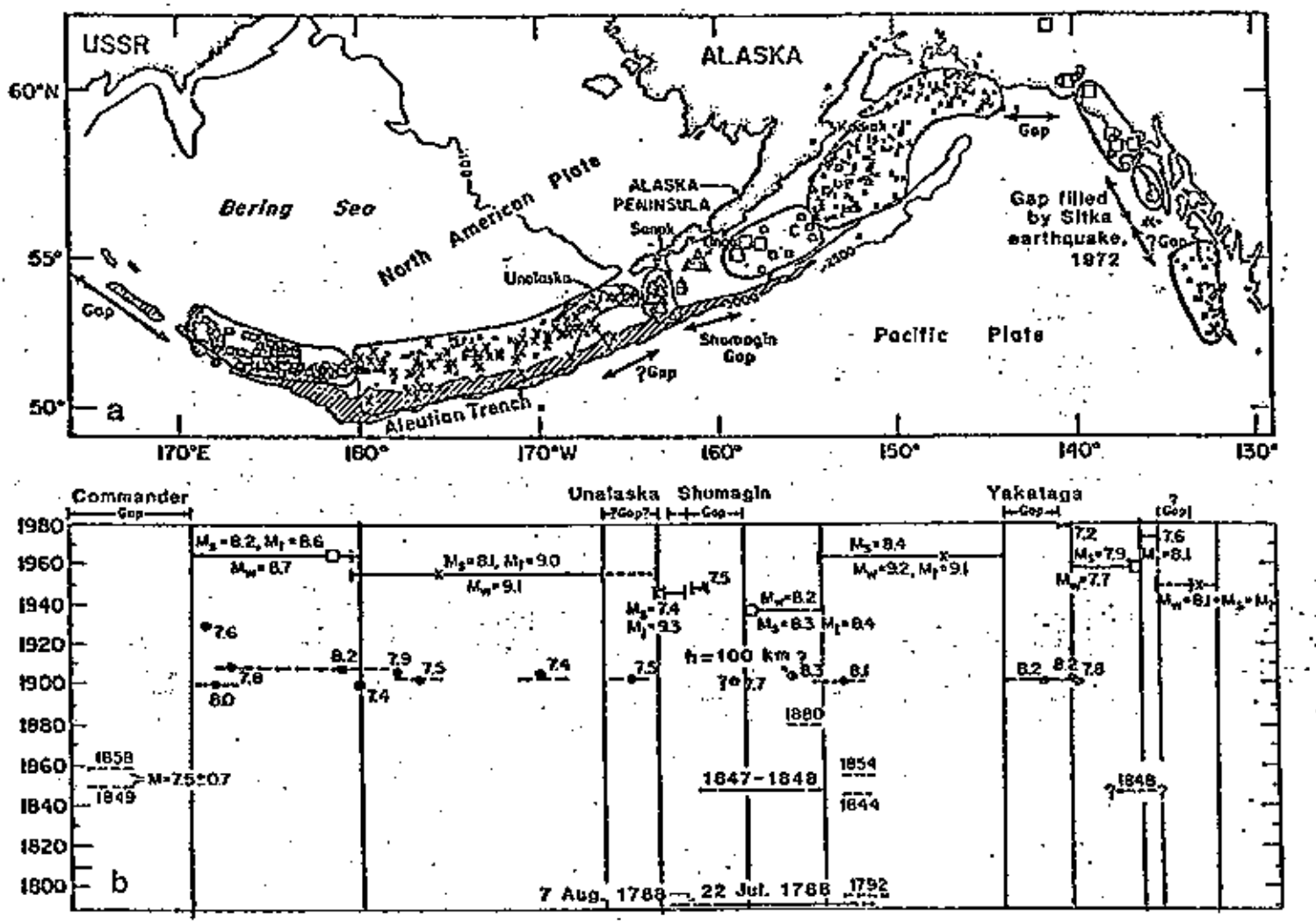
USSR
ALASKA
60°N
55°
50°
Bering Sea
North American Plate
ALASKA PENINSULA
Sanak
Unalaska
Gap
Shumagin Gap
?Gap
Pacific Plate
Aleutian Trench
Gap filled by Sitka earthquake, 1972
?Gap
Kodiak
a
170°E
180°
170°W
160°
150°
140°
130°
Commander
Unalaska
Shumagin
Yakataga
?
(Gap)
1980
1960
1940
1920
1900
1880
1860
1840
1820
1800
1858
1949
M=7.5±0.7
1880
1854
1847-1848
1844
1848
h=100 km ?
7 Aug. 1788
22 Jul. 1788
1792
b

Figure 5

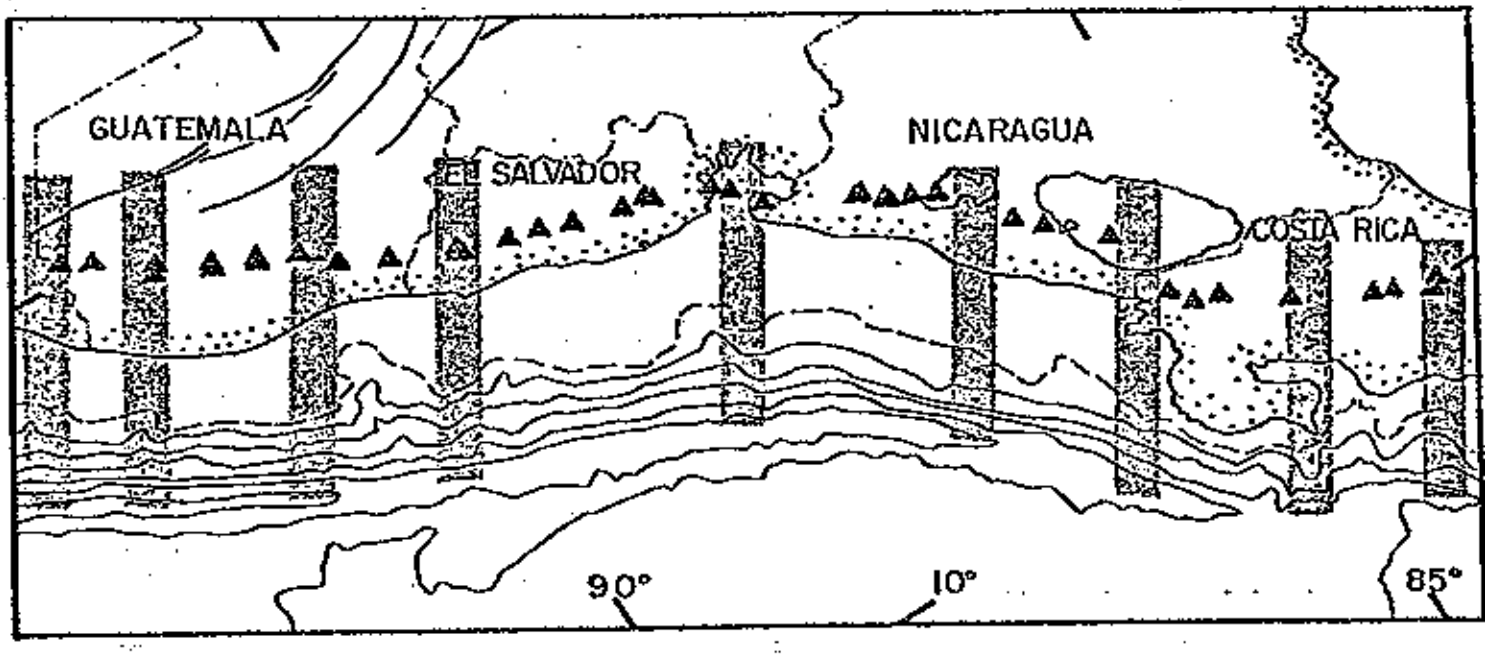

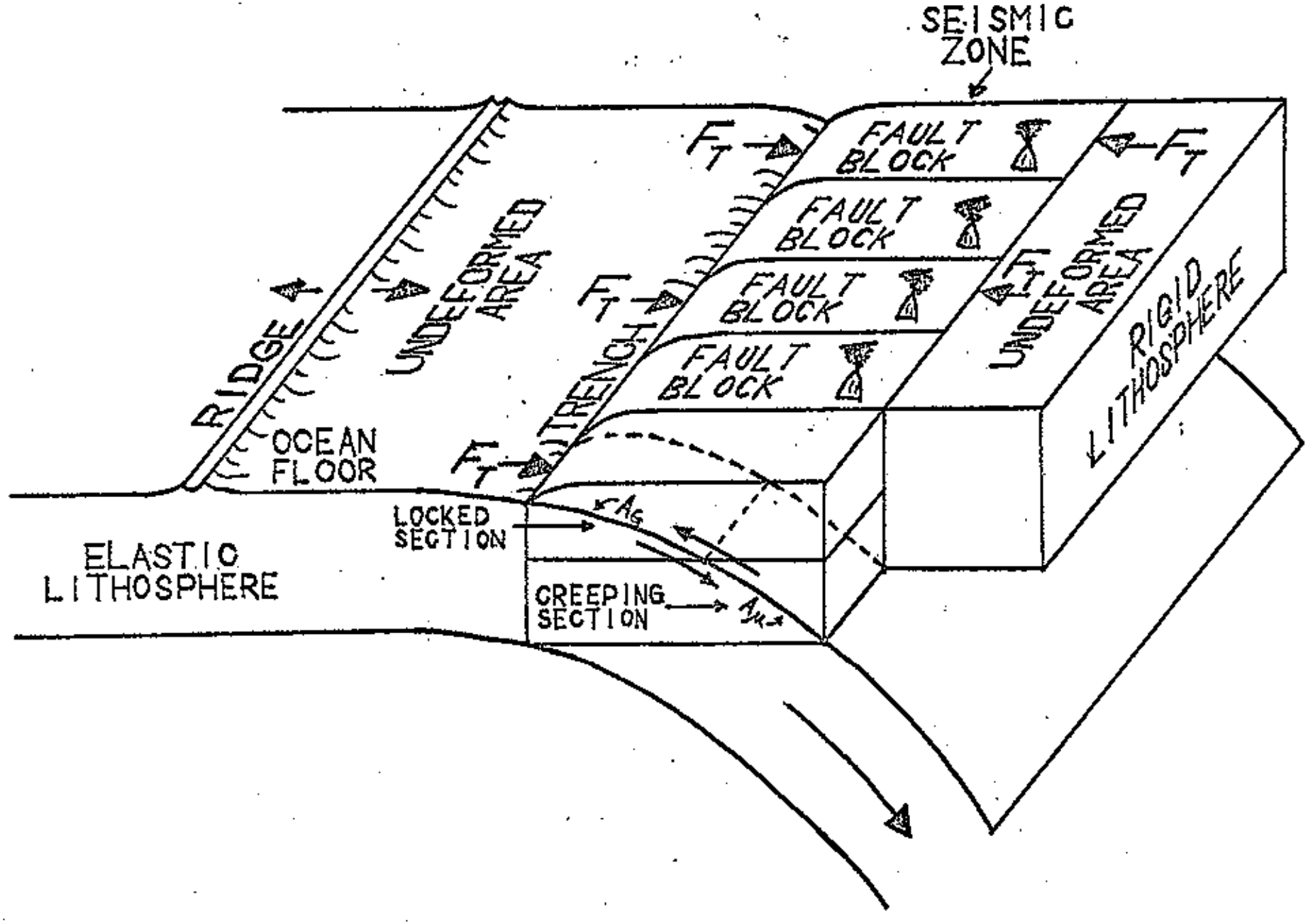

CONVERGENT PLATE MARGIN

NOT DRAWN TO SCALE

Figure 6

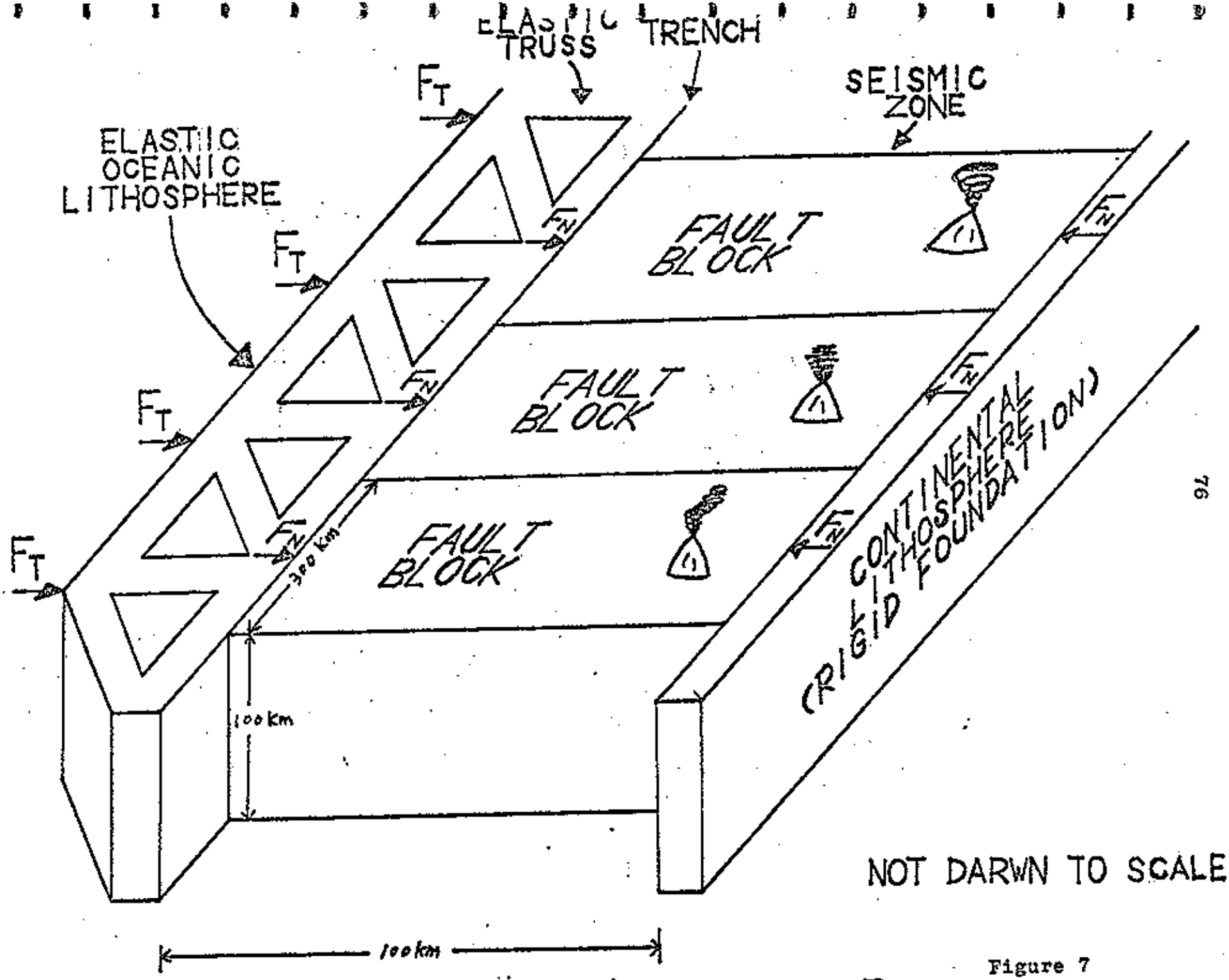

Figure 7

TRUSS-FAULT BLOCK ANALOGUE

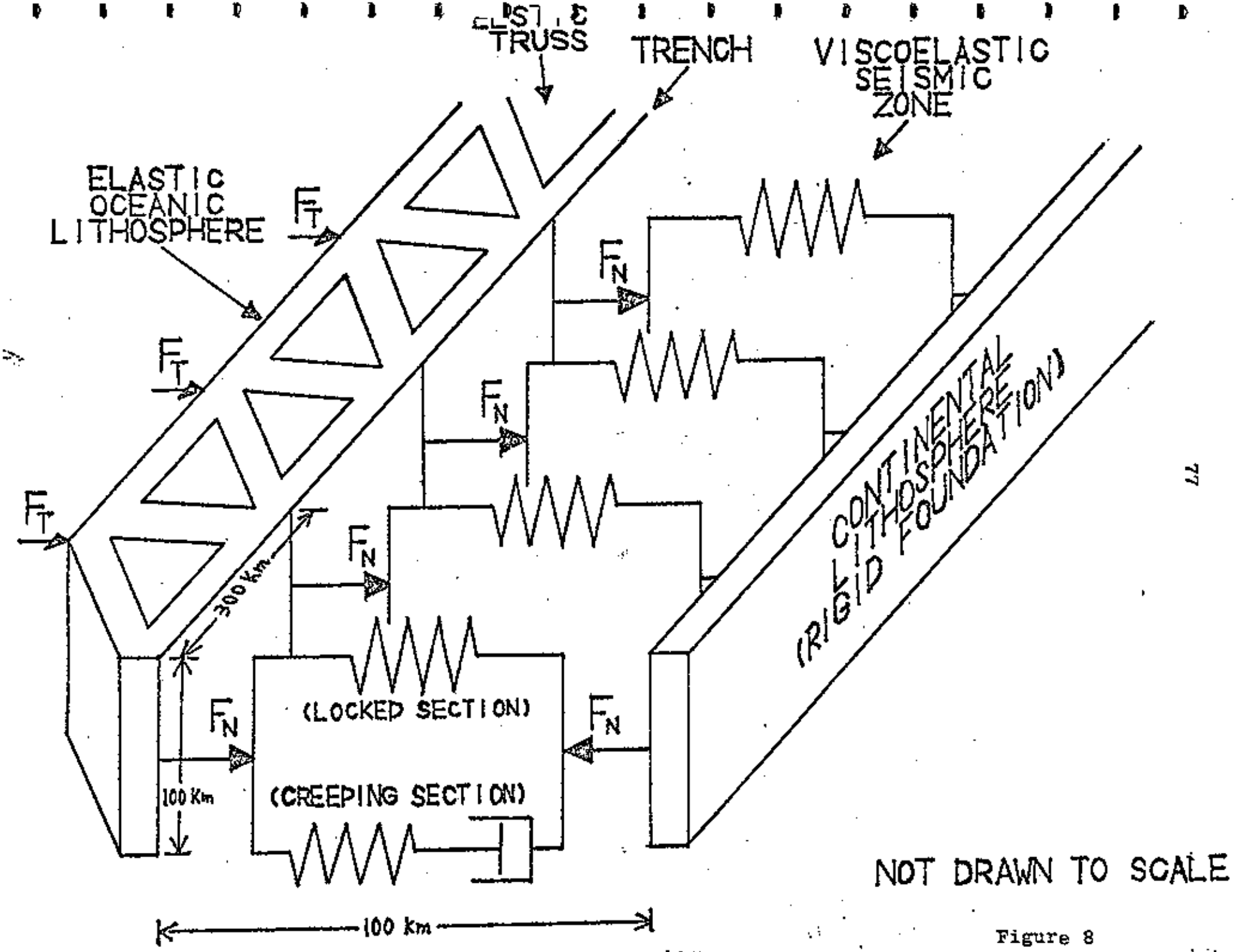

TRUSS-FAULT BLOCK AND STANDARD LINEAR SOLID ELEMENT

Figure 8

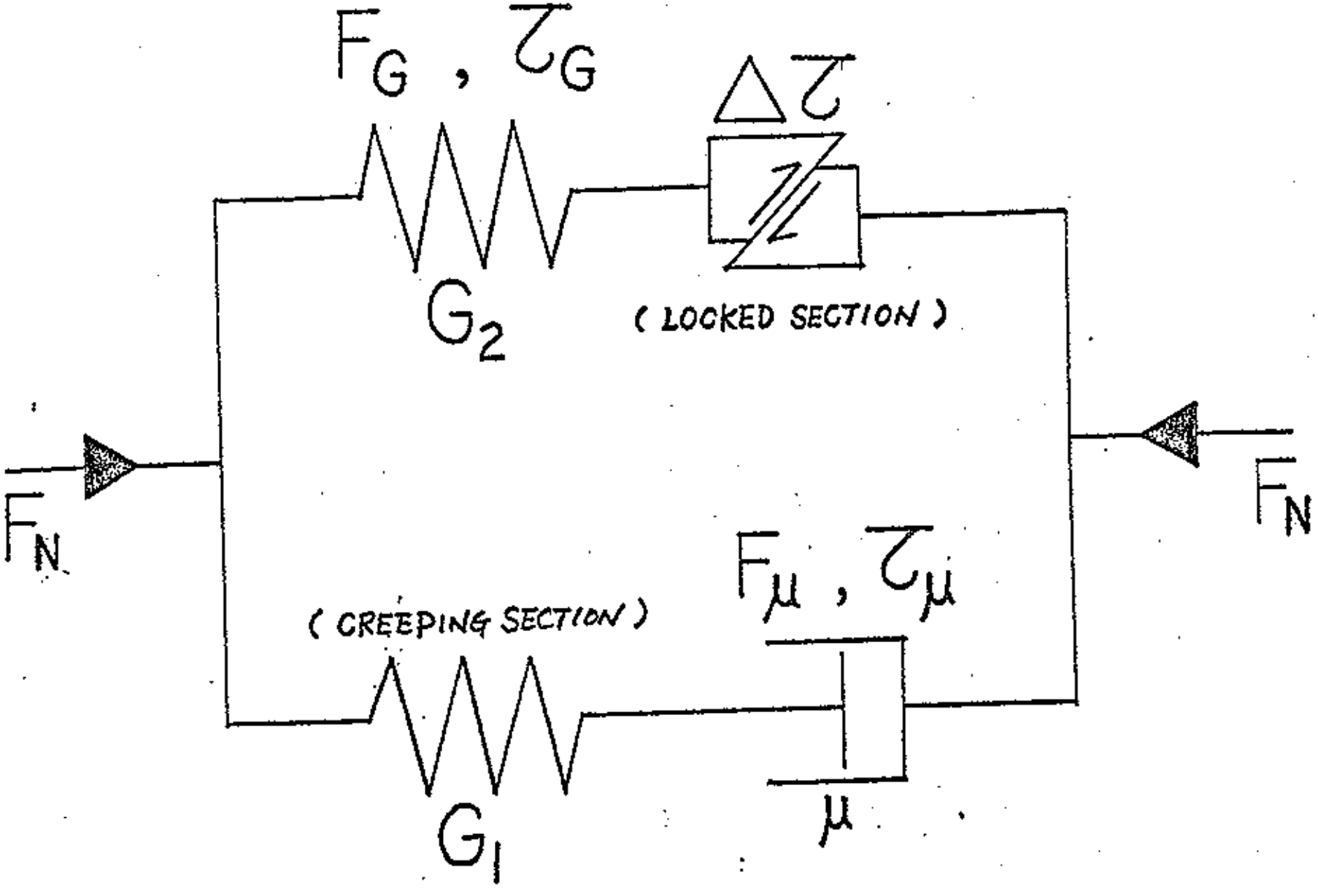

STANDARD LINEAR SOLID ELEMENT. Figure 9

Figure 10

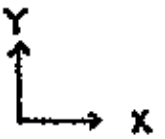

NO	STRESS	STRESS (MPS) 950 960 970 980 990
1	.9377364E+03	I
2	.9330328E+03	I
3	.9918581E+03	I
4	.9658891E+03	I
5	.9786105E+03	I
6	.9752501E+03	I
7	.9795587E+03	I
8	.9637177E+03	I
9	.9589006E+03	I
10	.9594891E+03	I
11	.9613989E+03	I
12	.9545952E+03	I
13	.9509694E+03	I
14	.9715845E+03	I
15	.9718392E+03	I
16	.9667645E+03	I
17	.9576559E+03	I
18	.9614191E+03	I
19	.9569396E+03	I
20	.9764693E+03	I
21	.9749081E+03	I
22	.9744944E+03	I
23	.9700078E+03	I
24	.9525477E+03	I
25	.9548680E+03	I
26	.9781307E+03	I
27	.9658787E+03	I
28	.9640333E+03	I
29	.9707251E+03	I
30	.9771558E+03	I
31	.9567085E+03	I
32	.9691133E+03	I
33	.9789193E+03	I
34	.9691482E+03	I
35	.9575986E+03	I
36	.9740286E+03	I
37	.9696160E+03	I
38	.9506632E+03	I
39	.9639770E+03	I
40	.9597278E+03	I
41	.9705619E+03	I
42	.9748429E+03	I
43	.9580667E+03	I
44	.9673641E+03	I
45	.9737298E+03	I
46	.9815313E+03	I
47	.9910575E+03	I
48	.1000754E+04	I
49	.9339541E+03	I

THE TOTAL TIME IS 3.0 YEARS

Figure 11

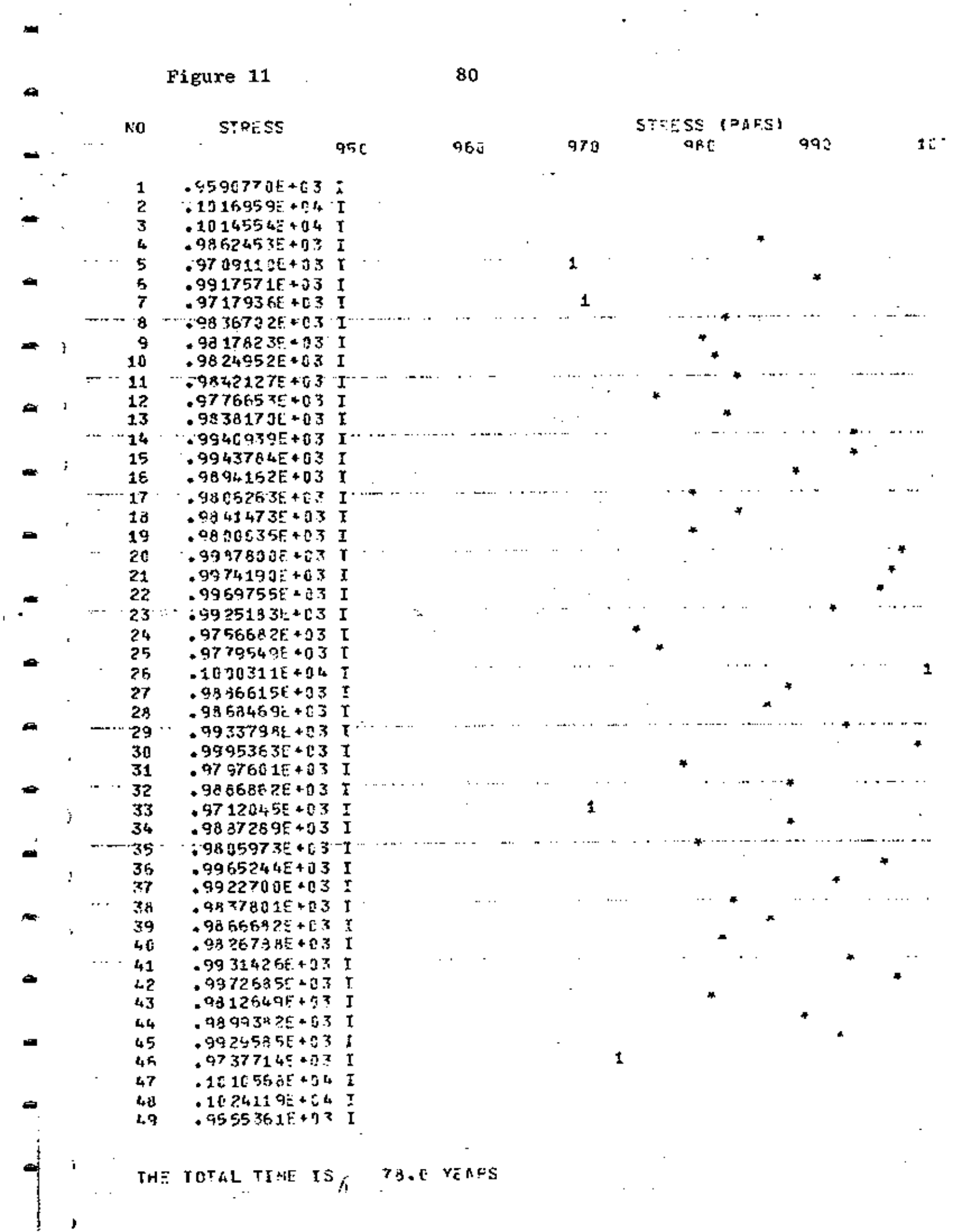

THE TOTAL TIME IS 78.0 YEARS

Figure 12

NO	STRESS	STRESS (BARS) 950 960 970 980 990 10
1	.9530770E+03	I
2	.1016959E+04	I
3	.1014554E+04	I
4	.9862453E+03	I
5	.9709110E+03	I 1
6	.9917571E+03	I
7	.9717936E+03	I 1
8	.9836702E+03	I
9	.9817823E+03	I
10	.9824952E+03	I
11	.9842127E+03	I
12	.9776653E+03	I
13	.9838170E+03	I
14	.9940939E+03	I
15	.9943784E+03	I
16	.9894162E+03	I
17	.9806261E+03	I
18	.9841465E+03	I
19	.9800009E+03	I
20	.9987717E+03	I
21	.9973944E+03	I
22	.9969094E+03	I
23	.9923895E+03	I
24	.9757362E+03	I
25	.9809586E+03	I
26	.9700661E+03	I 1
27	.9916957E+03	I
28	.9869194E+03	I
29	.9932504E+03	I
30	.9994698E+03	I
31	.9797358E+03	I
32	.9886780E+03	I
33	.9712018E+03	I 1
34	.9887291E+03	I
35	.9805971E+03	I
36	.9965244E+03	I
37	.9922700E+03	I
38	.9837801E+03	I
39	.9866662E+03	I
40	.9826788E+03	I
41	.9931426E+03	I
42	.9972685E+03	I
43	.9812549E+03	I
44	.9899382E+03	I
45	.9929585E+03	I
46	.9737714E+03	I 1
47	.1010568E+04	I
48	.1024119E+04	I
49	.9555361E+03	I

THE TOTAL TIME IS 73.0 YEARS

Figure 13

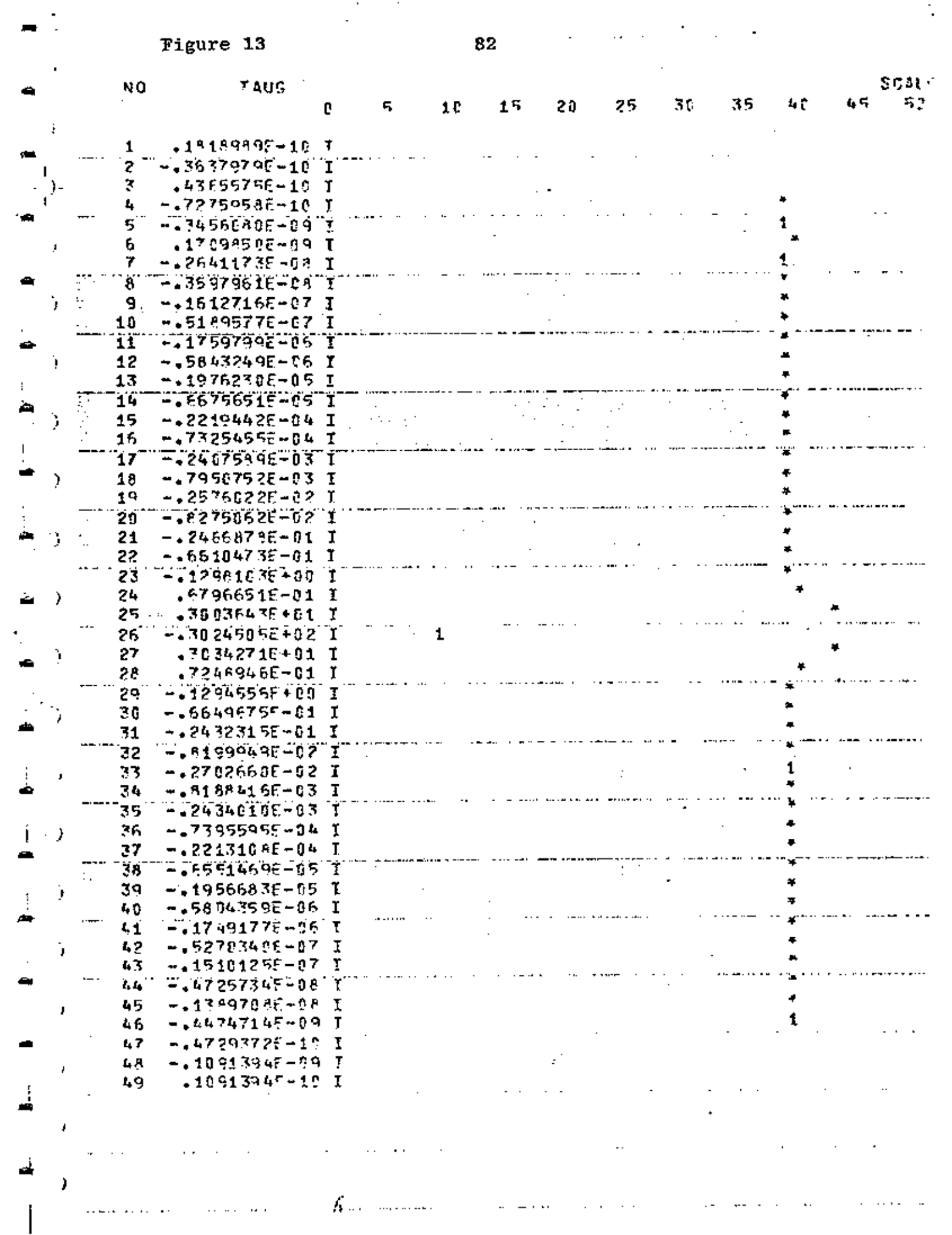
NO
TAUG
SCAL
0
5
10
15
20
25
30
35
40
45
50
1 .1918999E-10 I
2 -.3637979E-10 I
3 .4365575E-10 I
4 -.7275958E-10 I
5 -.3456080E-09 I
6 .1709450E-09 I
7 -.2641173E-08 I
8 -.3597961E-08 I
9 -.1612716E-07 I
10 -.5189577E-07 I
11 -.1759799E-06 I
12 -.5843249E-06 I
13 -.1976230E-05 I
14 -.6675651E-05 I
15 -.2219442E-04 I
16 -.7325455E-04 I
17 -.2407599E-03 I
18 -.7956752E-03 I
19 -.2576022E-02 I
20 -.8275062E-02 I
21 -.2466879E-01 I
22 -.6610473E-01 I
23 -.1298103E+00 I
24 .6796651E-01 I
25 .3503643E+01 I
26 -.3024505E+02 I
27 .7034271E+01 I
28 .7246946E-01 I
29 -.1294556E+00 I
30 -.6649675E-01 I
31 -.2432315E-01 I
32 -.8199949E-02 I
33 -.2702668E-02 I
34 -.8188416E-03 I
35 -.2434010E-03 I
36 -.7395595E-04 I
37 -.2213108E-04 I
38 -.6591469E-05 I
39 -.1956683E-05 I
40 -.5804359E-06 I
41 -.1749177E-06 I
42 -.5278340E-07 I
43 -.1510125E-07 I
44 -.4725734E-08 I
45 -.1349708E-08 I
46 -.4474714E-09 I
47 -.4729372E-10 I
48 -.1091394E-09 I
49 .1091394E-10 I

NO	STRESS	STRESS (PSI) 950 960 970 980 990
1	.9725139E+03	I
2	.1031871E+04	I
3	.1025960E+04	I
4	.9706169E+03	I
5	.9789386E+03	I
6	.9750664E+03	I
7	.9830453E+03	I
8	.9981301E+03	I
9	.9963444E+03	I
10	.9970654E+03	I
11	.9987153E+03	I
12	.9922845E+03	I
13	.9957955E+03	I
14	.9794473E+03	I
15	.9752780E+03	I
16	.9695462E+03	I
17	.9922257E+03	I
18	.9986397E+03	I
19	.9919225E+03	I
20	.9830812E+03	I
21	.9933848E+03	I
22	.9802987E+03	I
23	.9735009E+03	I
24	.9872628E+03	I
25	.9897923E+03	I
26	.9847215E+03	I
27	.1000246E+04	I
28	.9981053E+03	I
29	.9741436E+03	I
30	.9805186E+03	I
31	.9884957E+03	I
32	.9721059E+03	I
33	.9795440E+03	I
34	.9721776E+03	I
35	.9893010E+03	I
36	.9773831E+03	I
37	.9727381E+03	I
38	.9922837E+03	I
39	.9702831E+03	I
40	.9912402E+03	I
41	.9736248E+03	I
42	.9763140E+03	I
43	.9897990E+03	I
44	.9701442E+03	I
45	.9738201E+03	I
46	.9851570E+03	I
47	.1025195E+04	I
48	.1039063E+04	I
49	.9696459E+03	I

THE TOTAL TIME IS 120.0 YEARS

Figure 15

NO	STRESS	STRESS (BARS) 950 960 970 980 990 10
1	.9725139E+03 I	
2	.1031871E+04 I	
3	.1025860E+04 I	
4	.9706169E+03 I	
5	.9769386E+03 I	
6	.9790664E+03 I	
7	.9830453E+03 I	
8	.9981301E+03 I	
9	.9963444E+03 I	
10	.9970054E+03 I	
11	.9987153E+03 I	
12	.9922845E+03 I	
13	.9957955E+03 I	
14	.9794473E+03 I	
15	.9752780E+03 I	
16	.9695462E+03 I	
17	.9922256E+03 I	
18	.9986394E+03 I	
19	.9919217E+03 I	
20	.9830783E+03 I	
21	.9833759E+03 I	
22	.9862722E+03 I	
23	.9734312E+03 I	
24	.9871335E+03 I	
25	.9898849E+03 I	
26	.9879339E+03 I	
27	.9692670E+03 I	
28	.1001187E+04 I	
29	.9742223E+03 I	
30	.9833826E+03 I	
31	.9884284E+03 I	
32	.9720801E+03 I	
33	.9795352E+03 I	
34	.9721748E+03 I	
35	.9893002E+03 I	
36	.9773929E+03 I	
37	.9727380E+03 I	
38	.9922837E+03 I	
39	.9702831E+03 I	
40	.9912402E+03 I	
41	.9736248E+03 I	
42	.9783140E+03 I	
43	.9897990E+03 I	
44	.9701482E+03 I	
45	.9738201E+03 I	
46	.9851570E+03 I	
47	.1025195E+04 I	
48	.1039063E+04 I	
49	.9693459E+03 I	

THE TOTAL TIME IS 128.0 YEARS

NO	STRESS	STRESS (BARS) 950 960 970 980 990 10
1	.9596140E+03	I
2	.1017561E+04	I
3	.1015129E+04	I
4	.9866838E+03	I
5	.9714895E+03	I 1
6	.9923398E+03	I
7	.9723692E+03	I 1
8	.9842534E+03	I
9	.9823618E+03	I
10	.9830735E+03	I
11	.9847883E+03	I
12	.9762488E+03	I
13	.9843953E+03	I
14	.9946637E+03	I
15	.9949491E+03	I
16	.9899898E+03	I
17	.9812082E+03	I
18	.9847235E+03	I
19	.9805900E+03	I
20	.9933531E+03	I
21	.9980136E+03	I
22	.9976107E+03	I
23	.9932178E+03	I
24	.9761858E+03	I
25	.9755414E+03	I
26	.9706396E+03	I 1
27	.9862094E+03	I
28	.9873515E+03	I
29	.9946808E+03	I
30	.1006166E+04	I 1
31	.9603700E+03	I
32	.9892721E+03	I
33	.9717831E+03	I 1
34	.9893677E+03	I
35	.9811819E+03	I
36	.9970905E+03	I
37	.9926418E+03	I
38	.9843596E+03	I
39	.9872424E+03	I
40	.9832596E+03	I
41	.9937135E+03	I
42	.9978342E+03	I
43	.9818486E+03	I
44	.9905120E+03	I
45	.9935373E+03	I
46	.9743554E+03	I 1
47	.1011159E+04	I
48	.1024713E+04	I
49	.9560779E+03	I

THE TOTAL TIME IS 60.0 YEARS

NO	TAUG	0 5 10 15 20 25 30 35 40 45 50 SCAL
1	.5370719E+00	I
2	.5618690E+00	I
3	.5749240E+00	I
4	.5934522E+00	I *
5	.5784033E+00	I 1
6	.5926B4E+00	I *
7	.5755717E+00	I 1
8	.5932347E+00	I *
9	.5794983E+00	I *
10	.5783768E+00	I *
11	.5756234E+00	I *
12	.5934147E+00	I *
13	.5782499E+00	I *
14	.5698337E+00	I *
15	.5706837E+00	I *
16	.5736448E+00	I *
17	.5820383E+00	I *
18	.5770237E+00	I *
19	.5891439E+00	I *
20	.5813813E+00	I *
21	.6192510E+00	I *
22	.7012823E+00	I *
23	.8292972E+00	I *
24	.4495106E+00	I *
25	-.5417162E+01	I *
26	.5735590E+00	I 1
27	-.5486326E+01	I *
28	.4321283E+00	I *
29	.8304B39E+00	I *
30	.6959521E+00	I 1
31	.6342603E+00	I *
32	.5941040E+00	I *
33	.5812534E+00	I 1
34	.5795447E+00	I *
35	.5848373E+00	I *
36	.5661692E+00	I *
37	.5716214E+00	I *
38	.5795842E+00	I *
39	.5742083E+00	I *
40	.5808098E+00	I *
41	.5709420E+00	I *
42	.5657555E+00	I *
43	.5975547E+00	I *
44	.5737736E+00	I *
45	.5747933E+00	I *
46	.5840149E+00	I 1
47	.5863566E+00	I
48	.5941404E+00	I
49	.5419122E+00	I

Figure 18a

NO	STRESS	STRESS (BARS) 950 960 970 980 99[illegible] 1[illegible]
1	.9814221E+03 I	
2	.1041905E+04 I	
3	.1035558E+04 I	
4	.9807973E+03 I	1
5	.9889557E+03 I	1
6	.9850996E+03 I	1
7	.9902561E+03 I	1
8	.9791679E+03 I	1
9	.9752226E+03 I	1
10	.9779363E+03 I	1
11	.9775893E+03 I	1
12	.9961063E+03 I	*
13	.9745567E+03 I	1
14	.9863543E+03 I	1
15	.9852656E+03 I	1
16	.9794937E+03 I	1
17	.9991022E+03 I	*
18	.9775353E+03 I	1
19	.9987733E+03 I	*
20	.9926615E+03 I	1
21	.9933346E+03 I	1
22	.9902209E+03 I	1
23	.9833852E+03 I	1
24	.9972901E+03 I	*
25	.9996289E+03 I	*
26	.9910659E+03 I	1
27	.9792172E+03 I	1
28	.9786501E+03 I	1
29	.9813447E+03 I	1
30	.9902448E+03 I	1
31	.9986051E+03 I	*
32	.9820259E+03 I	1
33	.9893685E+03 I	1
34	.9820991E+03 I	1
35	.9993754E+03 I	*
36	.9870772E+03 I	1
37	.9794765E+03 I	1
38	.9732933E+03 I	1
39	.9736276E+03 I	1
40	.9692534E+03 I	1
41	.9803318E+03 I	1
42	.9879981E+03 I	1
43	.9997754E+03 I	*
44	.9800869E+03 I	1
45	.9937649E+03 I	1
46	.9949862E+03 I	1
47	.1034965E+04 I	
48	.1048952E+04 I	
49	.9780324E+03 I	

THE TOTAL TIME IS 162.0 YEARS

Figure 18b

NO	STRESS	STRESS (BARS) 950 960 970 980 990 1
1	.9819424E+03 I	
2	.1042491E+04 I	
3	.1036123E+04 I	
4	.9813876E+03 I	
5	.9895299E+03 I	
6	.9856795E+03 I	
7	.9908263E+03 I	
8	.9797512E+03 I	
9	.9758064E+03 I	
10	.9785179E+03 I	
11	.9781649E+03 I	
12	.9966852E+03 I	
13	.9751366E+03 I	
14	.9869303E+03 I	
15	.9858414E+03 I	
16	.9830790E+03 I	
17	.9996792E+03 I	
18	.9781076E+03 I	
19	.9993525E+03 I	
20	.9932259E+03 I	
21	.9939080E+03 I	
22	.9907952E+03 I	
23	.9839564E+03 I	
24	.9978653E+03 I	
25	.1000203E+04 I	
26	.9916302E+03 I	
27	.9797994E+03 I	
28	.9792340E+03 I	
29	.9819235E+03 I	
30	.9908101E+03 I	
31	.9991861E+03 I	
32	.9826007E+03 I	
33	.9899396E+03 I	
34	.9826740E+03 I	
35	.9999551E+03 I	
36	.9876455E+03 I	
37	.9900583E+03 I	
38	.9708816E+03 I	
39	.9742101E+03 I	
40	.9698429E+03 I	
41	.9809107E+03 I	
42	.9885660E+03 I	
43	.1000355E+04 I	
44	.9806634E+03 I	
45	.9843659E+03 I	
46	.9956695E+03 I	
47	.1035536E+04 I	
48	.1049531E+04 I	
49	.9785574E+03 I	

THE TOTAL TIME IS 164.0 YEARS

NO	STRESS	STRESS (BARS) 950 960 970 980 990
1	.9819424E+03	I 1
2	.1042491E+04	I
3	.1036123E+04	I
4	.9813675E+03	I 1
5	.9895299E+03	I 1
6	.9856795E+03	I 1
7	.9908263E+03	I 1
8	.9797512E+03	I 1
9	.9758064E+03	I 1
10	.9755179E+03	I 1
11	.9781649E+03	I 1
12	.9966852E+03	I
13	.9751366E+03	I 1
14	.9869303E+03	I 1
15	.9858413E+03	I 1
16	.9800698E+03	I 1
17	.9996784E+03	I
18	.9781048E+03	I 1
19	.9993440E+03	I
20	.9931993E+03	I 1
21	.9938374E+03	I 1
22	.9906589E+03	I 1
23	.9840352E+03	I 1
24	.1000940E+04	I 1
25	.9691317E+03	I 1
26	.9948696E+03	I 1
27	.9798991E+03	I 1
28	.9791001E+03	I 1
29	.9818523E+03	I 1
30	.9907830E+03	I 1
31	.9991774E+03	I
32	.9825978E+03	I 1
33	.9899346E+03	I 1
34	.9826734E+03	I 1
35	.9999542E+03	I
36	.9876426E+03	I 1
37	.9800492E+03	I 1
38	.9708548E+03	I 1
39	.9741386E+03	I 1
40	.9697375E+03	I 1
41	.9810094E+03	I 1
42	.9916188E+03	I 1
43	.9688114E+03	I 1
44	.9838894E+03	I 1
45	.9844608E+03	I 1
46	.9954229E+03	I 1
47	.1035466E+04	I
48	.1049505E+04	I
49	.9795495E+03	I

THE TOTAL TIME IS 164.0 YEARS

Figure 18d

NO	STRESS	STRESS (BARS) 950 960 970 980 990 1
1	.9824624E+03	I
2	.1043077E+04	I
3	.1036689E+04	I
4	.9819775E+03	I
5	.9901036E+03	I
6	.9862591E+03	I
7	.9913961E+03	I
8	.9833342E+03	I
9	.9763898E+03	I
10	.9730995E+03	I
11	.9787400E+03	I
12	.9972639E+03	I
13	.9757162E+03	I
14	.9875060E+03	I
15	.9864172E+03	I
16	.9806469E+03	I
17	.1000259E+04	I
18	.9786895E+03	I
19	.9999612E+03	I
20	.9938756E+03	I
21	.9946626E+03	I
22	.9914264E+03	I
23	.9818157E+03	I
24	.9690533E+03	I
25	.9697164E+03	I
26	.9868854E+03	I
27	.9803924E+03	I
28	.9800089E+03	I
29	.9825949E+03	I
30	.9914095E+03	I
31	.9997777E+03	I
32	.9831786E+03	I
33	.9905114E+03	I
34	.9832491E+03	I
35	.1000535E+04	I
36	.9882165E+03	I
37	.9806468E+03	I
38	.9714969E+03	I
39	.9748637E+03	I
40	.9705673E+03	I
41	.9813907E+03	I
42	.9858864E+03	I
43	.9694033E+03	I
44	.9750192E+03	I
45	.9846518E+03	I
46	.9962720E+03	I
47	.1036177E+04	I
48	.1050135E+04	I
49	.9790900E+03	I

THE TOTAL TIME IS 166.0 YEARS

Figure 18e

NO	STRESS	STRESS (BARS) 950 960 970 980 990
1	.9824624E+03 I	
2	.1043077E+04 I	
3	.1036688E+04 I	
4	.9819775E+03 I	1
5	.9901036E+03 I	1
6	.9862591E+03 I	1
7	.9913961E+03 I	1
8	.9803339E+03 I	1
9	.9763890E+03 I	1
10	.9790967E+03 I	1
11	.9787311E+03 I	1
12	.9972378E+03 I	*
13	.9756450E+03 I	1
14	.9873692E+03 I	1
15	.9865129E+03 I	1
16	.9836800E+03 I	1
17	.9684682E+03 I	1
18	.9619105E+03 I	1
19	.1000051E+04 I	1
20	.9937367E+03 I	1
21	.9945966E+03 I	1
22	.9913993E+03 I	1
23	.9818066E+03 I	1
24	.9690559E+03 I	1
25	.9697175E+03 I	1
26	.9838849E+03 I	1
27	.9803914E+03 I	1
28	.9800660E+03 I	1
29	.9825858E+03 I	1
30	.9913625E+03 I	1
31	.9997085E+03 I	*
32	.9630420E+03 I	1
33	.9906681E+03 I	1
34	.9864827E+03 I	1
35	.9689688E+03 I	1
36	.9914698E+03 I	1
37	.9807454E+03 I	1
38	.9713608E+03 I	1
39	.9747921E+03 I	1
40	.9705404E+03 I	1
41	.9813816E+03 I	1
42	.9856835E+03 I	1
43	.9694024E+03 I	1
44	.9738169E+03 I	1
45	.9848517E+03 I	1
46	.9962720E+03 I	1
47	.1036177E+04 I	
48	.1050135E+04 I	
49	.9790900E+03 I	

THE TOTAL TIME IS 156.0 YEARS

Figure 18f

NO	STRESS	STRESS (RAPS) 950 966 978 98 99 1
1	.9929820E+03	I
2	.1043563E+04	I
3	.1037253E+04	I
4	.9825670E+03	I
5	.9906770E+03	I
6	.9668383E+03	I
7	.9919657E+03	I
8	.9809170E+03	I
9	.9769738E+03	I
10	.9796837E+03	I
11	.9793244E+03	I
12	.9978702E+03	I
13	.9753739E+03	I
14	.9882400E+03	I
15	.9869558E+03	I
16	.9781074E+03	I
17	.9690575E+03	I
18	.9734079E+03	I
19	.9735657E+03	I
20	.9919040E+03	I
21	.9952255E+03	I
22	.9921391E+03	I
23	.9824592E+03	I
24	.9696690E+03	I
25	.9793160E+03	I
26	.9894567E+03	I
27	.9809755E+03	I
28	.9805948E+03	I
29	.9831820E+03	I
30	.9920010E+03	I
31	.1050427E+04	I
32	.9838899E+03	I
33	.9909851E+03	I
34	.9805953E+03	I
35	.9695599E+03	I
36	.9855365E+03	I
37	.9811275E+03	I
38	.9722195E+03	I
39	.9755169E+03	I
40	.9711827E+03	I
41	.9819781E+03	I
42	.9864622E+03	I
43	.9699957E+03	I
44	.9746009E+03	I
45	.9854323E+03	I
46	.9966454E+03	I
47	.1036747E+04	I
48	.1050712E+04	I
49	.9796143E+03	I

THE TOTAL TIME IS 168.0 YEARS

Figure 18g

NO.	STRESS	STRESS (BARS) 950 960 970 980 990 1000
1	.9850563E+03	I
2	.1046002E+04	I
3	.1033960E+04	I
4	.9849216E+03	I 1
5	.9929670E+03	I 1
6	.9891515E+03	I 1
7	.9942400E+03	I 1
8	.9832478E+03	I 1
9	.9793023E+03	I 1
10	.9820048E+03	I 1
11	.9816200E+03	I 1
12	.1030179E+04	I 1
13	.9786665E+03	I 1
14	.9905364E+03	I 1
15	.9892529E+03	I 1
16	.9830428E+03	I 1
17	.9714114E+03	I 1
18	.9757320E+03	I 1
19	.9759214E+03	I 1
20	.9941727E+03	I 1
21	.9975113E+03	I 1
22	.9944286E+03	I 1
23	.9847571E+03	I 1
24	.9720321E+03	I 1
25	.9726786E+03	I 1
26	.9917539E+03	I 1
27	.9833665E+03	I 1
28	.9830568E+03	I 1
29	.9853996E+03	I 1
30	.9910161E+03	I 1
31	.9713380E+03	I 1
32	.9829710E+03	I 1
33	.9931671E+03	I 1
34	.9830469E+03	I 1
35	.9719940E+03	I 1
36	.9876532E+03	I 1
37	.9834498E+03	I 1
38	.9745679E+03	I 1
39	.9778404E+03	I 1
40	.9735334E+03	I 1
41	.9842879E+03	I 1
42	.9827503E+03	I 1
43	.9723583E+03	I 1
44	.9869271E+03	I 1
45	.9877506E+03	I 1
46	.9991353E+03	I 1
47	.1039026E+04	I
48	.1053019E+04	I
49	.9817076E+03	I

THE TOTAL TIME IS 176.0 YEARS

Figure 19

NO	STRESS	STRESS (BARS) 950 960 970 980 990 1
1	.9850563E+03 I	
2	.1046002E+04 I	
3	.1039568E+04 I	
4	.9849207E+03 I	1
5	.9929641E+03 I	1
6	.9891423E+03 I	1
7	.9942126E+03 I	1
8	.9831725E+03 I	1
9	.9791666E+03 I	1
10	.9820989E+03 I	1
11	.9846486E+03 I	1
12	.9683542E+03 I	1
13	.9819093E+03 I	1
14	.9906305E+03 I	1
15	.9891151E+03 I	1
16	.9803559E+03 I	1
17	.9713645E+03 I	1
18	.9757230E+03 I	1
19	.9759186E+03 I	1
20	.9941718E+03 I	1
21	.9975111E+03 I	1
22	.9944286E+03 I	1
23	.9847571E+03 I	1
24	.9720321E+03 I	1
25	.9726786E+03 I	1
26	.9917539E+03 I	1
27	.9833685E+03 I	1
28	.9830569E+03 I	1
29	.9853986E+03 I	1
30	.9910161E+03 I	1
31	.9713380E+03 I	1
32	.9829710E+03 I	1
33	.9931671E+03 I	1
34	.9830469E+03 I	1
35	.9719940E+03 I	1
36	.9876532E+03 I	1
37	.9834498E+03 I	1
38	.9746679E+03 I	1
39	.9778404E+03 I	1
40	.9735334E+03 I	1
41	.9842679E+03 I	1
42	.9887503E+03 I	1
43	.9723589E+03 I	1
44	.9839231E+03 I	1
45	.9877506E+03 I	1
46	.9991353E+03 I	1
47	.1039826E+04 I	
48	.1053619E+04 I	
49	.9817876E+03 I	

THE TOTAL TIME IS 176.0 YEARS

Figure 20a

NO	STRESS	STRESS (BARS) 950 960 970 980 990
1	.1011647E+04	I
2	.1076080E+04	I
3	.1065616E+04	I
4	.9842138E+03	I 2
5	.9870925E+03	I 2
6	.9829954E+03	I 2
7	.9891735E+03	I 2
8	.9882140E+03	I 2
9	.9866203E+03	I 2
10	.9789830E+03	I 2
11	.9729979E+03	I 2
12	.9926563E+03	I 1
13	.9727413E+03	I 2
14	.9890047E+03	I 2
15	.9897579E+03	I 2
16	.9785625E+03	I 2
17	.9958279E+03	I 1
18	.9756697E+03	I 2
19	.9884444E+03	I 2
20	.9864702E+03	I 2
21	.9944387E+03	I 2
22	.9935066E+03	I 2
23	.9830373E+03	I 2
24	.9995447E+03	I 1
25	.1000158E+04	I 2
26	.9893326E+03	I 2
27	.9841058E+03	I 2
28	.9849971E+03	I 2
29	.9875649E+03	I 2
30	.9886708E+03	I 2
31	.9960494E+03	I 1
32	.9796423E+03	I 2
33	.9871588E+03	I 2
34	.9799143E+03	I 2
35	.9964544E+03	I 1
36	.9847225E+03	I 2
37	.9804272E+03	I 2
38	.9988242E+03	I 1
39	.9779438E+03	I 2
40	.9978647E+03	I 1
41	.9811814E+03	I 2
42	.9856658E+03	I 2
43	.9967301E+03	I 1
44	.9775029E+03	I 2
45	.9821532E+03	I 2
46	.9947696E+03	I 2
47	.1065551E+04	I
48	.1042604E+04	I
49	.1005532E+04	I

THE TOTAL TIME IS 280.0 YEARS

Figure 20b

NO	STRESS	STRESS (BARS) 950 960 970 980 990 1.
1	.1011647E+04	I
2	.1076000E+04	I
3	.1065616E+04	I
4	.9842138E+03	I 2
5	.9870925E+03	I 2
6	.9629954E+03	I 2
7	.9891735E+03	I 2
8	.9882140E+03	I 2
9	.9866203E+03	I 2
10	.9769630E+03	I 2
11	.9729979E+03	I 2
12	.9926583E+03	I 1
13	.9727413E+03	I 2
14	.9890047E+03	I 2
15	.9897578E+03	I 2
16	.9765622E+03	I 2
17	.9958270E+03	I 1
18	.9758669E+03	I 2
19	.9804356E+03	I 2
20	.9864430E+03	I 2
21	.9943677E+03	I 2
22	.9983745E+03	I 2
23	.9831322E+03	I 2
24	.1032553E+04	I 2
25	.9683493E+03	I 2
26	.9925650E+03	I 2
27	.9842217E+03	I 2
28	.9846564E+03	I 2
29	.9874936E+03	I 2
30	.9886432E+03	I 2
31	.9960405E+03	I 1
32	.9796394E+03	I 2
33	.9871579E+03	I 2
34	.9799140E+03	I 2
35	.9964444E+03	I 1
36	.9847225E+03	I 2
37	.9804272E+03	I 2
38	.9986242E+03	I 1
39	.9779438E+03	I 2
40	.9978647E+03	I 1
41	.9811814E+03	I 2
42	.9856658E+03	I 2
43	.9967301E+03	I 1
44	.9775620E+03	I 2
45	.9821572E+03	I 2
46	.9947696E+03	I 2
47	.1065591E+04	I
48	.1092604E+04	I
49	.1088932E+04	I

THE TOTAL TIME IS 280.0 YEARS

Figure 20c

NO	STRESS	STRESS (BARS) 950 960 970 980 990 10.
1	.10131395+04	I
2	.10776935+04	I
3	.10672665+04	I
4	.98596885+03	I 2
5	.98681785+03	I 2
6	.98473905+03	I 2
7	.99088155+03	I 2
8	.98994935+03	I 2
9	.98435215+03	I 2
10	.98072275+03	I 2
11	.97473265+03	I 2
12	.99439955+03	I 1
13	.97446425+03	I 2
14	.99072355+03	I 2
15	.99148215+03	I 2
16	.98029005+03	I 2
17	.99756545+03	I 1
18	.97760395+03	I 2
19	.98223255+03	I 2
20	.98425455+03	I 2
21	.99631215+03	I 2
22	.10002755+04	I 3
23	.98254605+03	I 2
24	.97729825+03	I 2
25	.97021355+03	I 2
26	.98779325+03	I 2
27	.98582065+03	I 2
28	.98669715+03	I 2
29	.98938355+03	I 2
30	.99039935+03	I 2
31	.99760625+03	I 1
32	.98157395+03	I 2
33	.98487565+03	I 2
34	.98164345+03	I 2
35	.99818765+03	I 1
36	.98643125+03	I 2
37	.98215365+03	I 2
38	.10305545+04	I 2
39	.97966175+03	I 2
40	.99959775+03	I 1
41	.98290565+03	I 2
42	.98737375+03	I 2
43	.99947285+03	I 1
44	.97923725+03	I 2
45	.98789905+03	I 2
46	.99650255+03	I 2
47	.10672175+04	I
48	.10944745+04	I
49	.10190375+04	I

THE TOTAL TIME IS 286.0 YEARS

Figure 20d

NO	STRESS	STRESS (BARS) 950 960 970 980 990 1000
1	.1013635E+04 I	
2	.1072257E+04 I	
3	.1067615E+04 I	
4	.9865530E+03 I	2
5	.9833921E+03 I	2
6	.9853195E+03 I	2
7	.9914501E+03 I	2
8	.9965270E+03 I	2
9	.9889246E+03 I	2
10	.9813018E+03 I	2
11	.9755102E+03 I	2
12	.9949793E+03 I	1
13	.9750646E+03 I	2
14	.9912964E+03 I	2
15	.9920584E+03 I	2
16	.9888724E+03 I	2
17	.9981652E+03 I	1
18	.9782379E+03 I	2
19	.9929272E+03 I	2
20	.9887283E+03 I	2
21	.9942511E+03 I	2
22	.9746330E+03 I	3
23	.9804796E+03 I	2
24	.9777939E+03 I	2
25	.9709117E+03 I	2
26	.9884216E+03 I	2
27	.9864236E+03 I	2
28	.9874513E+03 I	2
29	.9899617E+03 I	2
30	.9909650E+03 I	2
31	.9933906E+03 I	1
32	.9821587E+03 I	2
33	.9894750E+03 I	2
34	.9822916E+03 I	2
35	.9988982E+03 I	1
36	.9868840E+03 I	2
37	.9795283E+03 I	2
38	.9705562E+03 I	2
39	.9776465E+03 I	2
40	.1000665E+04 I	2
41	.9836157E+03 I	2
42	.9860153E+03 I	2
43	.9996800E+03 I	1
44	.9798241E+03 I	2
45	.9844831E+03 I	2
46	.9970736E+03 I	2
47	.1067772E+04 I	
48	.1084831E+04 I	
49	.1010538E+04 I	

THE TOTAL TIME IS 288.0 YEARS

Figure 20e

NO	STRESS	STRESS (RAPS) 950 960 970 980 990 1000
1	.1014627E+04	I
2	.1379364E+04	I
3	.1368912E+04	I
4	.9877205E+03	I 2
5	.9905397E+03	I 2
6	.9864794E+03	I 2
7	.9925862E+03	I 2
8	.9916813E+03	I 2
9	.9900806E+03	I 2
10	.9824590E+03	I 2
11	.9764641E+03	I 2
12	.9961375E+03	I 1
13	.9762240E+03	I 2
14	.9924396E+03	I 2
15	.9932051E+03	I 2
16	.9820210E+03	I 2
17	.9993192E+03	I 1
18	.9793654E+03	I 2
19	.9840984E+03	I 2
20	.9895651E+03	I 2
21	.9953998E+03	I 2
22	.9759938E+03	I 3
23	.9816323E+03	I 2
24	.9789694E+03	I 2
25	.9720865E+03	I 2
26	.9895557E+03	I 2
27	.9875827E+03	I 2
28	.9886332E+03	I 2
29	.9911119E+03	I 2
30	.9920924E+03	I 2
31	.9995823E+03	I 1
32	.9833091E+03	I 2
33	.9906192E+03	I 2
34	.9834559E+03	I 2
35	.1003084E+04	I 2
36	.9886944E+03	I 2
37	.9808226E+03	I 2
38	.9716201E+03	I 2
39	.9750233E+03	I 2
40	.9708240E+03	I 2
41	.9815658E+03	I 2
42	.9830344E+03	I 2
43	.1000369E+04	I 2
44	.9810507E+03	I 2
45	.9856724E+03	I 2
46	.9982224E+03	I 2
47	.1062684E+04	I
48	.1045943E+04	I
49	.1011539E+04	I

THE TOTAL TIME IS 292.0 YEARS

Figure 20f

NO	STRESS	STRESS (MPa) 950 960 970 980 990 1000
1	.1015122E+04	I
2	.1073947E+04	I
3	.1069460E+04	I
4	.9883037E+03	I 2
5	.9911139E+03	I 2
6	.9870589E+03	I 2
7	.9931538E+03	I 2
8	.9922579E+03	I 2
9	.9956660E+03	I 2
10	.9830371E+03	I 2
11	.9770485E+03	I 2
12	.9967161E+03	I 1
13	.9766031E+03	I 2
14	.9930187E+03	I 2
15	.9937779E+03	I 2
16	.9825947E+03	I 2
17	.9998956E+03	I 1
18	.9799586E+03	I 2
19	.9846834E+03	I 2
20	.9964329E+03	I 2
21	.9959736E+03	I 2
22	.9765736E+03	I 3
23	.9822081E+03	I 2
24	.9795566E+03	I 2
25	.9726734E+03	I 2
26	.9901224E+03	I 2
27	.9881626E+03	I 2
28	.9892115E+03	I 2
29	.9916956E+03	I 2
30	.9926833E+03	I 2
31	.1000203E+04	I 2
32	.9840176E+03	I 2
33	.9910736E+03	I 2
34	.9808352E+03	I 2
35	.9705681E+03	I 2
36	.9854561E+03	I 2
37	.9812934E+03	I 2
38	.9723688E+03	I 2
39	.9757476E+03	I 2
40	.9715736E+03	I 2
41	.9820352E+03	I 2
42	.9863907E+03	I 2
43	.9707199E+03	I 2
44	.9748397E+03	I 2
45	.9861384E+03	I 2
46	.9989269E+03	I 2
47	.1066506E+04	I
48	.1086524E+04	I
49	.1012047E+04	I

THE TOTAL TIME IS 294.0 YEARS

Figure 20g

NO	STRESS	STRESS (RMS) 95(96(97(98(99(1.
1	.1015617E+04 I	
2	.1040510E+04 I	
3	.1070038E+04 I	
4	.9818865E+03 I	2
5	.9916859E+03 I	2
6	.9876379E+03 I	2
7	.9937209E+03 I	2
8	.9928342E+03 I	2
9	.9912311E+03 I	2
10	.9836147E+03 I	2
11	.9776165E+03 I	2
12	.9972943E+03 I	1
13	.9773819E+03 I	2
14	.9935814E+03 I	2
15	.9943504E+03 I	2
16	.9831680E+03 I	2
17	.1008472E+04 I	2
18	.9805315E+03 I	2
19	.9852681E+03 I	2
20	.9910004E+03 I	2
21	.9965471E+03 I	2
22	.9771533E+03 I	3
23	.9827844E+03 I	2
24	.9861463E+03 I	2
25	.9732691E+03 I	2
26	.9907167E+03 I	2
27	.9868135E+03 I	2
28	.9899196E+03 I	2
29	.9921517E+03 I	2
30	.9900266E+03 I	2
31	.9737749E+03 I	2
32	.9814028E+03 I	2
33	.9915277E+03 I	2
34	.9815489E+03 I	2
35	.9712314E+03 I	2
36	.9860570E+03 I	2
37	.9818915E+03 I	2
38	.9729586E+03 I	2
39	.9763295E+03 I	2
40	.9721619E+03 I	2
41	.9826132E+03 I	2
42	.9869632E+03 I	2
43	.9713109E+03 I	2
44	.9790208E+03 I	2
45	.9867183E+03 I	2
46	.9994954E+03 I	2
47	.1070061E+04 I	
48	.1037079E+04 I	
49	.1012546E+04 I	

THE TOTAL TIME IS 236.0 YEARS

Figure 20h

NO	STRESS	STRESS (BARS) 950 960 970 980 990 10.
1	.1018036E+04	I
2	.1083317E+04	I
3	.1072742E+04	I
4	.9917951E+03	I 2
5	.9945451E+03	I 2
6	.9905276E+03	I 2
7	.9965515E+03	I 2
8	.9957103E+03	I 2
9	.9941020E+03	I 2
10	.9865036E+03	I 2
11	.9805004E+03	I 2
12	.1000207E+04	I 2
13	.9803425E+03	I 2
14	.9965637E+03	I 2
15	.9970935E+03	I 2
16	.9828513E+03	I 2
17	.9727748E+03	I 2
18	.9802240E+03	I 2
19	.9880763E+03	I 2
20	.9939683E+03	I 2
21	.9994820E+03	I 2
22	.9800732E+03	I 2
23	.9656654E+03	I 2
24	.9830779E+03	I 2
25	.9761966E+03	I 2
26	.9935420E+03	I 2
27	.9917007E+03	I 2
28	.9927653E+03	I 2
29	.9950181E+03	I 2
30	.9928636E+03	I 2
31	.9737381E+03	I 2
32	.9842925E+03	I 2
33	.9943728E+03	I 2
34	.9844390E+03	I 2
35	.9741807E+03	I 2
36	.9889157E+03	I 2
37	.9847698E+03	I 2
38	.9758685E+03	I 2
39	.9792319E+03	I 2
40	.9751050E+03	I 2
41	.9855226E+03	I 2
42	.9898873E+03	I 2
43	.9743816E+03	I 2
44	.9818157E+03	I 2
45	.9866684E+03	I 2
46	.9723392E+03	I 3
47	.1070026E+04	I
48	.1089754E+04	I
49	.1015133E+04	I

THE TOTAL TIME IS 306.6 YEARS

Figure 21

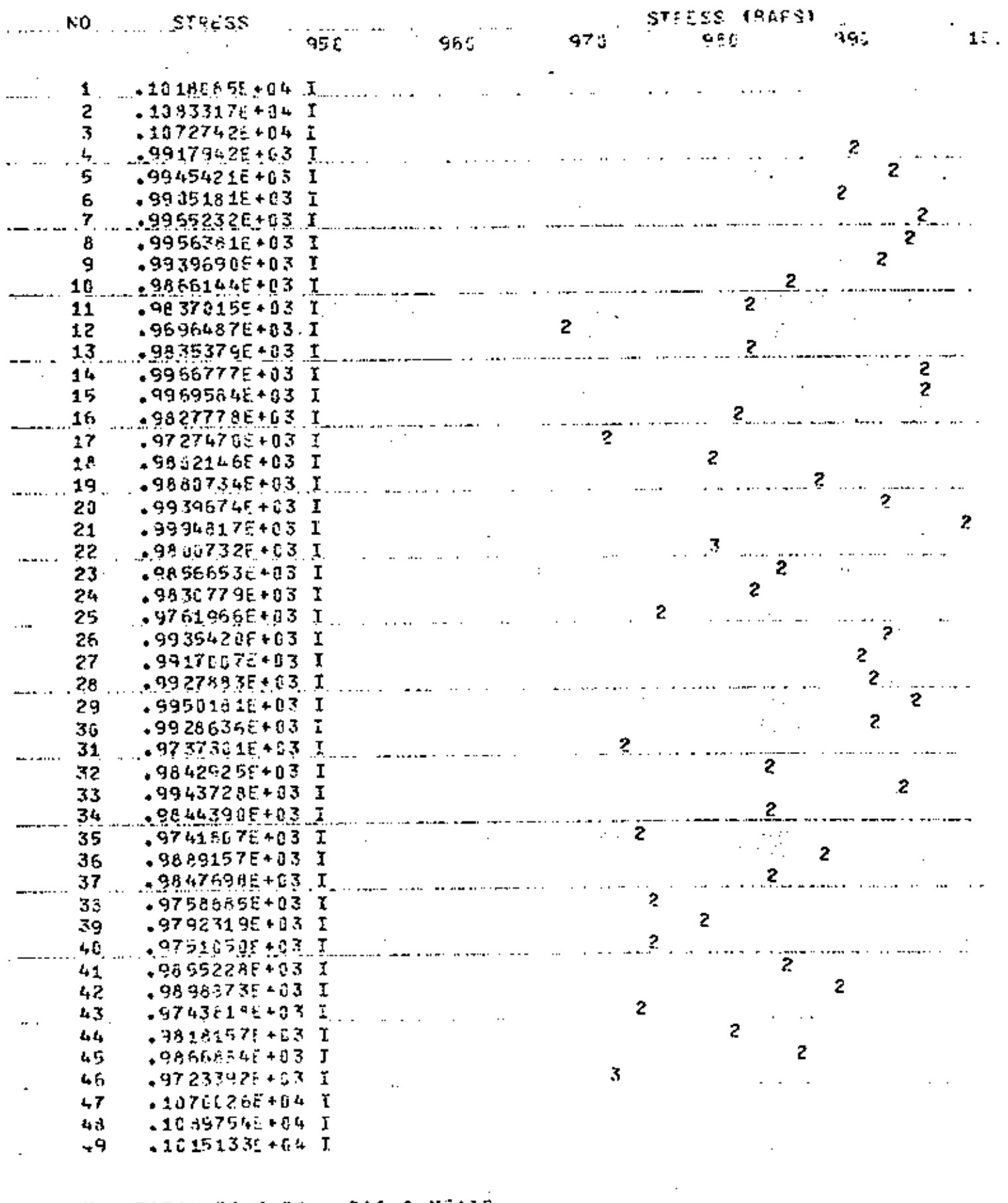

THE TOTAL TIME IS 306.0 YEARS

Figure 22

NO	STRESS	STRESS (BARS) 95(96(97(98(99(1...
1	.1048630E+04	I
2	.1116010E+04	I
3	.1102432E+04	I
4	.9788233E+03	I 4
5	.9942632E+03	I 3
6	.9832473E+03	I 3
7	.9961145E+03	I 3
8	.9903098E+03	I 4
9	.9748251E+03	I 4
10	.9836100E+03	I 3
11	.9816579E+03	I 3
12	.9683377E+03	I 3
13	.9811772E+03	I 3
14	.9719419E+03	I 4
15	.9726143E+03	I 4
16	.9796638E+03	I 3
17	.9715599E+03	I 3
18	.9781078E+03	I 3
19	.9986683E+03	I 3
20	.9954153E+03	I 3
21	.9987026E+03	I 3
22	.9826909E+03	I 4
23	.9882952E+03	I 3
24	.9934404E+03	I 3
25	.9746962E+03	I 3
26	.9920041E+03	I 3
27	.9933764E+03	I 3
28	.9952131E+03	I 3
29	.9732192E+03	I 4
30	.9954209E+03	I 3
31	.9742857E+03	I 3
32	.9829989E+03	I 3
33	.9930695E+03	I 3
34	.9830450E+03	I 3
35	.9735563E+03	I 3
36	.9872446E+03	I 3
37	.9832902E+03	I 3
38	.9746139E+03	I 3
39	.9778203E+03	I 3
40	.9737776E+03	I 3
41	.9839312E+03	I 3
42	.9842143E+03	I 3
43	.9735417E+03	I 3
44	.9801305E+03	I 3
45	.9865609E+03	I 3
46	.9766534E+03	I 4
47	.1102153E+04	I
48	.1124842E+04	I
49	.1045894E+04	I

THE TOTAL TIME IS 432.0 YEARS

Figure 23

NO	STRESS	STRESS (BARS) 950 960 970 980 990 1
1	.1078094E+04 I	
2	.1151909E+04 I	
3	.1133656E+04 I	
4	.9861904E+03 I	5
5	.9928582E+03 I	4
6	.9897132E+03 I	4
7	.9953195E+03 I	4
8	.9899079E+03 I	5
9	.9901804E+03 I	5
10	.9858974E+03 I	4
11	.9808354E+03 I	4
12	.9886435E+03 I	4
13	.9818842E+03 I	4
14	.9786917E+03 I	5
15	.9737185E+03 I	5
16	.9796777E+03 I	4
17	.9716686E+03 I	4
18	.9783516E+03 I	4
19	.9858852E+03 I	5
20	.9925890E+03 I	4
21	.9701045E+03 I	5
22	.9820660E+03 I	5
23	.9844758E+03 I	4
24	.9731654E+03 I	5
25	.9734682E+03 I	4
26	.9905038E+03 I	4
27	.9972901E+03 I	4
28	.9763011E+03 I	5
29	.9739259E+03 I	5
30	.9961689E+03 I	4
31	.9760524E+03 I	4
32	.9831679E+03 I	4
33	.9931697E+03 I	4
34	.9831711E+03 I	4
35	.9747028E+03 I	4
36	.9869172E+03 I	4
37	.9833341E+03 I	4
38	.9749443E+03 I	4
39	.9779817E+03 I	4
40	.9741736E+03 I	4
41	.9838739E+03 I	4
42	.9879009E+03 I	4
43	.9745105E+03 I	4
44	.9797774E+03 I	4
45	.9874795E+03 I	4
46	.9797063E+03 I	5
47	.1133691E+04 I	
48	.1157473E+04 I	
49	.1075646E+04 I	

THE TOTAL TIME IS 566.0 YEARS

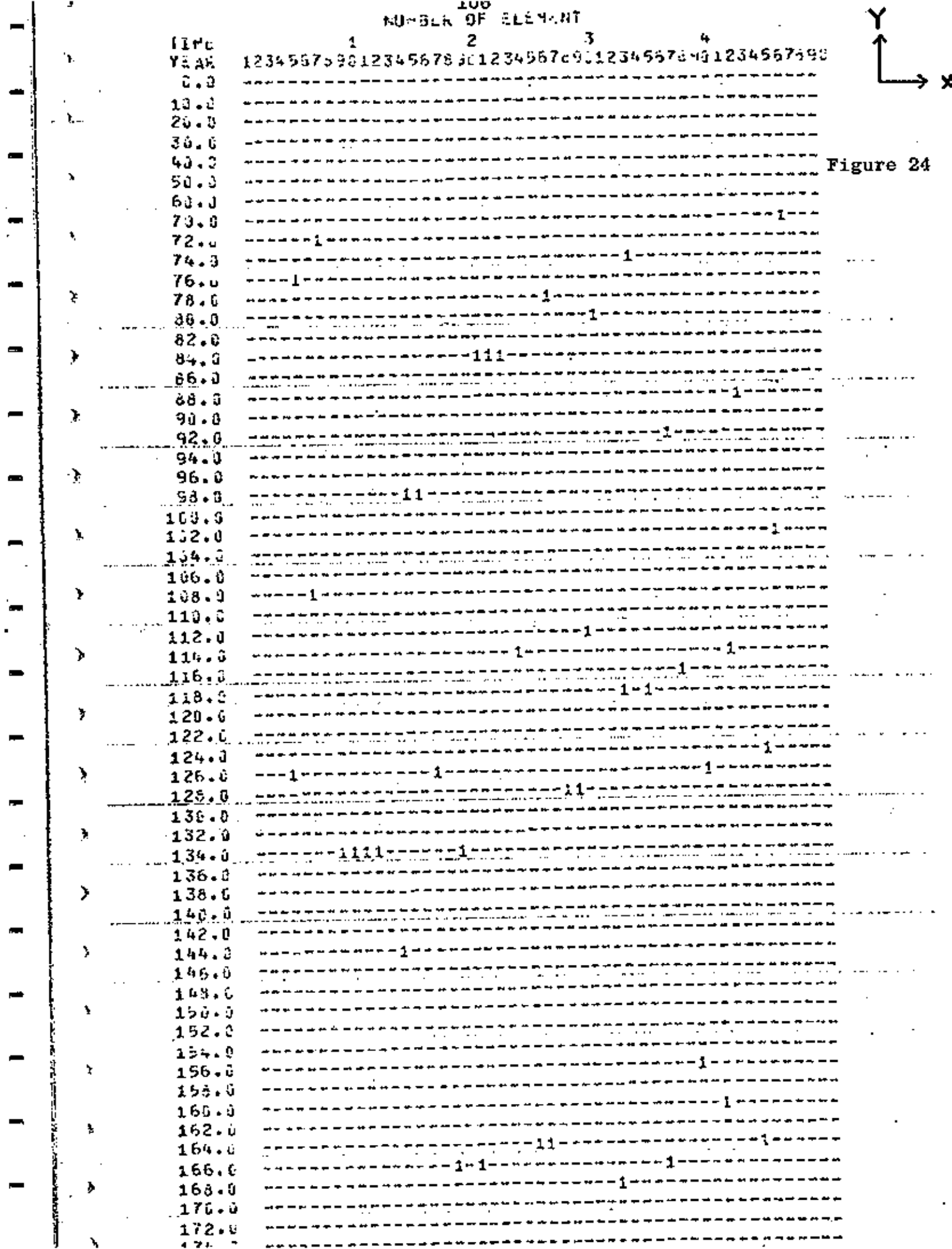

Figure 24

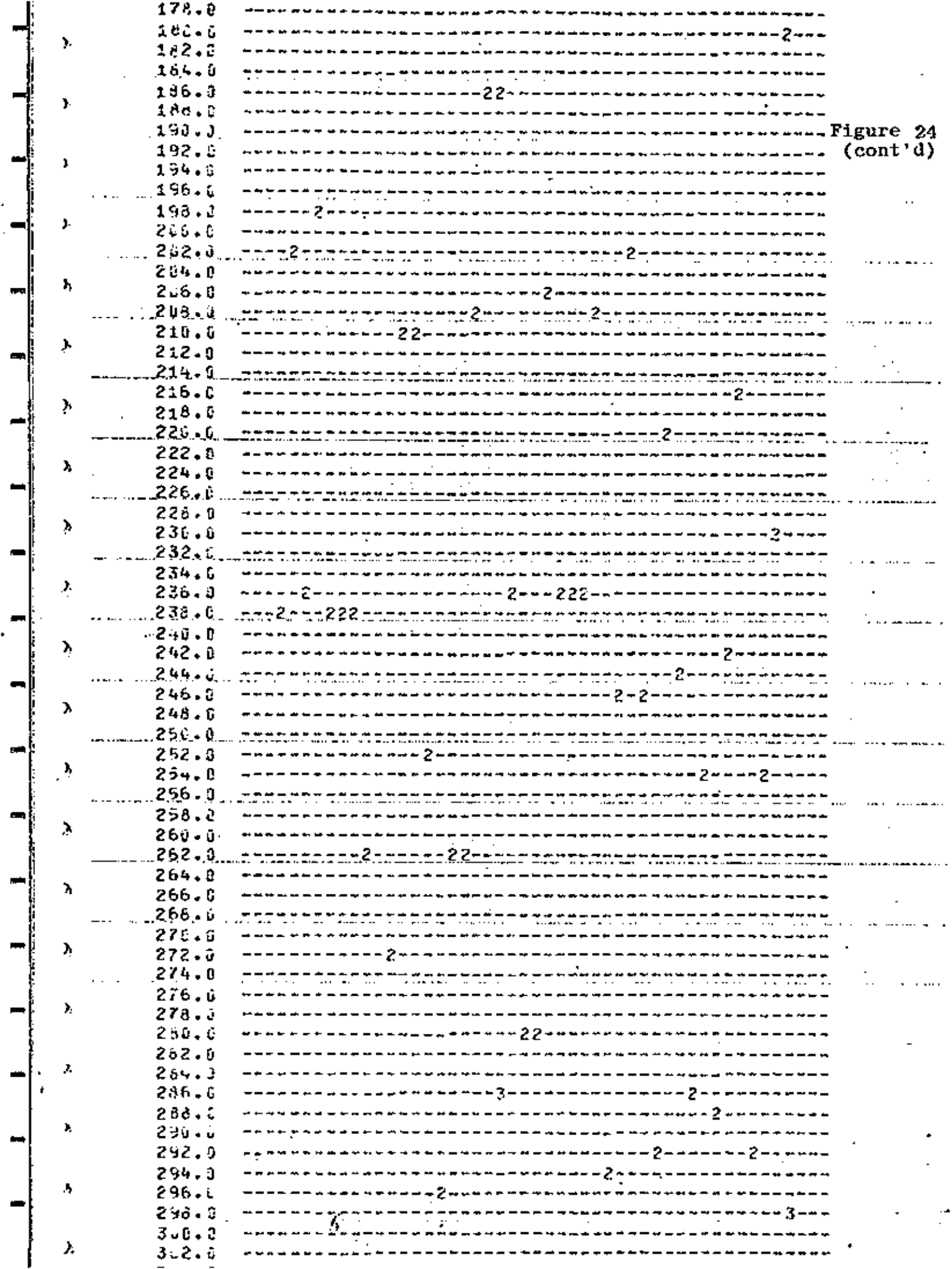

Figure 24 (cont'd)

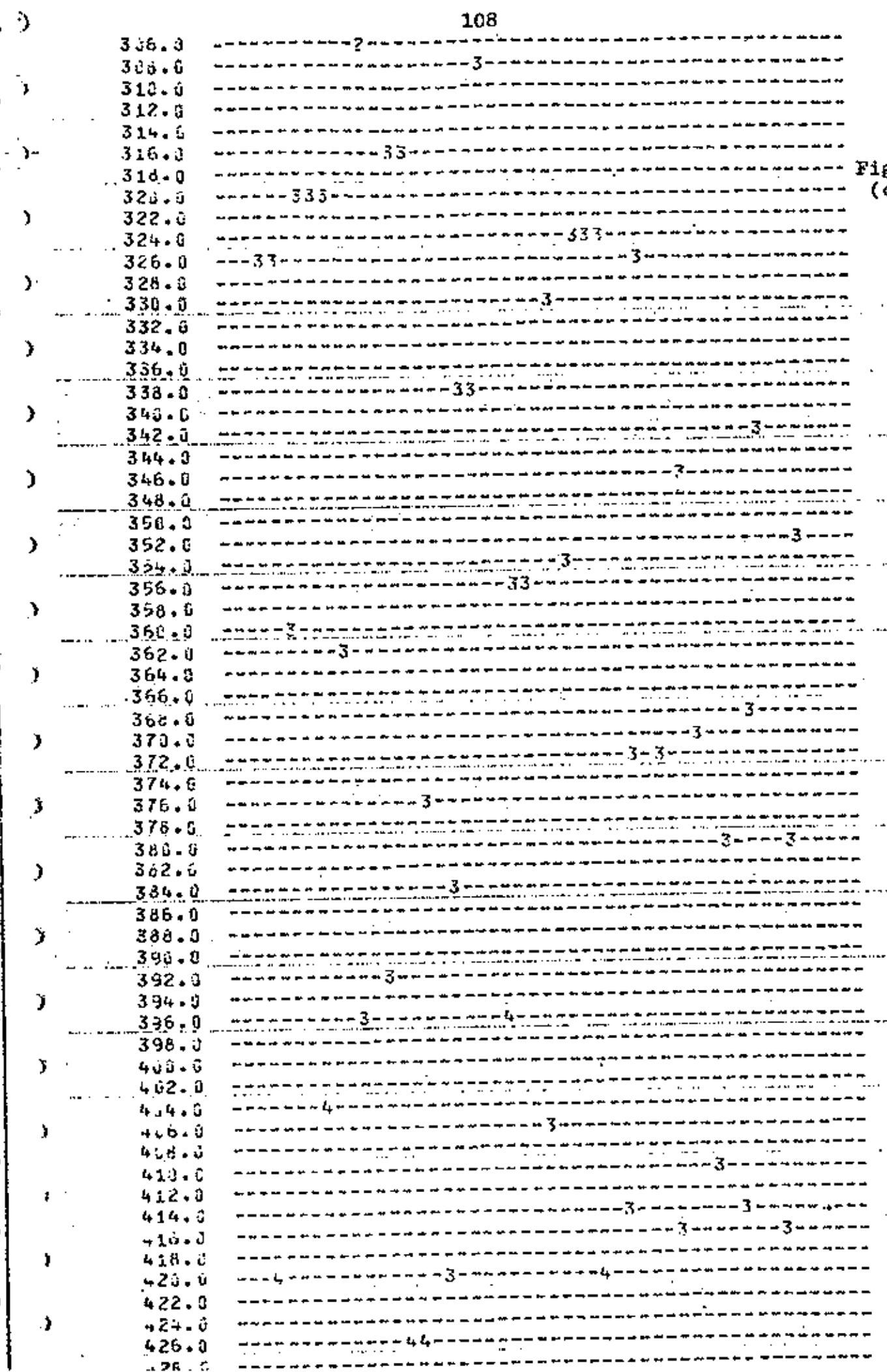

Figure 24 (cont'd)

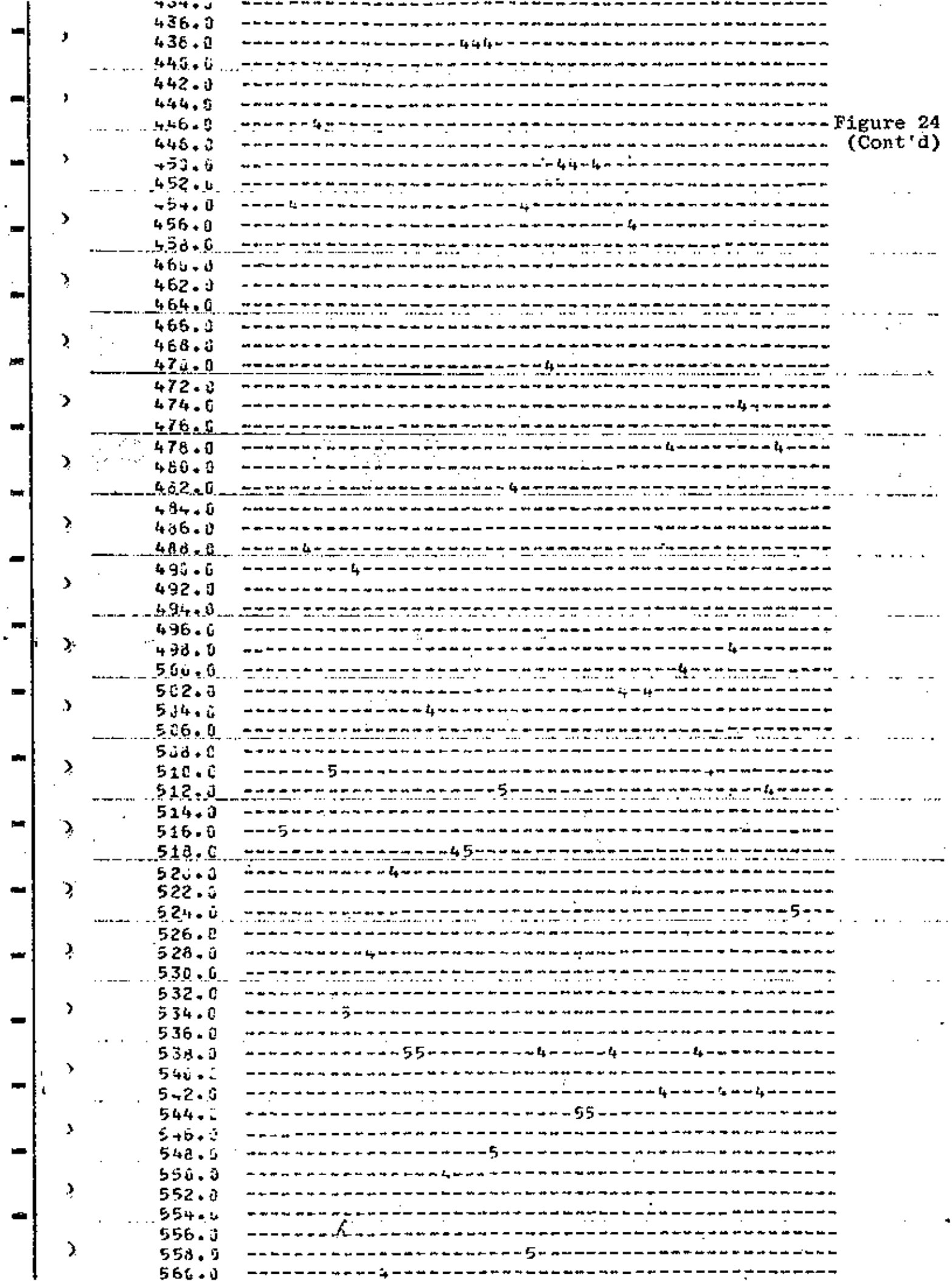

Figure 24
(Cont'd)

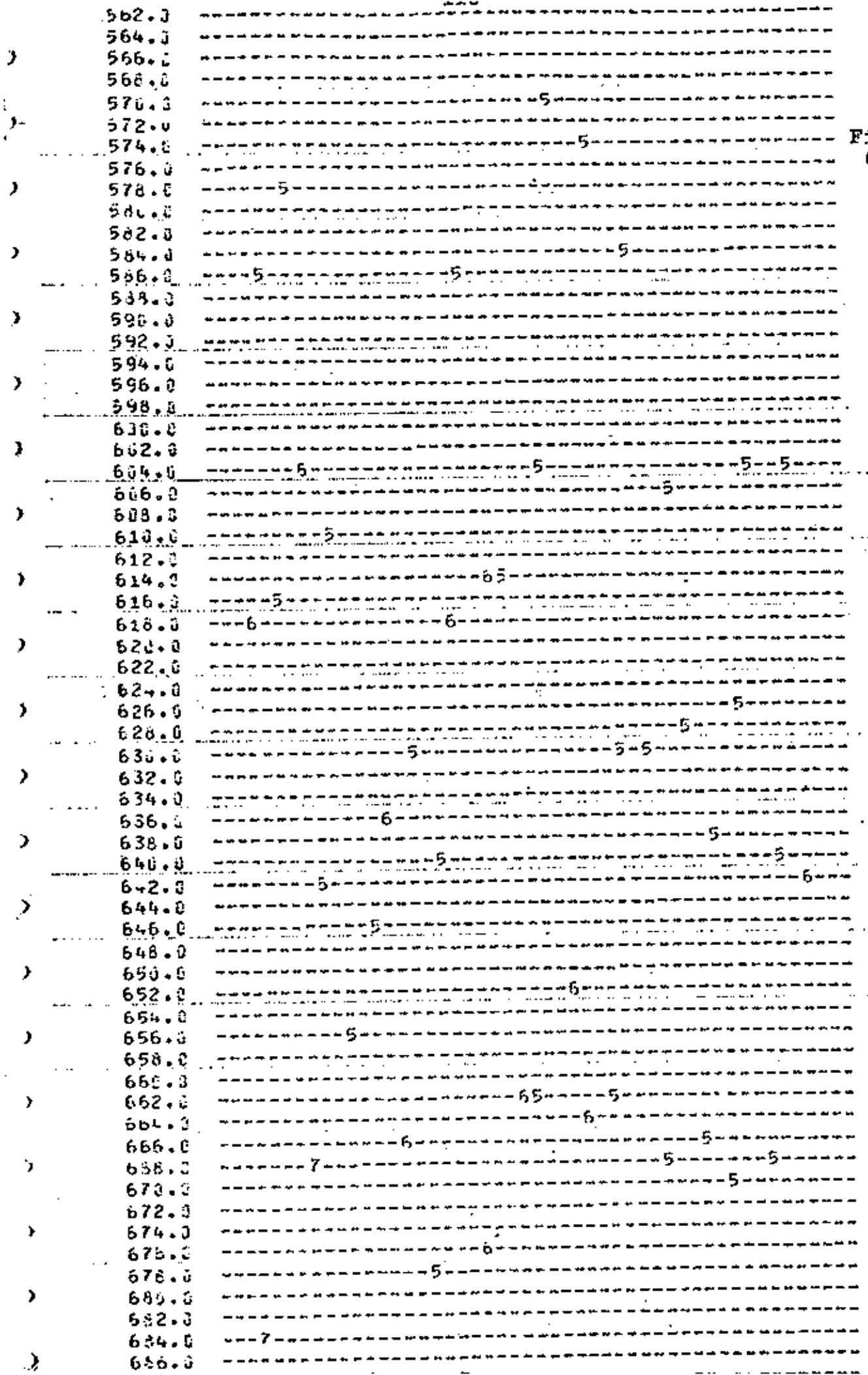

Figure 24
(Cont'd)

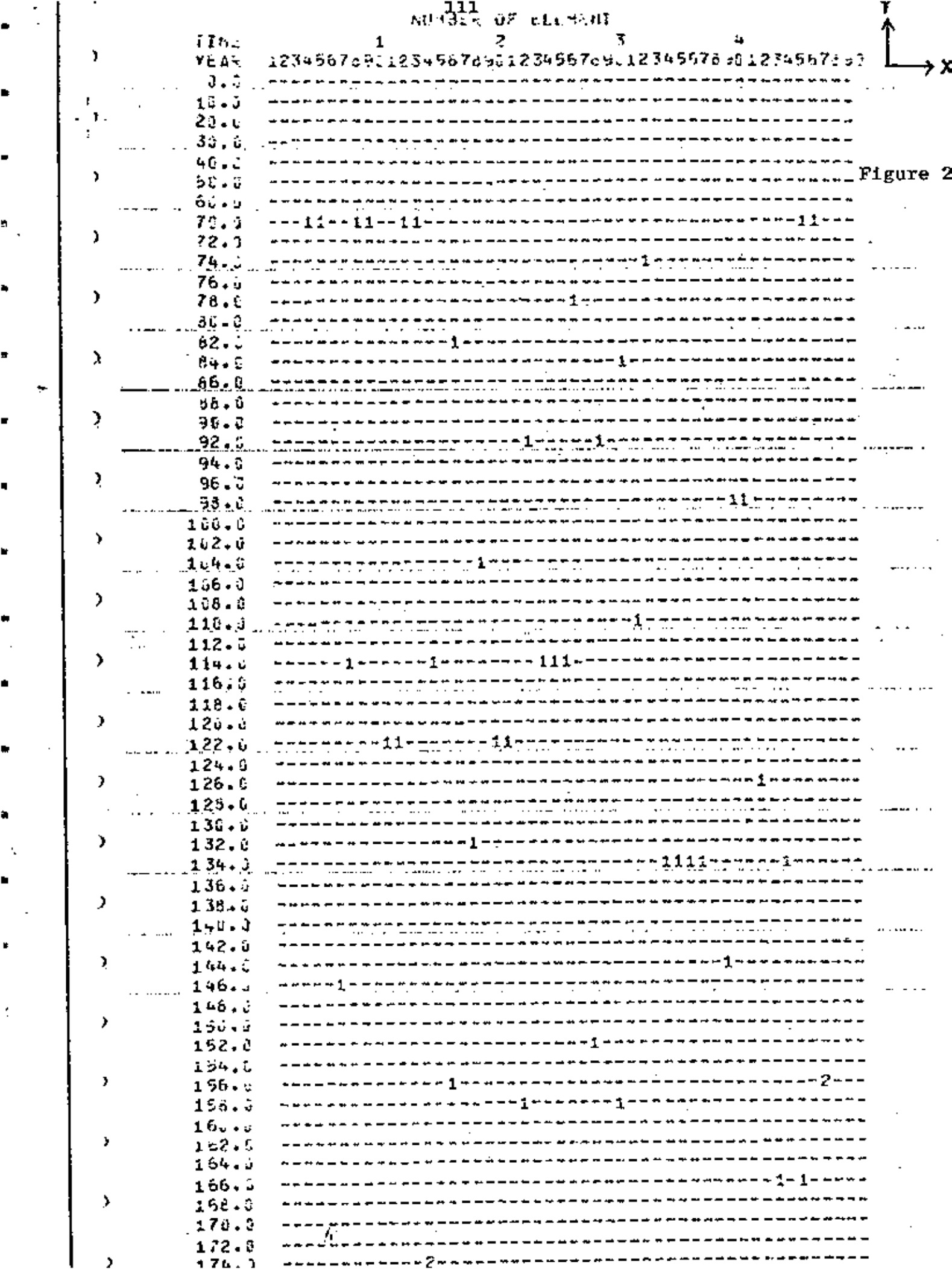

Figure 2

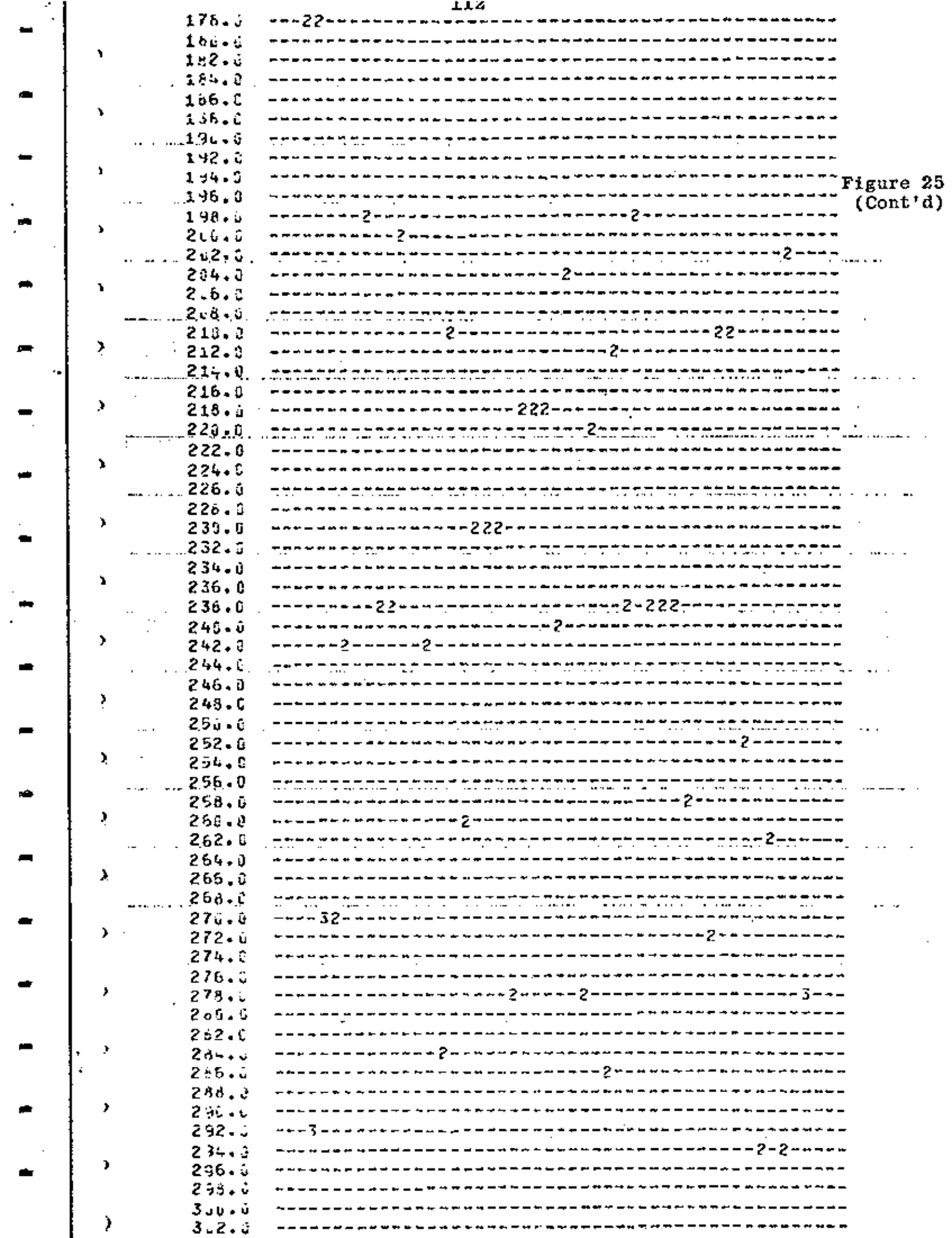

Figure 25 (Cont'd)

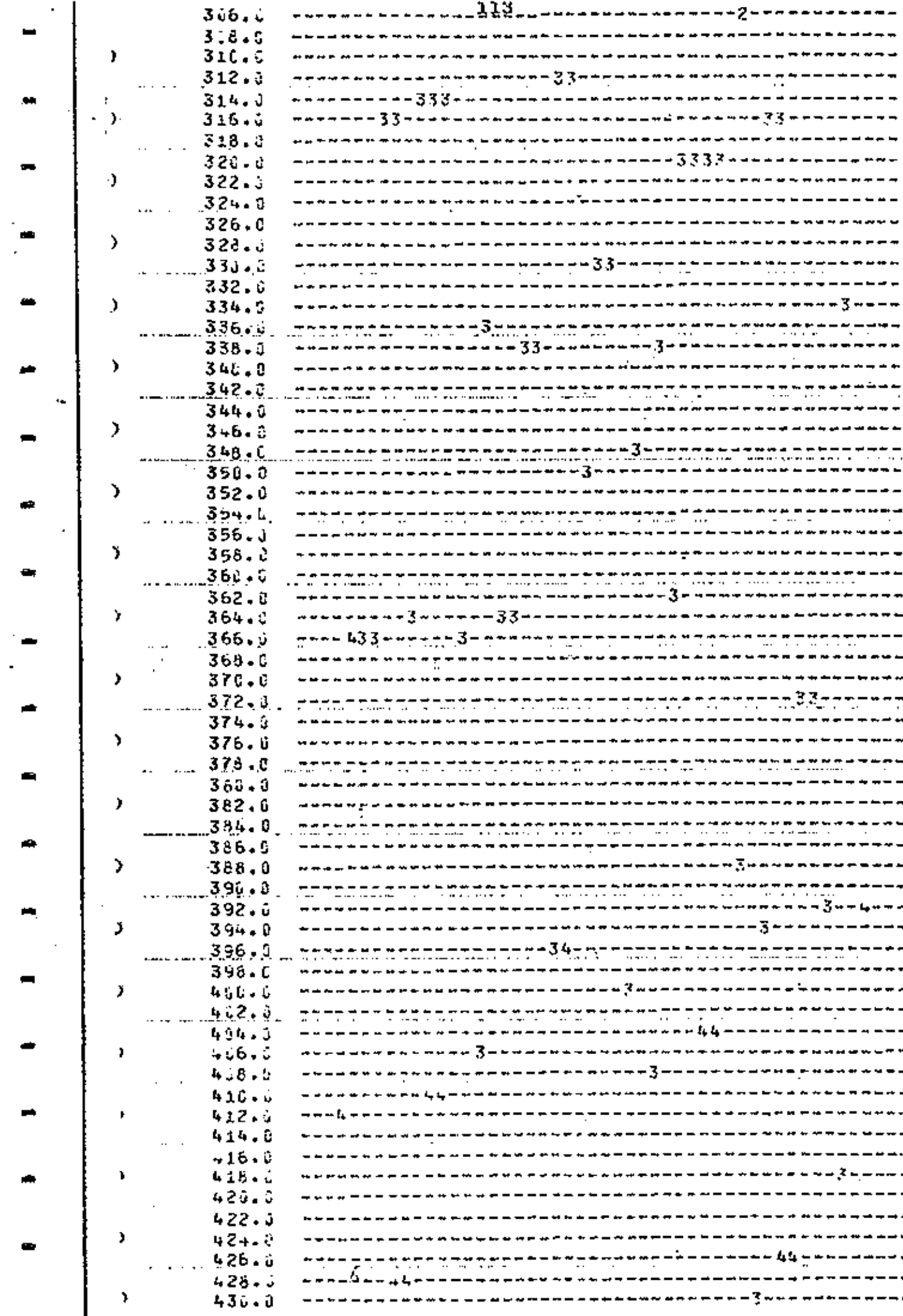

Figure 25 (Cont'd)

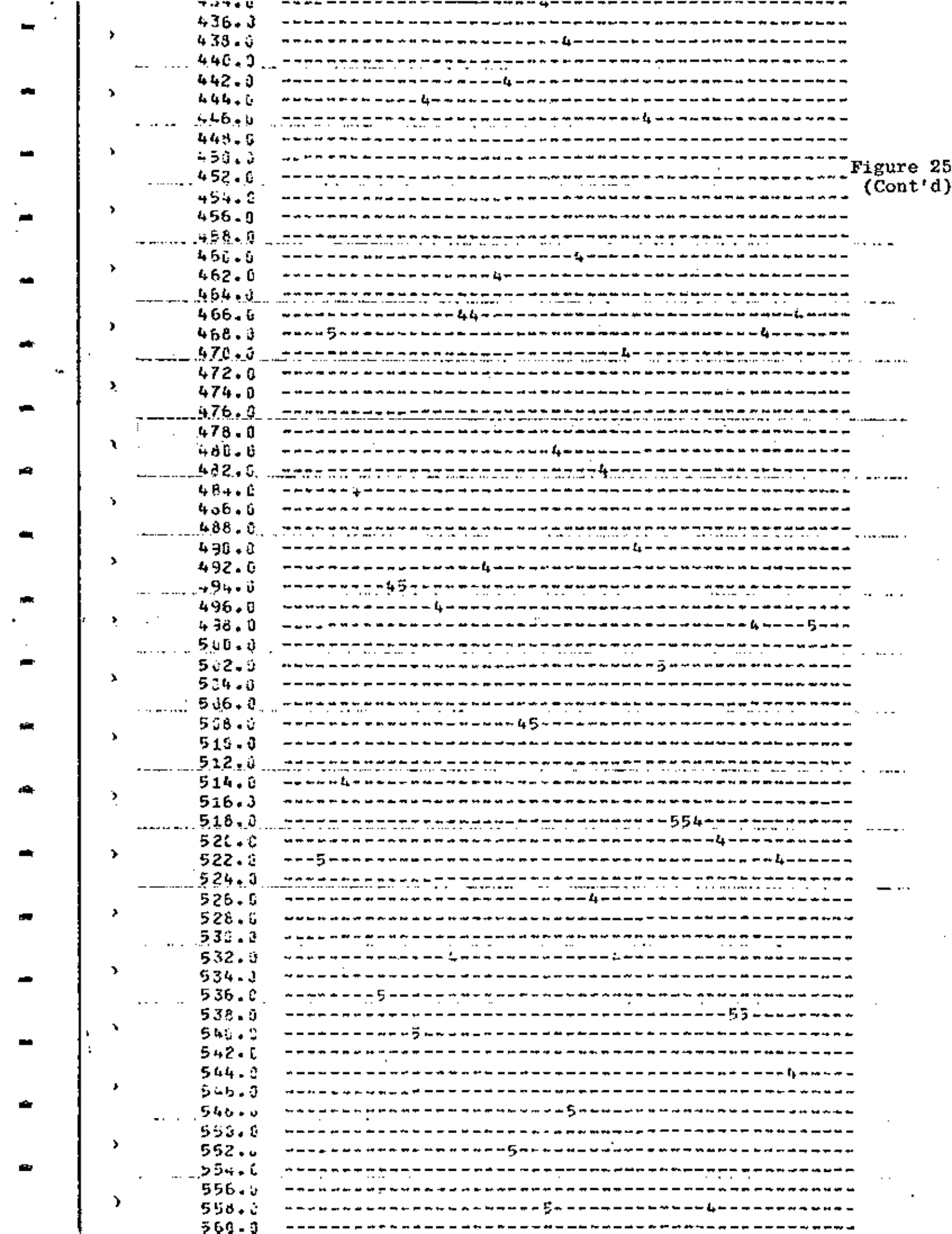

Figure 25
(Cont'd)

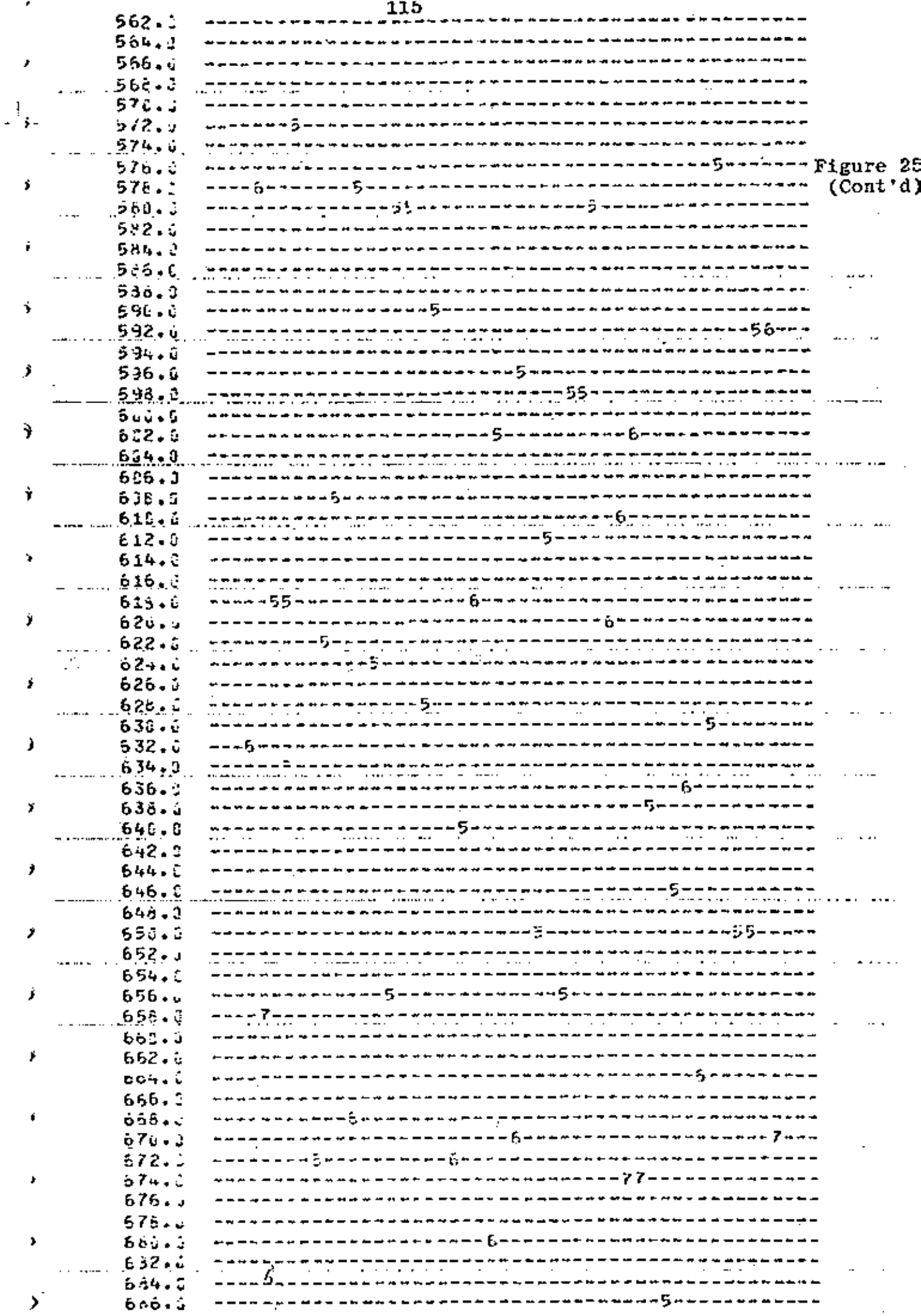

Figure 25 (Cont'd)

Figure 26

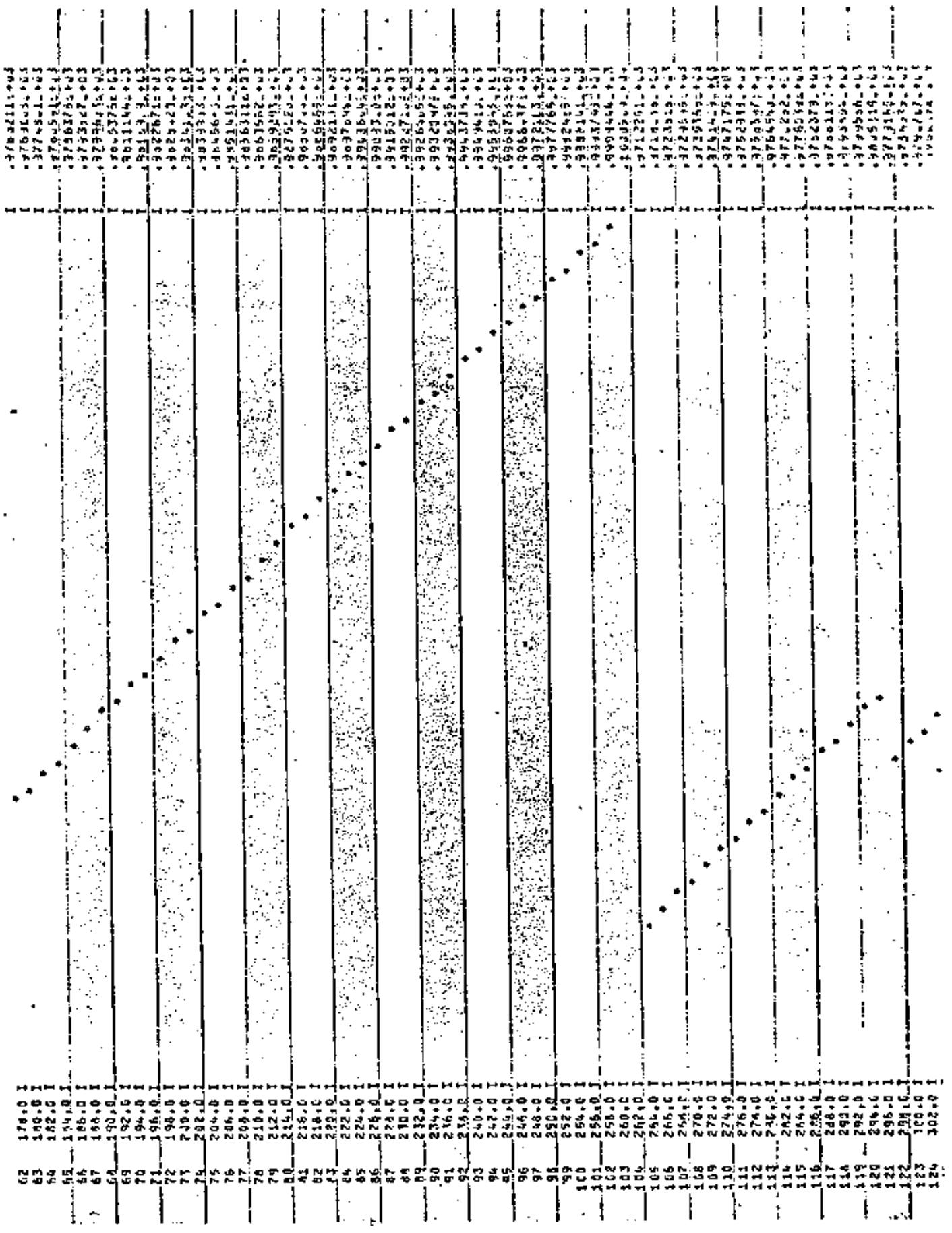

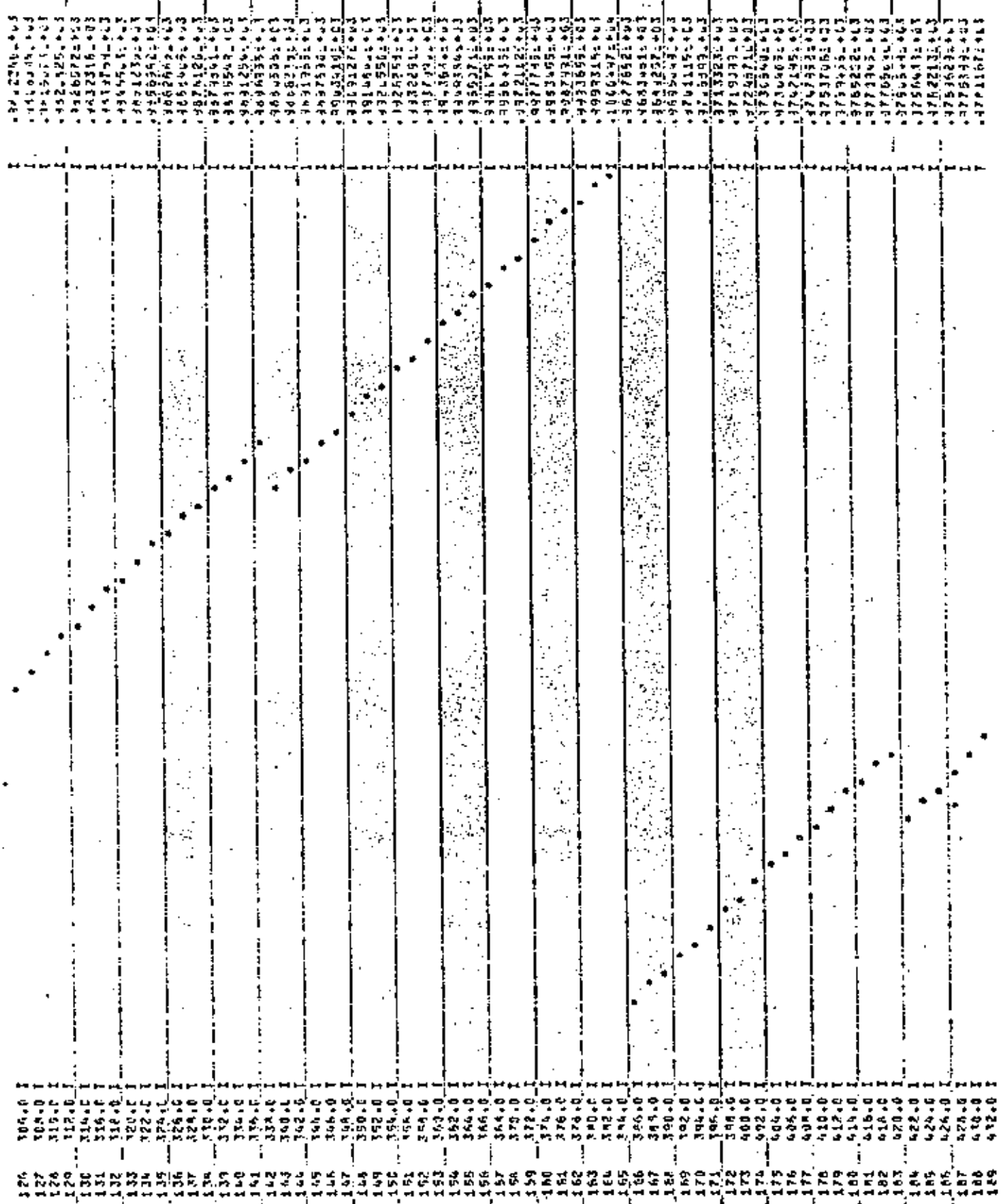

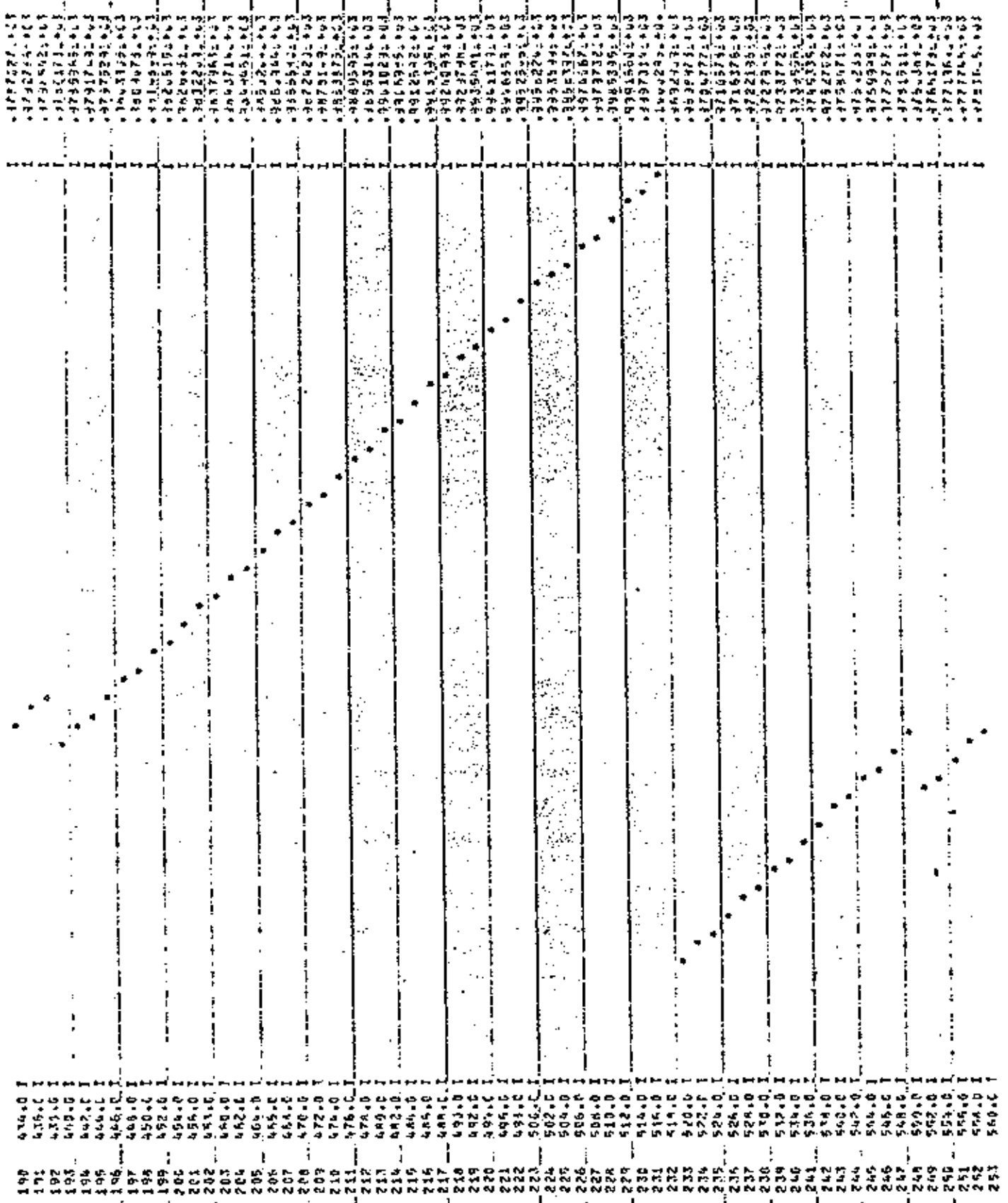

Figure 26 (Cont'd)

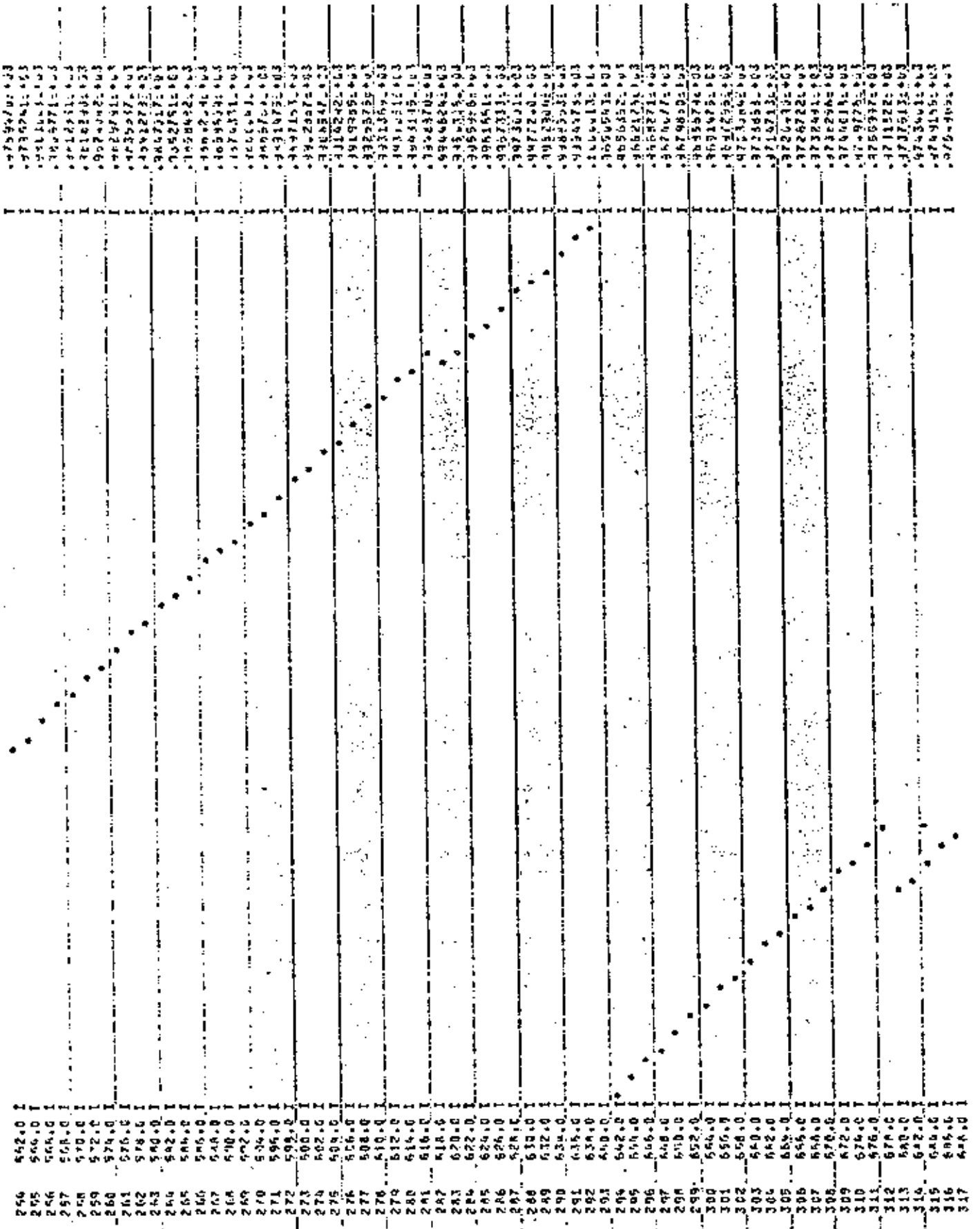

Figure 27

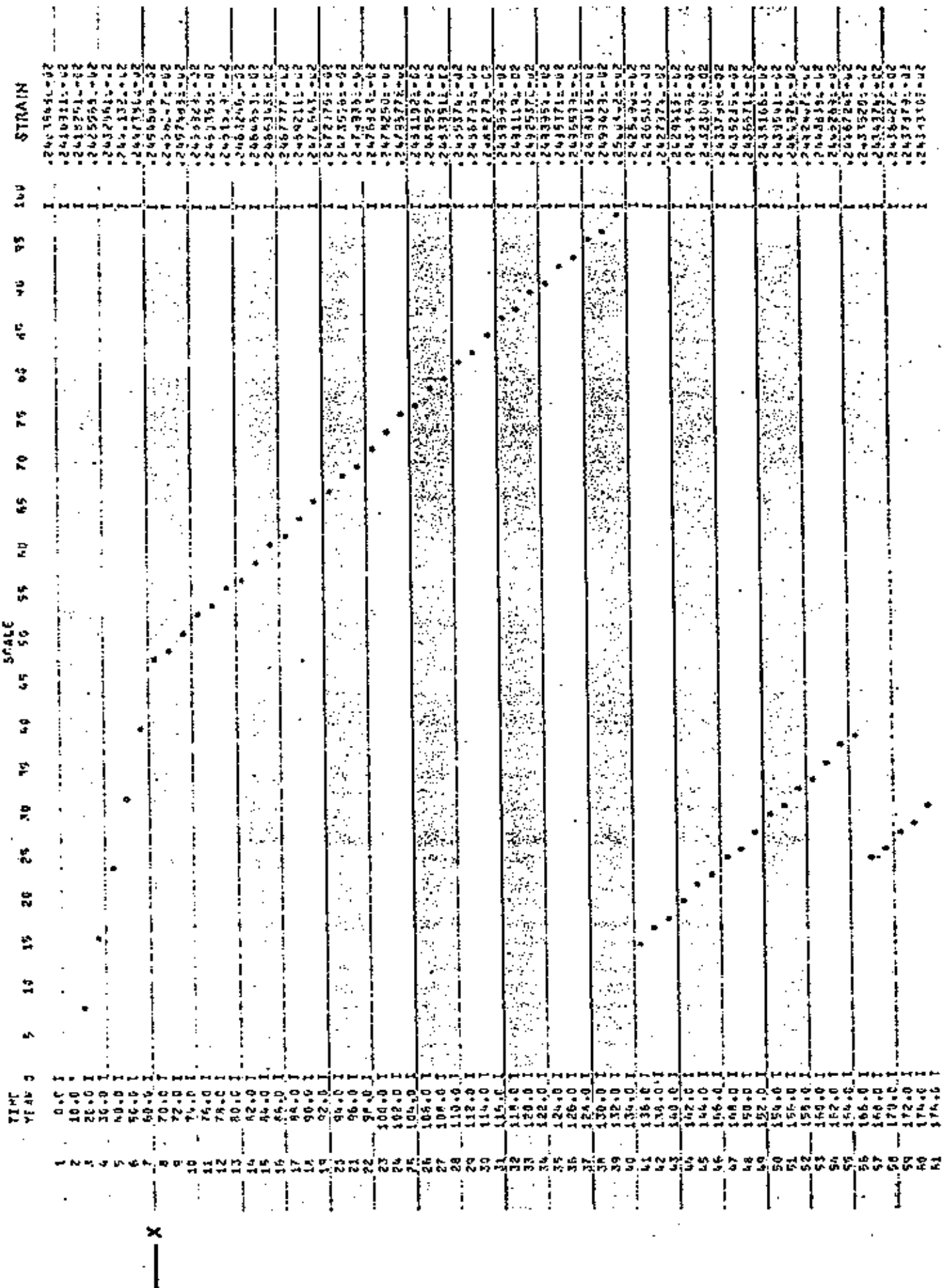

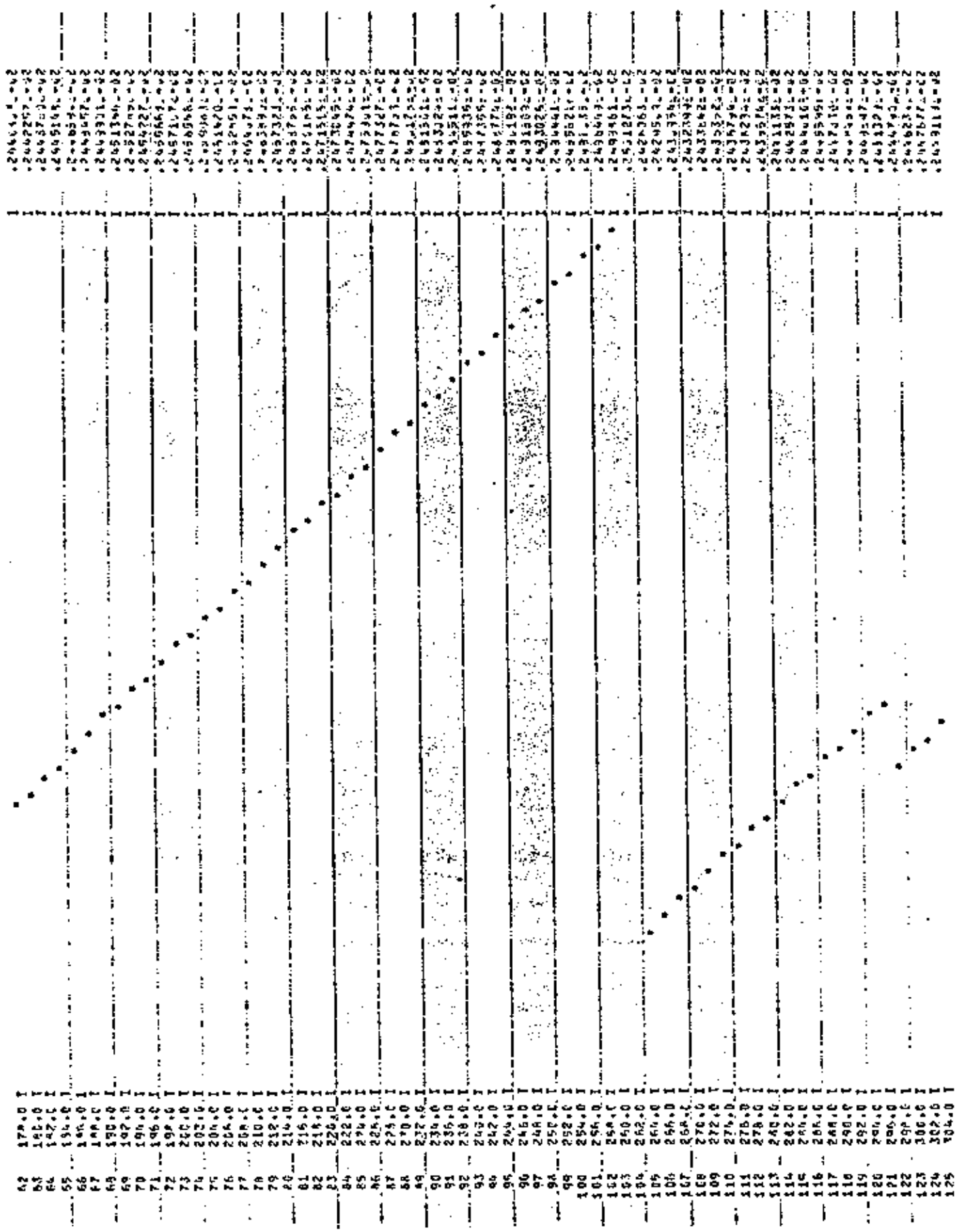

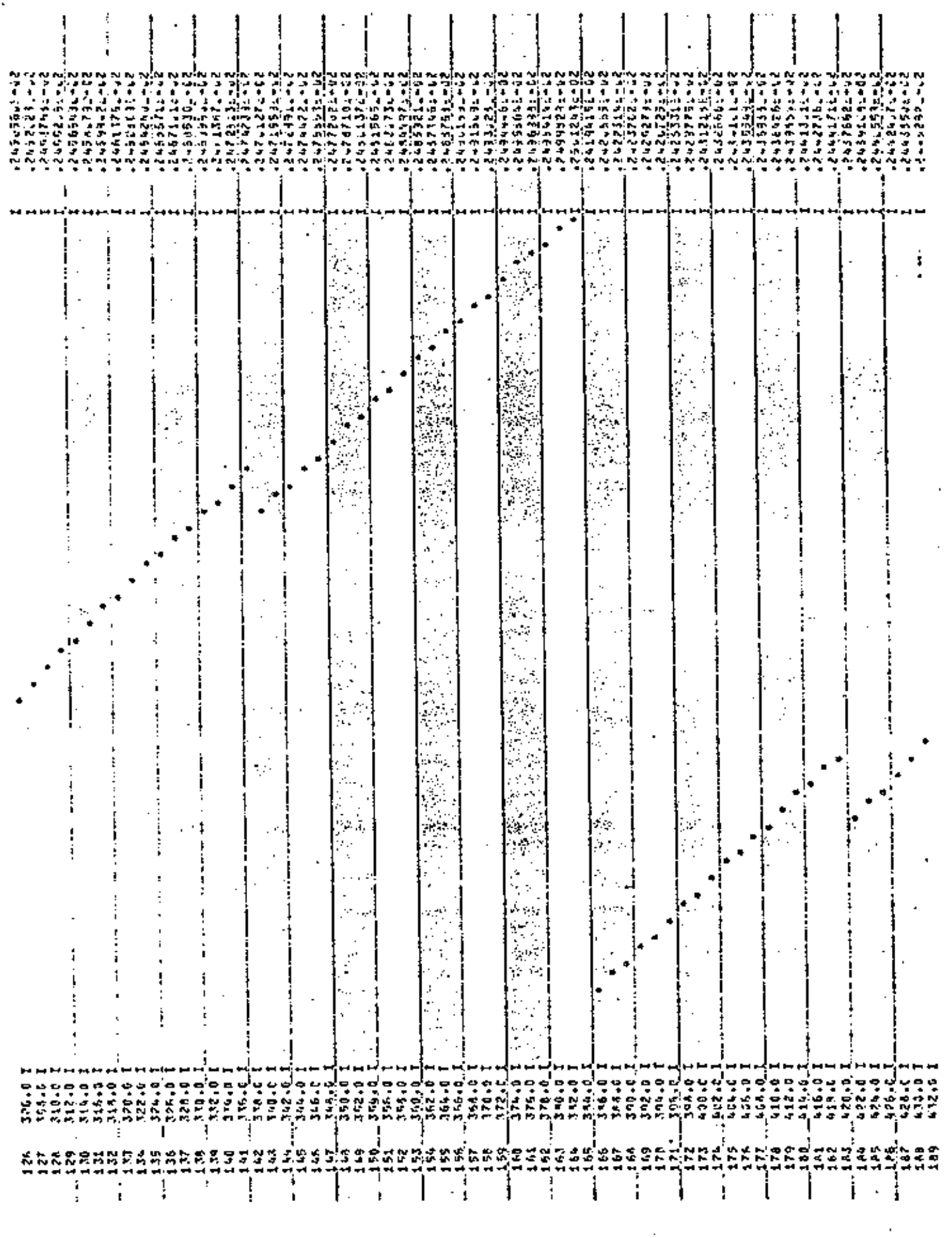

Figure 27 (Cont'd)

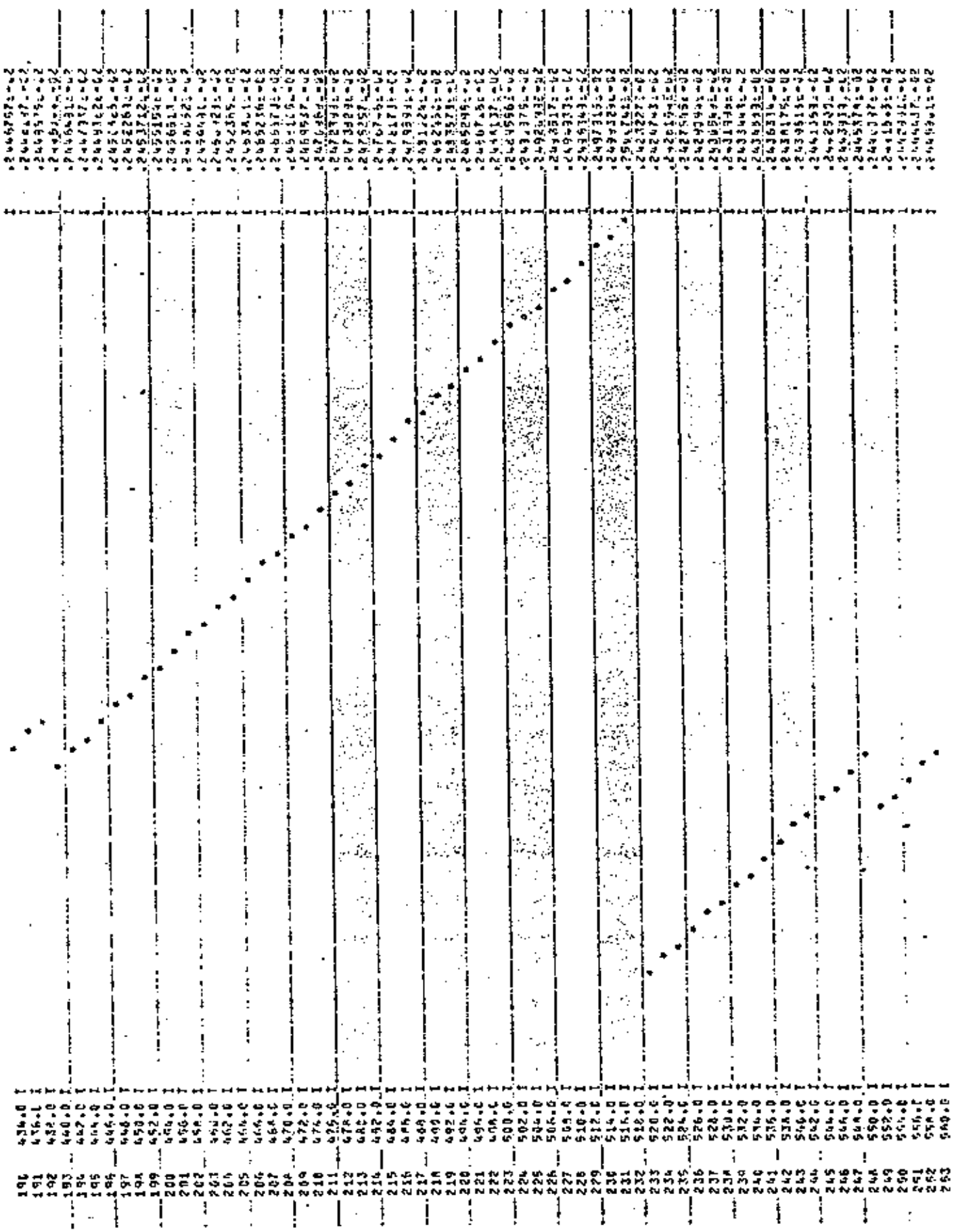

Figure 27 (Cont'd)

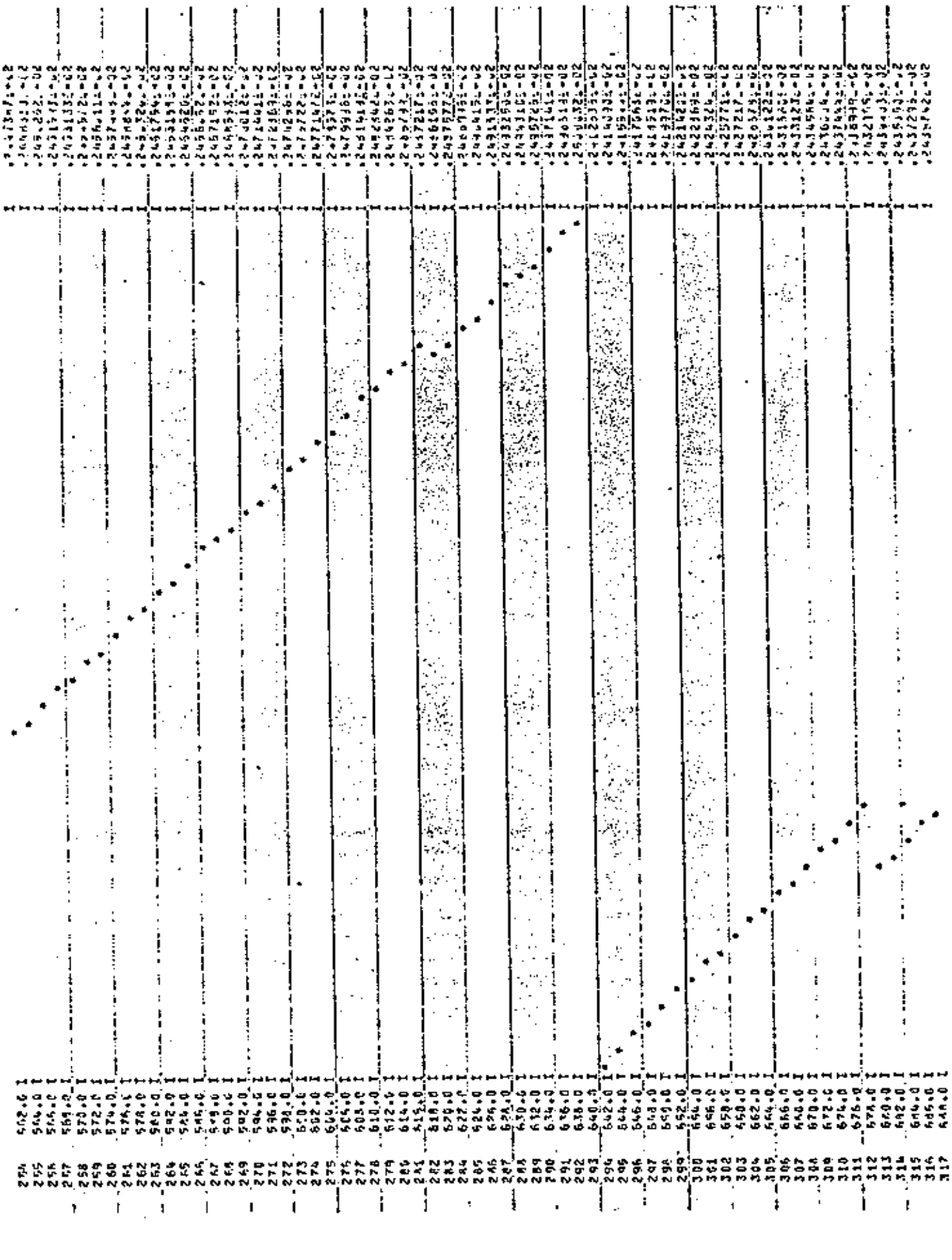

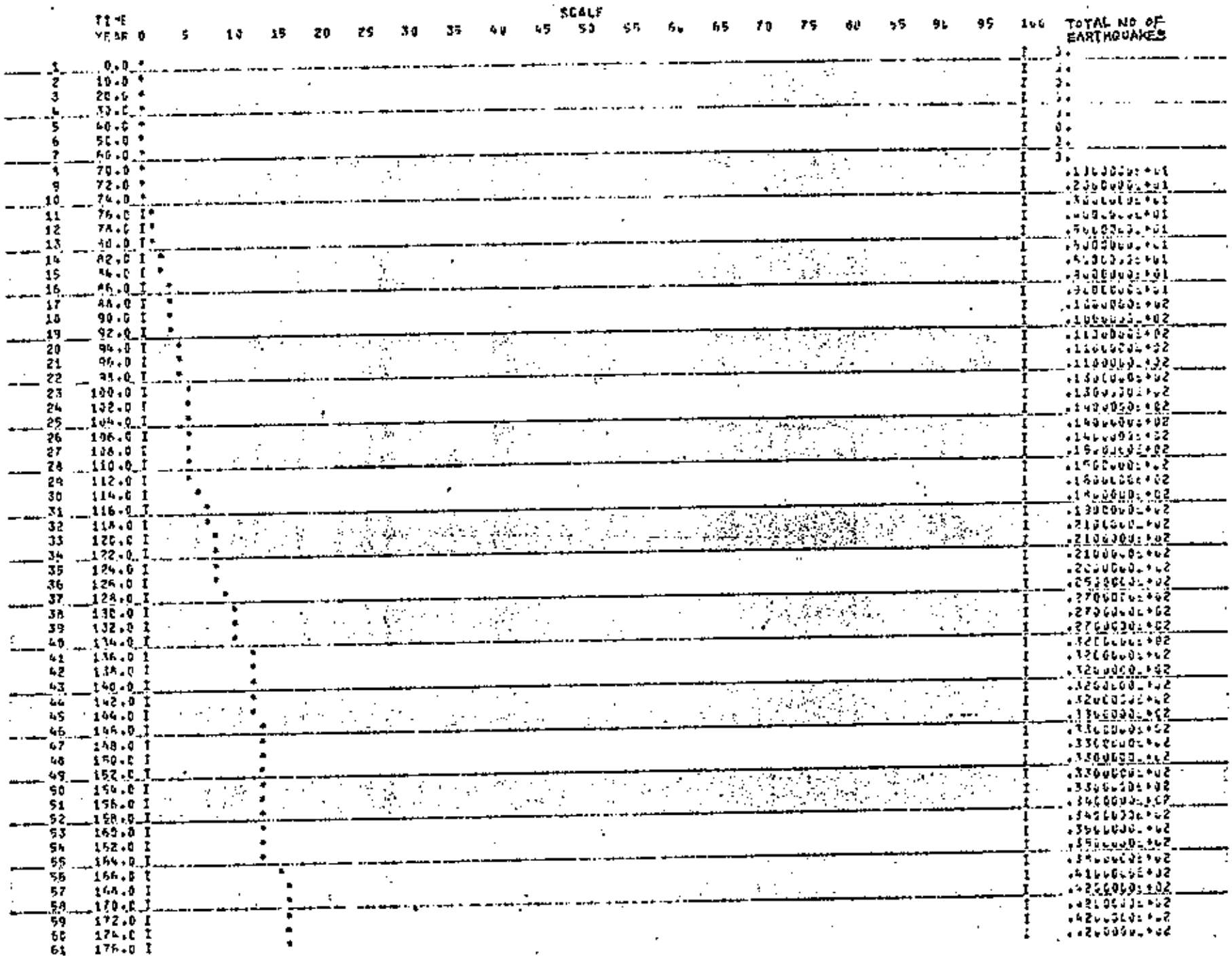
SCALE
TIME
YEAR
0
5
10
15
20
25
30
35
40
45
50
55
60
65
70
75
80
85
90
95
100
TOTAL NO OF EARTHQUAKES

Figure 28

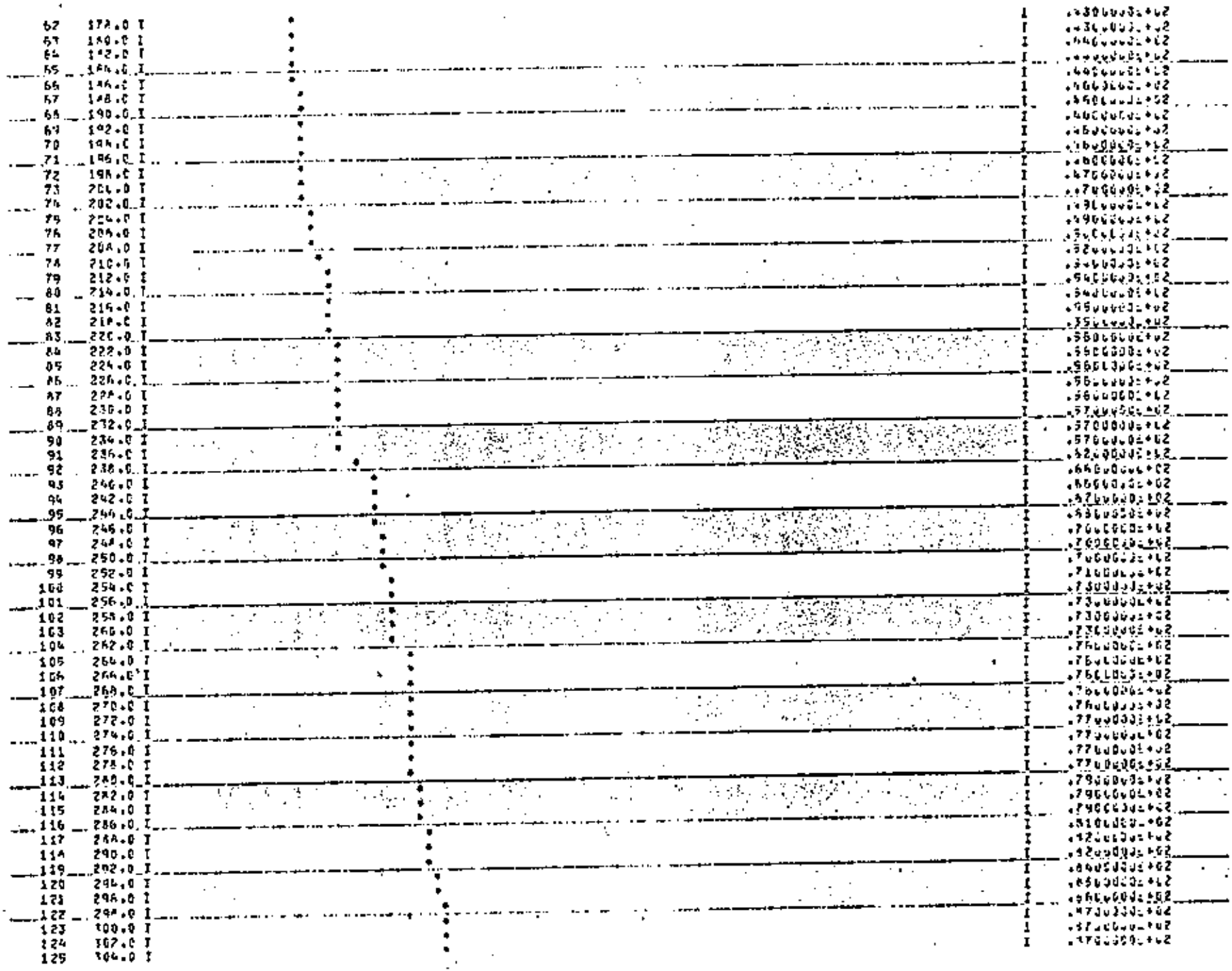

Figure 28 (Cont'd)

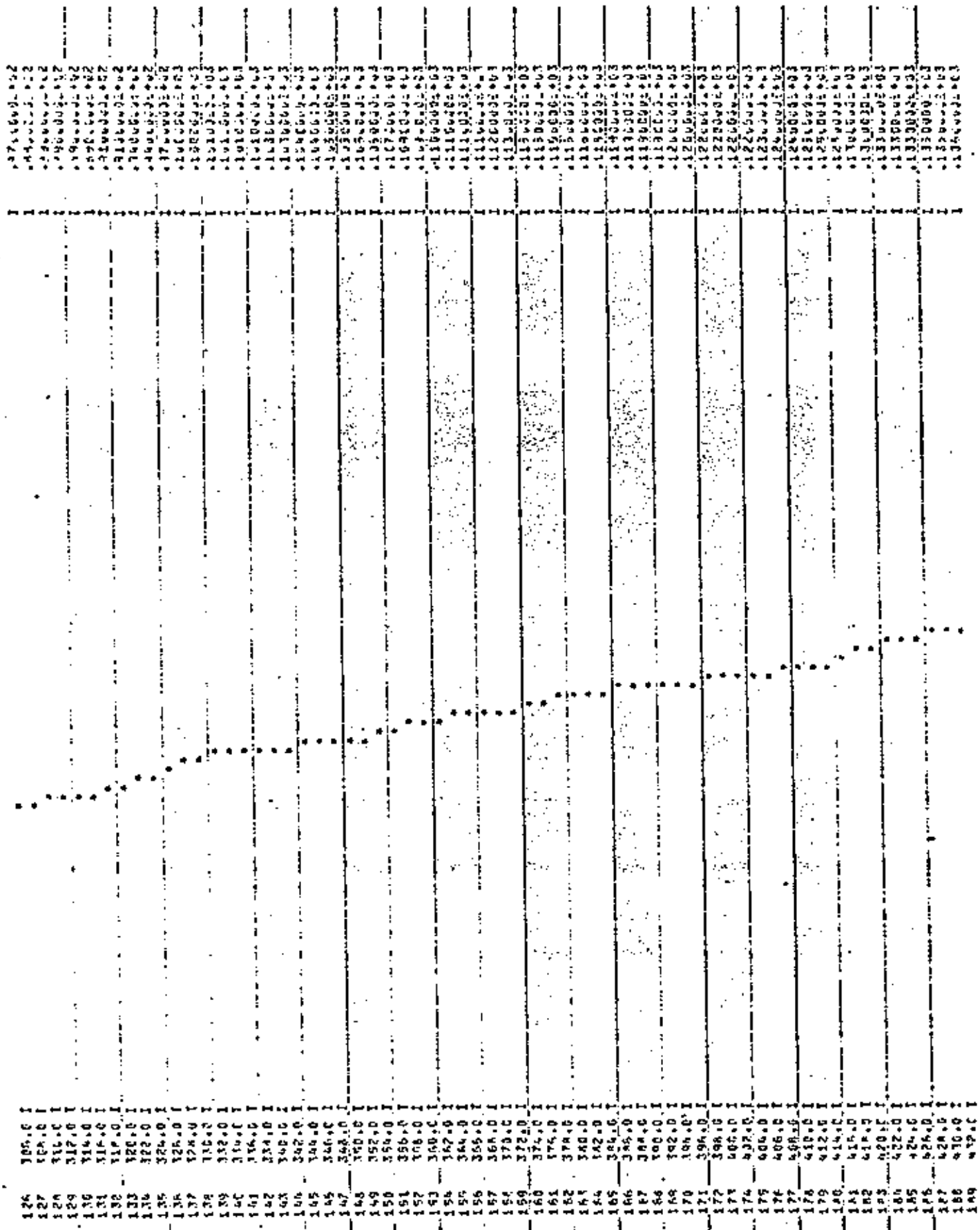

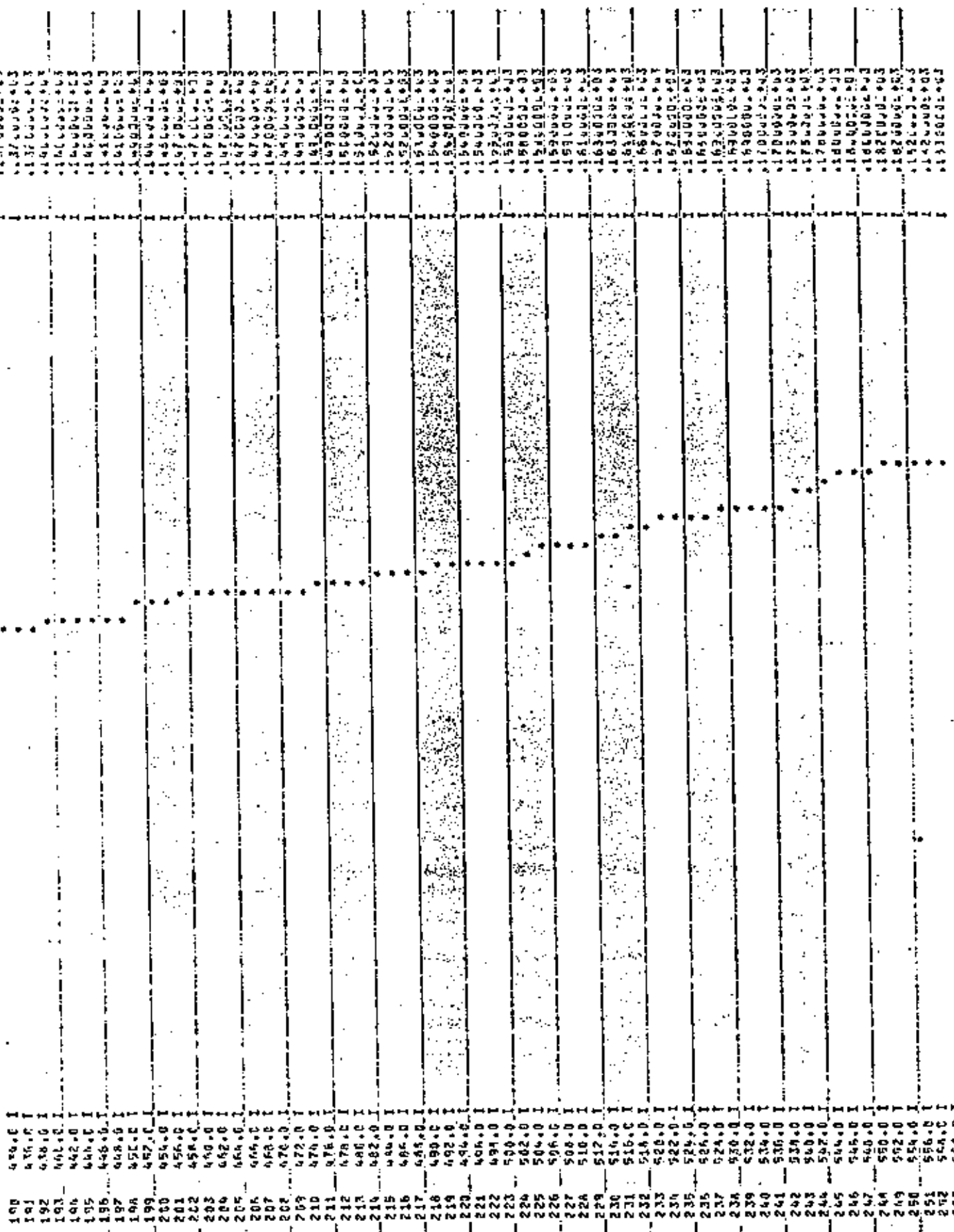

Figure 28 (Cont'd)

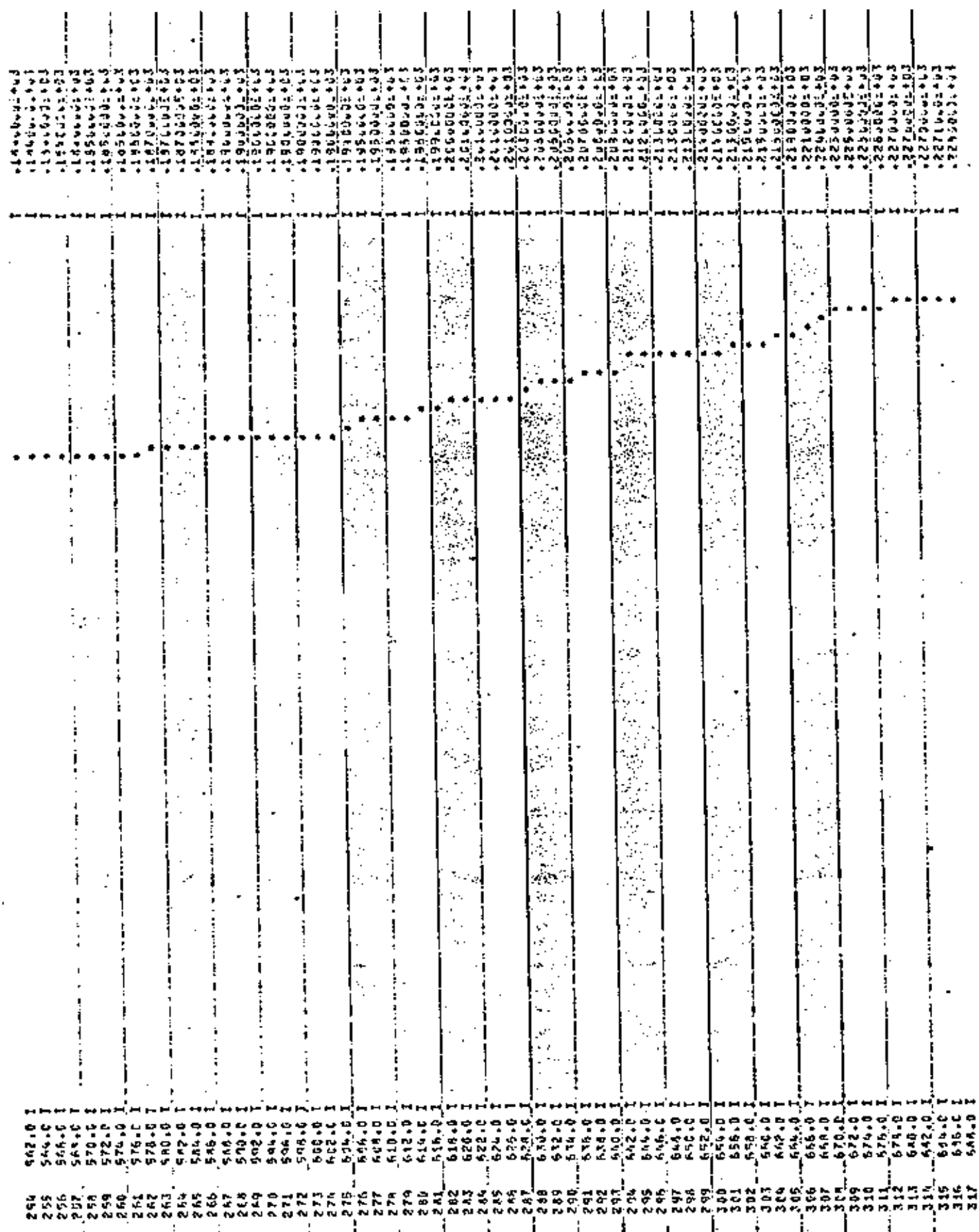

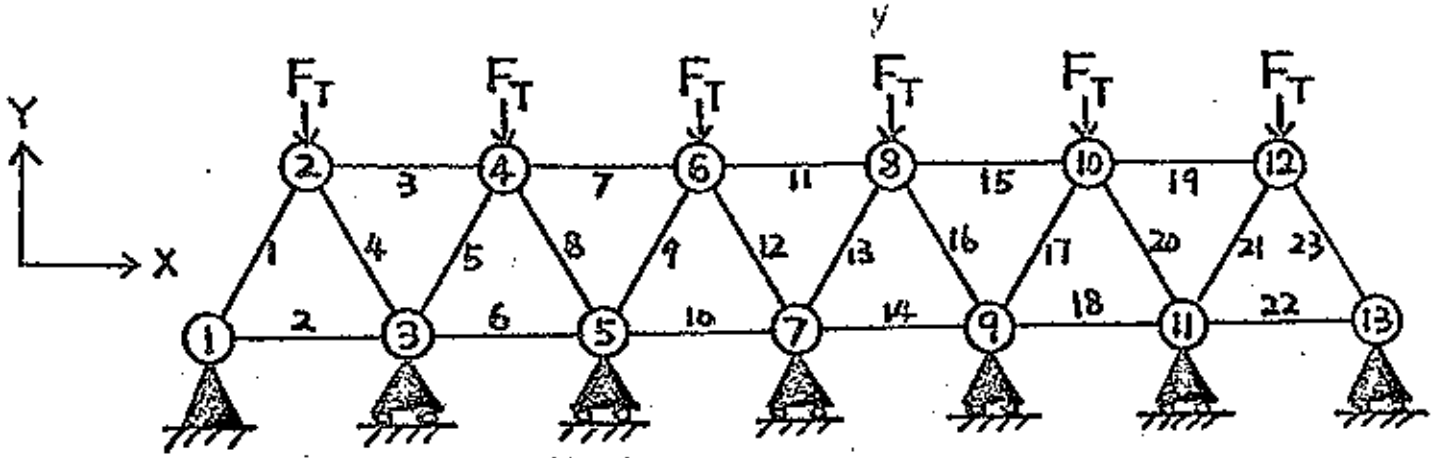

(29a)

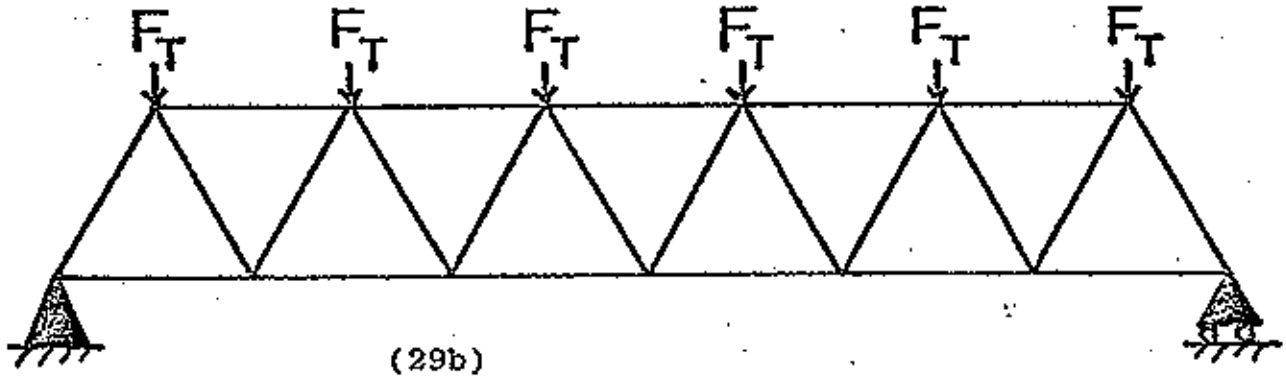

(29b)

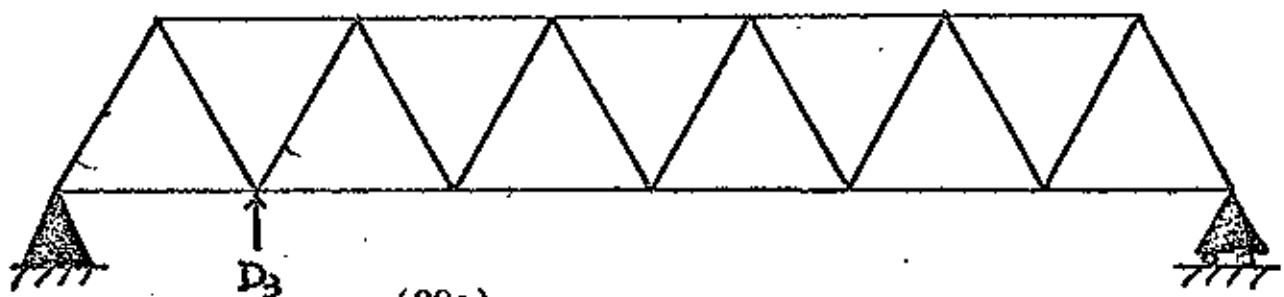

(29c)

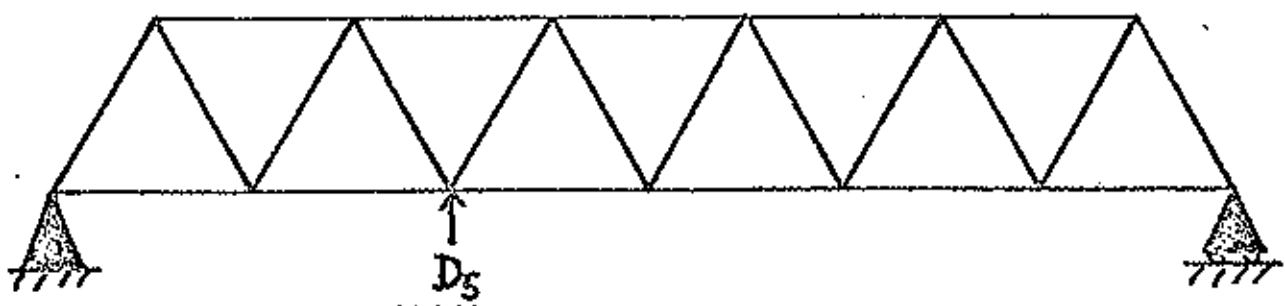

(29d)

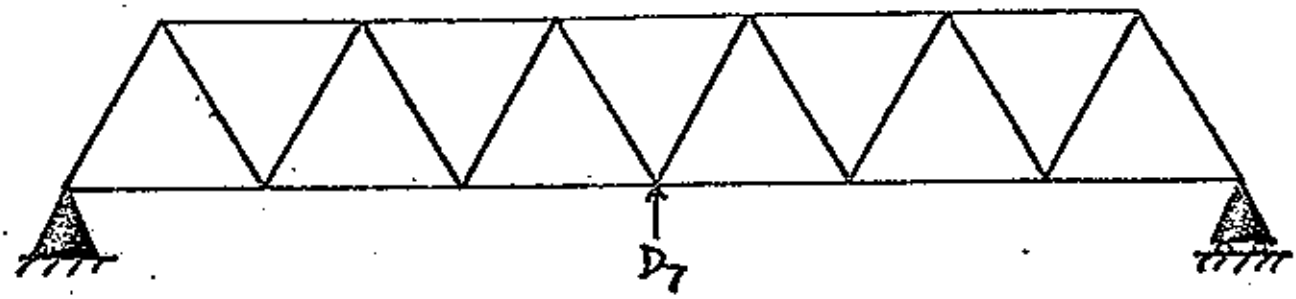

(29e)

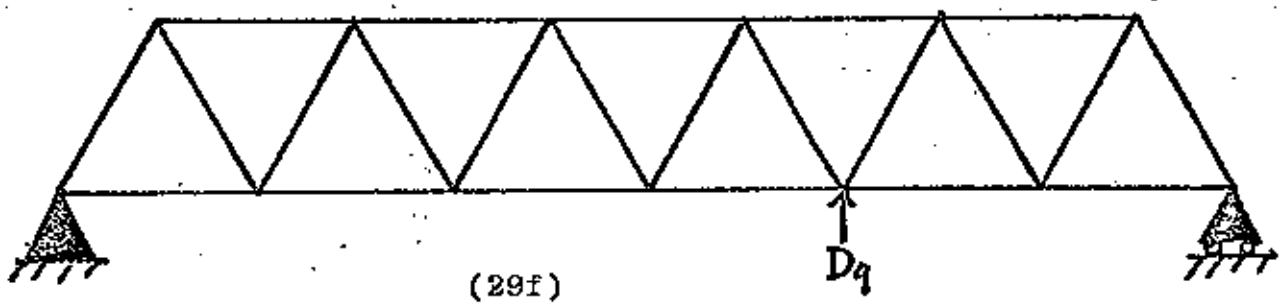

(29f)

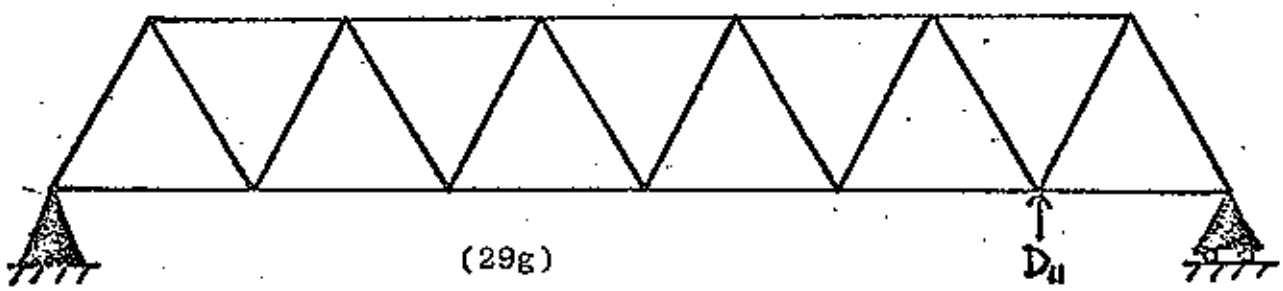

(29g)

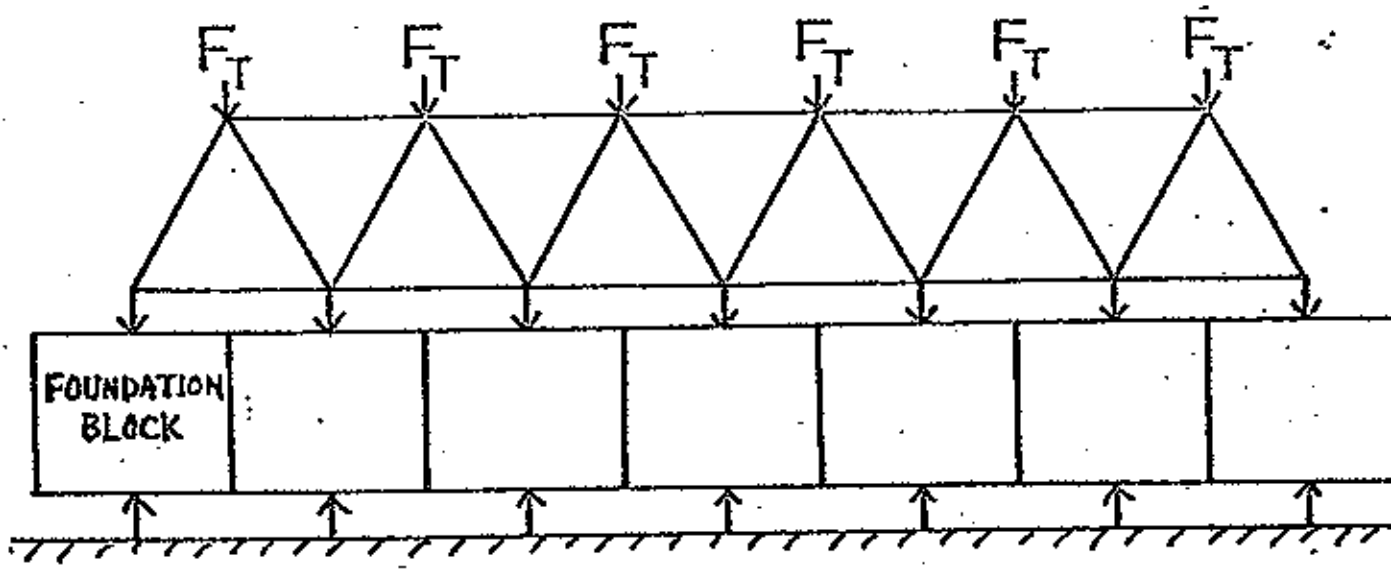
F_T
F_T
F_T
F_T
F_T
F_T
FOUNDATION BLOCK

(30a)

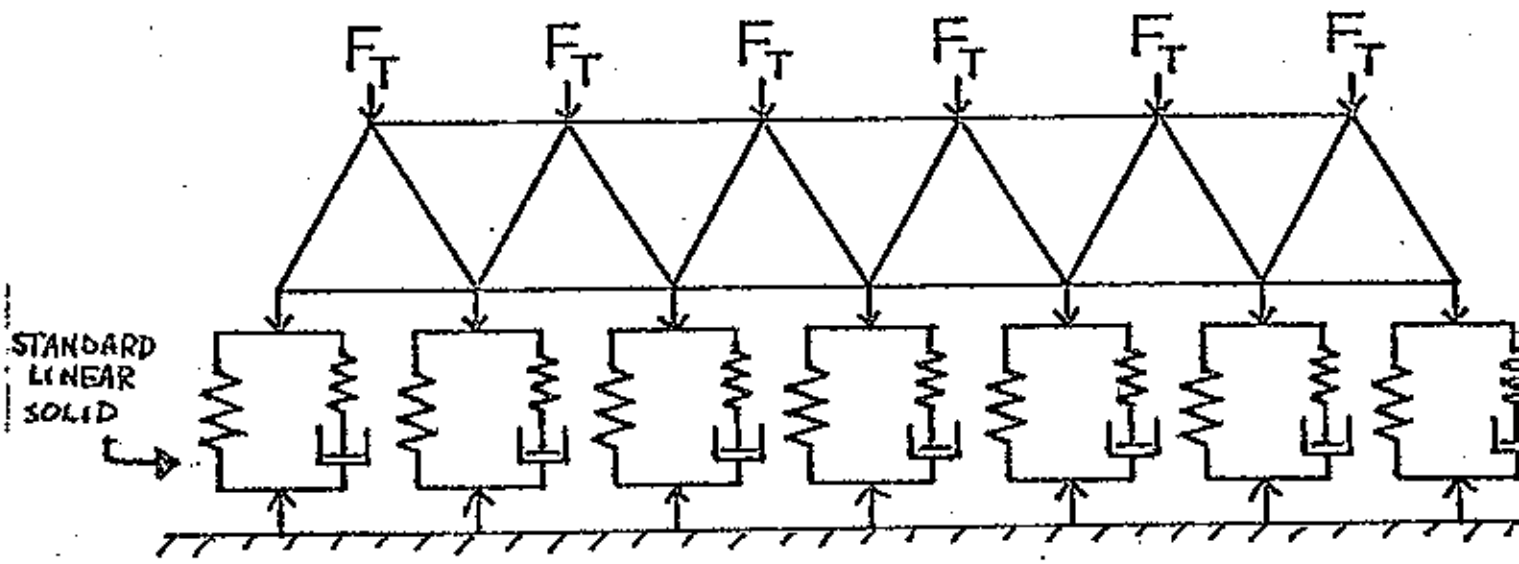
F_T
F_T
F_T
F_T
F_T
F_T
STANDARD LINEAR SOLID

(30b)

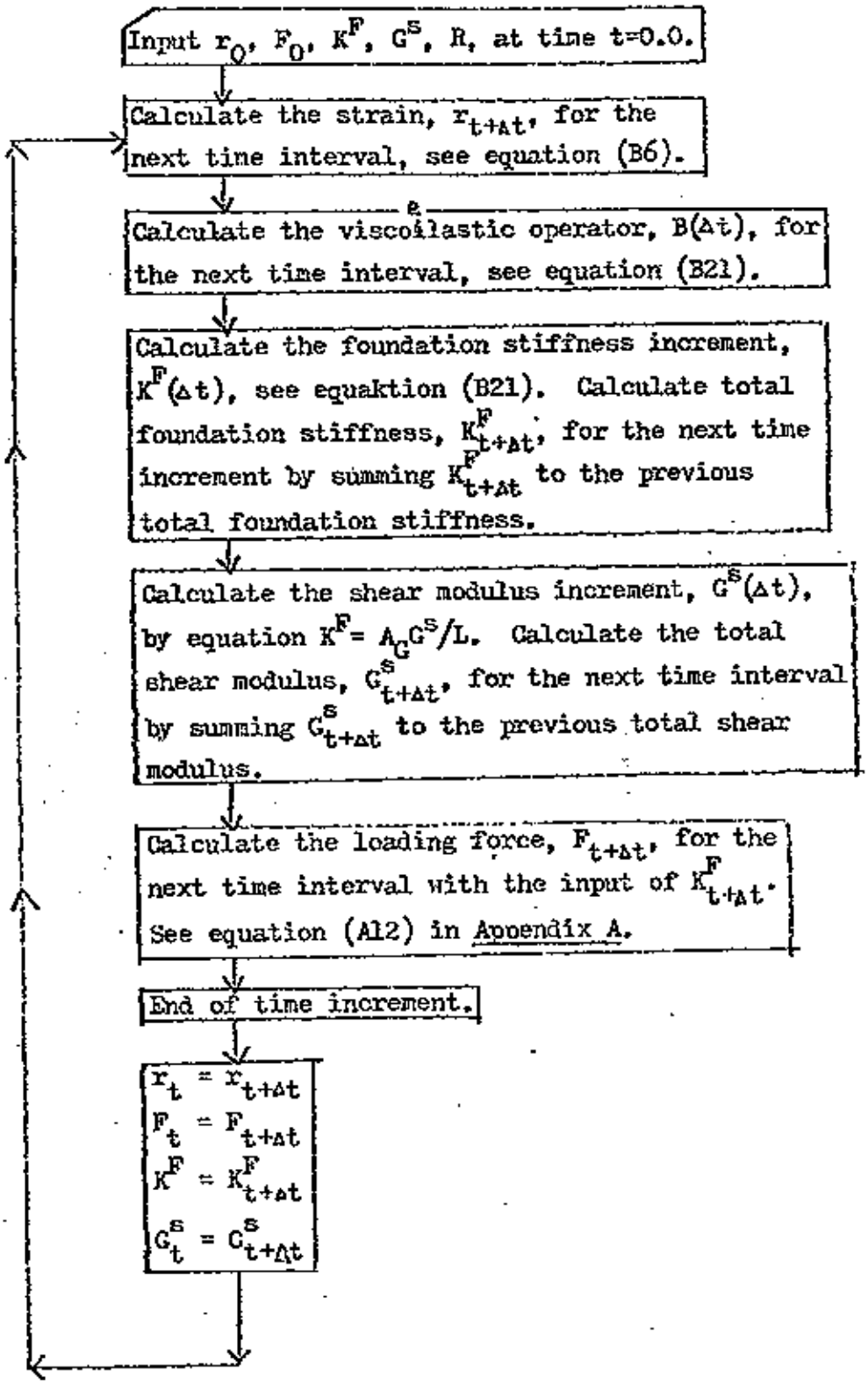
Input r_0, F_0, K^F, G^S, R, at time t=0.0.
Calculate the strain, $r_{t+\Delta t}$, for the next time interval, see equation (B6).
Calculate the viscoelastic operator, $B(\Delta t)$, for the next time interval, see equation (B21).
Calculate the foundation stiffness increment, $K^F(\Delta t)$, see equaktion (B21). Calculate total foundation stiffness, $K^F_{t+\Delta t}$, for the next time increment by summing $K^F_{t+\Delta t}$ to the previous total foundation stiffness.
Calculate the shear modulus increment, $G^S(\Delta t)$, by equation $K^F = A_G G^S/L$. Calculate the total shear modulus, $G^S_{t+\Delta t}$, for the next time interval by summing $G^S_{t+\Delta t}$ to the previous total shear modulus.
Calculate the loading force, $F_{t+\Delta t}$, for the next time interval with the input of $K^F_{t+\Delta t}$. See equation (A12) in Appendix A.
End of time increment.
$r_t = r_{t+\Delta t}$
$F_t = F_{t+\Delta t}$
$K^F = K^F_{t+\Delta t}$
$G^S_t = G^S_{t+\Delta t}$

Figure 32